Methyltransferase inhibitors interfere with Snail1 action on myofibroblast activity to prevent fibrosis and metastasis

Laura Sala Romanyà

TESI DOCTORAL UPF / 2018

DIRECTOR DE LA TESI

Dr. Josep Baulida i Estadella

DEPARTAMENT DE CIÈNCIES EXPERIMENTALS I DE LA SALUT

ACKNOWLEDGEMENTS

Durant la tesis hi ha hagut de tot, però l'he gaudida molt i en gran part ha sigut per les moltes persones que he conegut durant el camí i que m'han ajudat durant la tesis fent-la més bonica.

Jepi, volia agrair-te la confiança que vas dipositar amb mi des del principi. Sinó potser no hauria fet la tesis i era una cosa que tenia molta il·lusió per fer. Tot i que aquestes últimes setmanes escrivint m'he preguntat més d'un cop què perquè ho vaig fer. Sempre has estat disponible per resoldre tots el dubtes i per animar-me a seguir, a més a més m'he sentit molt lliure per proposar i fer experiments i això ho he agraït moltíssim.

També volia agrair-li tot el suport a l'Antonio, per totes les propostes al projecte i també per la confiança. Víctor, gràcies per el teu humor en el laboratori i també per animar-me sempre.

Ser part del Snail team és molt xulo, volia agrair al David, Jordi, Hèctor, Willy, Aida, Rubén, Raúl, Alba, Laura i Raulillo tot el bon rotllo i les bones estones que em passat junts. Al laboratori sempre hi ha bon ambient i algú disposat a alegrar-te el dia si està anant malament. David, gracias por los momentazos que nos haces vivir cada día, me encantas. Hèctor, ànims amb la tesis que comences, segur que la

gaudeixes moltíssim. Willy, de veritat que no puc riure més amb tu, el teu humor m'ha ajudat molts cops! Aida, gràcies per la xocolata, tant necessària, i per entendre'm tant amb aquestes coses! Jordi, merci per portar tant bé els ratolins, per ajudar-me amb les operacions i els inhibidors, la teva ajuda ha estat vital per la meva qualitat de vida i per últim gràcies pels berenars terapèutics, les tardes de zumba i un llarg etc. Raúl, gràcies per la portada, els consells, les IHQ, i per ser un tècnic molt guai. A l'Alba, la Laura i el Raulillo gràcies per aportar més alegria al laboratori. Rubén, gràcies per ser com ets, de maco i afectuós, sempre em fas somriure i m'ho passo tant bé treballant amb tu!

Volia agrair també el que ja no estan al lab però que em van ajudar moltíssim en els seu moment. Àlex, gràcies pel Rumi. Txell, merci per iniciar-nos a la zumba i per ser una persona tant positiva i alegre, encara et trobo a faltar al lab. Lorena, em vas ensenyar tot el món *in vivo* i m'has ajudat molt amb el projecte també, gràcies perquè amb tu he après moltíssim. Maria, va ser genial treballar juntes i tinc tant bon rècord del mini equip que vam fer!

Volia donar les gràcies a tothom de la segona planta, ha sigut fàcil treballar aquí. Als laboratoris veïns, als treballadors de la cuina, de la neteja i de tots els serveis, moltes gràcies pel tracte durant aquests anys, pels reactius i pels somriures al llarg del passadís. Vull agrair especialment al Joan Gibert pel seu interès en el projecte i els seus súper consells.

Chromatin team, per mi va ser un drama que marxéssiu del PRBB. A vegades encara se'm fa estrany que no estigueu al lab i us hi trobo molt a faltar. Gràcies, Gemma, Jess, Joan Pau i Laura pels anys al laboratori, per mi van ser els millors. Gràcies a la Sandra també pels consells i els ànims durant aquest temps.

Laura i Joan Pau, d'aquí m'enduc dos grans amics. Gràcies per entendre'm, preocupar-vos i suportar-me. Laura, m'encantes ja ho saps, ànims amb la teva tesis que ja quasi ho tens i gràcies per estar sempre al meu costat, escoltar-me i recolzar-me tant! Joan Pau, amb tu sempre és complicat, al principi quan ens vam conèixer et vaig odiar una mica per lo del panda, però bé suposo que t'haig de donar les gràcies pel panda també, li he agafat estima. Que estiguessis al lab feia sempre que el dia fos més senzill i feliç i encara ho fa. Gràcies per estar allà sempre.

Encara que no has intervingut directament en aquesta tesis, volia agrair-te Josep els dos anys que vaig passar al teu laboratori. Allà va ser on vaig decidir que volia fer investigació i vaig aprendre'n moltíssim, gràcies pel tracte tant humà i proper que tens sempre. Gràcies Mónica per ensenyar-me tantes tècniques per primer cop i per compartir amb mi part del teu doctorat, m'ho vaig passar tant bé!!! There, Mònica, Jonathan, Pablo, Pepe, Lecho, gràcies pels riures i pels vídeos.

Per descomptat, el recolzament de família i els amics ha estat fonamental, la majoria de setmanes només tenia ganes que arribés divendres per anar a sopar amb vosaltres, Jordi, Meri i Eli, i fer una copa de vi o dues.

Als meus compis de pis, David i Judith, sou la canya. Jud gràcies també per ajudar-me al laboratori, per la paella dels teus avis, de veritat que no pot haver cosa més bona, per convidar-me a Nules sempre i per ser tant bona amiga.

Als biòlegs, Mel, Jan, Ana, Laureska i Sílvia, gràcies per compartir amb mi tantes classes i tantes hores de bar, i ara per seguir al meu costat encara que a vegades amb milers de quilòmetres pel mig. És bonic compartir tantes aficions amb vosaltres.

I el gràcies més gran és per la meva família, pels meus pares, per recolzar-me sempre, per fer-me feliç i ensenyar-m'ho tot. Marcel, merci per suportar-me com a germana gran que sé que és pesat.

Per acabar, gràcies als membres del tribunal per acceptar formar-ne part i per llegir-vos la tesis. També agraeixo a la Fundació IMIM l'ajuda econòmica per la impressió d'aquesta tesis.

ABSTRACT

Snail1 is a transcription factor which activity is required for the fibroblasts-to-myofibroblast differentiation. In the first part of the thesis we characterize a protein complex involving Snail1, PRMT1 and PRMT4, two related members of the protein arginine methyltransferase (PRMT) family. Upon fibroblast activation with TGF-β, these enzymes interact with Snail1 and with the proximal Fibronectin promoter where Snail1 was described to bind. In fact, TGF-β induces Snail1-dependent arginine dimethylation on a set of proteins, including the H3 at the proximal Fibronectin promoter and several splicing regulators. We describe some TGF-β-induced alternative splicing events that are Snail1-dependent. In the second part, we use the methyltransferases inhibitors AMI-1 or Sinefungin to prevent myofibroblast activity in both cell culture and *in vivo* models. Of therapeutic interest for fibrosis and cancer, the inhibitors are effective in blocking the exacerbated activity of fibroblasts from idiopathic pulmonary fibrosis patients and Sinefungin efficiently interfered with the desmoplastic deposition in breast tumours and reduced the metastatic burden in mice. Our data reveal a new molecular pathway induced by Snail1 and point to methyltransferase inhibitors as potential reagents to prevent fibrosis and metastasis.

RESUM

L'activitat del factor de transcripció Snail1 és necessària per l'activació de fibroblasts a miofibroblasts. En la primera part de la tesis caracteritzem un complex proteic que inclou Snail1, PRMT1 i PRMT4, dos membres d'una família de proteïnes que transfereixen grups metils a arginines (PRMTs). L'activació de fibroblasts amb TGF-β indueix la interacció d'aquests dos enzims amb Snail1 i amb el promotor proximal de Fibronectina on s'havia descrit que hi interaccionava Snail1. De fet, TGF-β indueix la dimetilació en arginines d'un conjunt de proteïnes en les que s'hi inclou la H3 del promotor proximal de Fibronectina i factors reguladors del processament (splicing) alternatiu de l'ARN. Hem descrit que TGF-β promou varis events de splicing alternatiu que depenen de Snail1. En la segona part, hem utilitzat els inhibidors de l'activitat de les metiltransferases, AMI-1 i Sinefungin per prevenir l'activitat dels miofibroblasts en cultius cel·lulars i en models *in vivo*. Els inhibidors bloquegen la hiperactivació de fibroblasts provinents de pacients amb fibrosis pulmonar idiopàtica i en ratolins la Sinefungin redueix la deposició d'estroma als tumours de mama i el número de metàstasi. El nostre treball revela una nova via molecular induïda per Snail1 i proposa els inhibidors de metiltransferases com a molècules amb potencial per a prevenir la fibrosis i les metàstasi.

TABLE OF CONTENTS

FIGURE INDEX

INTRODUCTION

RESULTS

DISCUSSION

ABBREVIATIONS

3D-ECMs: Three dimensional ExtraCellular Matrices

AMI-1: Arginine N-Methyltransferase Inhibitor-1.

BSA: Bovine Serum Albumin

CAFs: Cancer-associated Fibroblasts

ChIP: Chromatin ImmunoPrecipitation

cDNA: Complementary Desoxyribonucleic Acid

Cre: Circular recombinase specific

CTD: C-terminal domain

DAPI: 4',6-diamidino-2-phenylindole

DMEM: Dulbecco's Modified Eagle's Medium

ECM: Extracellular matrix

EGF: Epidermal Growth Factor

EMT: Epithelial-to-Mesenchymal Transition

EMT-TFs: Epithelial-to-Mesenchymal Transition Transciption factors

FAP: Fibroblast Activation Protein

FBS: Fetal Bovine Serum

FGF: Fibroblast growth factor

GFP: Green fluorescent protein

IF: Immunofluorescence

IgG: Immunoglobulin G

IHC: ImmunoHistoChemistry

IP: Immunoprecipitation

kDa: Kilo Dalton

KO: Knock-out

MEFs: Mouse embryonic fibroblasts

MET: Mesenchymal-to-Epithelial transition

MMTV: Mouse Mammary Tumour Virus

MSCs: Mesenchymal stem cells

MTA: 5′-Deoxy-5′-(methylthio)adenosine

MTT: 3-(4,5-dimethylthiazol-2-yl)-2,5-diphenyltetrazolium bromide

mRNA: messenger Ribonucleic Acid

NF-κB: Nuclear Factor kappa B

OHT: 4-Hydroxytamoxifen

PARP1: Poly (ADP-ribose) polymerase 1

PCR: Polymerase chain reaction

PGE_2: Prostaglandin E2

PI3K: Phosphatidylinositol-3-kinases

PKMTs: Protein Lysine Methyltransferases

PRMTs: Protein Arginine Methiltransferases

PTEN: Phosphatidylinositol-3,435-trisphosphate 3-phosphatase

PyMT: Polyoma Virus Middle T-antigen

RIPA: Radioimmunoprecipitation assay buffer

RNA: Ribonucleic Acid

RT: Reverse transcription

SET7/9: SET Domain Containing Lysine Methyltransferase 7/9

SCID: Severe combined immunodeficiency

SNAI1: Snail family transcriptional factor 1

TAFs: Tumor-associated fibroblasts

TBS-T: Tris Buffer Saline-Tween

TGF-β: Transforming Growth Factor beta

TFs: Transcription factors

WT: Wild type

αSMA: α-Smooth Muscle Actin

INTRODUCTION

INTRODUCTION

1. THE STROMAL CONTRIBUTION TO CANCER PROGRESSION

1.1 Cancer overview

Cancer is the second leading cause of death globally and accounted for 8.8 million deaths in 2015 according to the World Health Organization. Cancer is the generic term for a various groups of diseases characterized by an abnormal cell growth.

Human beings have had cancer throughout recorded history, some of the earliest evidence of cancer is found in human mummies in ancient Egypt. Growth suggestive of bone cancer osteosarcoma has been seen in mummies. The oldest description of cancer (although the word cancer was not used) was also discovered in Egypt and dates back to about 3000 BC.

Cancer can be divided in two major subtypes; solid and liquid tumours. Solid tumours are composed of parenchyma and stroma. Parenchyma consist of the cells that perform the function of the tissue or organ, stroma is the part of the tissue with a structural or connective role; it is made up of connective tissue, blood vessels, nerves and ducts. Cancer cells belong to the parenchyma whereas non-malignant cells

and the extracellular matrix (ECM) compose the stroma. Solid tumours are classified according to the cell type where the tumour is originated. Carcinomas originates from the epithelium and account for 80 to 90% of all cancers. Sarcomas are tumours that arise from mesenchymal cells differentiating into bone, muscle, fat and cartilage. Liquid tumours are the ones that arise from blood cells precursors, such as myelomas (uncontrolled growth of plasma cells in the bone marrow), leukaemia (the same in leukocytes of the bone marrow) and lymphomas (develops in the nodes of the lymphatic system).

But the main cause of death in solid cancer patients is not the primary growth of these tumours, but the metastasis formation[1]. In order for a metastasis to occur, cancer cells must acquire invasive capabilities, intravasate into the circulation, survive in the blood stream, arrive at the target organ, seed, extravasate into the parenchyma and show persistent growth. Seeding can occur to multiple organs, but metastatic tumours may grow in only one or a few[2].

In 2000, Douglas Hanahan and Robert A.Weinberg defined six essential alterations in cell physiology that dictate malignant growth[3] (Figure 1). These hallmarks of cancer are the following: sustaining proliferative signalling, insensitivity to antigrowth signals, evasion to apoptosis, limitless replicative potential, sustained angiogenesis and tissue invasion and metastasis. This last property is the main feature that

deciphers a malignant tumour from a benign one. Underlying these hallmarks there is genome instability which generates the genetic diversity necessary for the acquisition of these traits. Somatic mutations drive the transformation from a normal to malignant cells. The most frequently mutated oncogenes and oncosupressors in cancer cells are PI3K, Ras, p53 and PTEN, however there is a large number of low-frequency mutations that are also contributing[4].

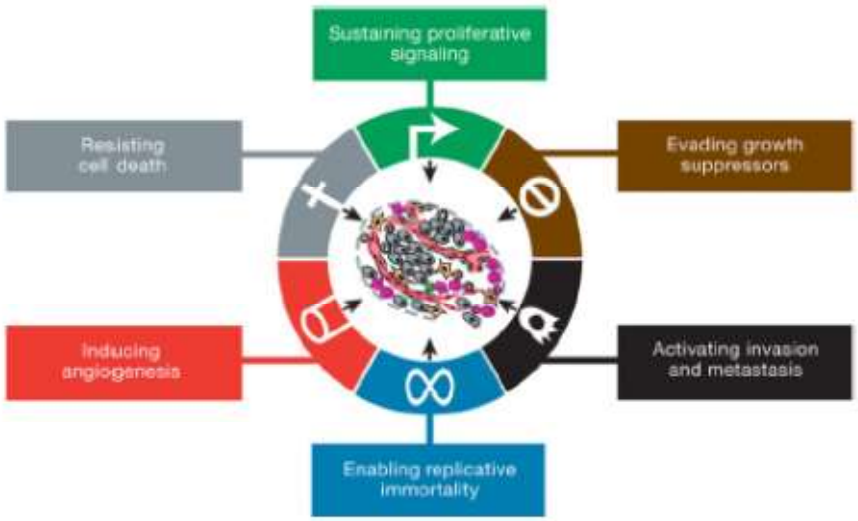

Figure 1. The hallmarks of cancer. Representative cartoon of the six capabilities originally proposed by Weinberg and Hanahan in 2000[3].

In 2011 Hanahan and Weinberg actualized their original concept by adding two new characteristics; reprogramming of cellular energy metabolism and evasion to the immune system[5]. Importantly, the paradigm that cancer cells were the

only element contributing to tumour progression evolved. In general, an oncogenic mutation is not enough to trigger cancer progression, there is also the need of a change in the stromal signalling that alters tissue homeostasis[6]. Tumour stroma has the capacity to limit cancer initiation acting as a natural barrier but once homeostasis is lost changes in the microenvironment can shift the balance and drive disease progression. Tumours are complex and recruit normal cells that contribute to the acquisition of the hallmarks traits by creating a tumour microenvironment or stroma that supports and enhances tumour growth and metastasis.

1.2 Tumour stroma

Tumours are like new organs and are made of different cell types and components. Within the stroma compartment there are all the non-tumour cells; including cells of the immune and vascular systems as well as fibroblasts and interstitial extracellular matrix (ECM) (Figure 2).

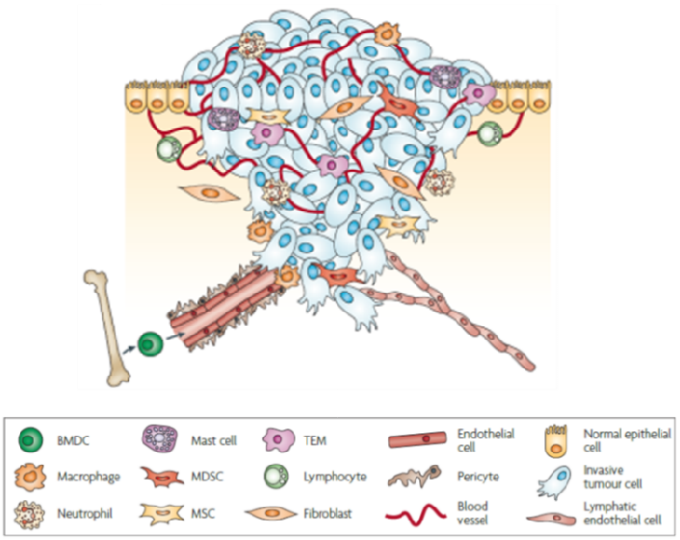

Figure 2: The primary tumour microenvironment. Cancer cells are surrounded by a complex microenvironment comprising numerous cells including endothelial cells, stromal fibroblasts and a variety of bone marrow-derived cells including macrophages, and mesenchymal stem cells. Adapted from Joyce and Pollard[2].

The change in stromal signalling comes from cancer cells that alter the adjacent stroma to form a permissive and supportive microenvironment. Changes in the stroma accompanying tumour progression include appearance of discontinuities in the basement membrane surrounding the growing tumour, several immune responses, formation of new blood vessels (angiogenesis), activation of the stromal fibroblasts and the subsequent remodelling of the extracellular matrix (ECM). Cancer alters these processes in a way to favour its own development.

1.2.1 Fibroblast to myofibroblast transition

Fibroblasts are the main cellular type of the stroma. Virchow[7] and later Duvall[8] used classic histological techniques to describe cells residing in connective tissues. Fibroblasts were first described as cells in the connective tissue that synthesize collagen. Normal fibroblasts are present in the interstitial space usually close to a capillar and embedded within the ECM. Fibroblasts are non-epithelial, non-immune cells with a likely mesenchymal lineage origin. They are very heterogeneous and exhibit a spindle-shape morphology. Fibroblasts in a normal tissue are considered metabolically and transcriptomically inactive being in a quiescent or resting state.

But these fibroblasts have the potential to proliferate once activated by different stimuli, for example, transforming growth factor β (TGF-β), plateled-derived growth factor (PDGF) and interleukin-6 (IL-6) among others. In such conditions, these cells are proliferative, with higher secretory activity and they express α-smooth muscle actin (αSMA), Fibroblast activation protein (FAP) and Vimentin among others. The appearance of these characteristics is called fibroblast activation and fibroblasts positive for αSMA are refer to as myofibroblasts, to stress out the contractile resemblance with smooth muscle cells (Figure 3). Myofibroblast or activated fibroblast functions include synthesizing ECM, secrete cytokines, and exert physical

forces to modify tissue architecture[9]; therefore, they modify their microenvironment physically and biochemically.

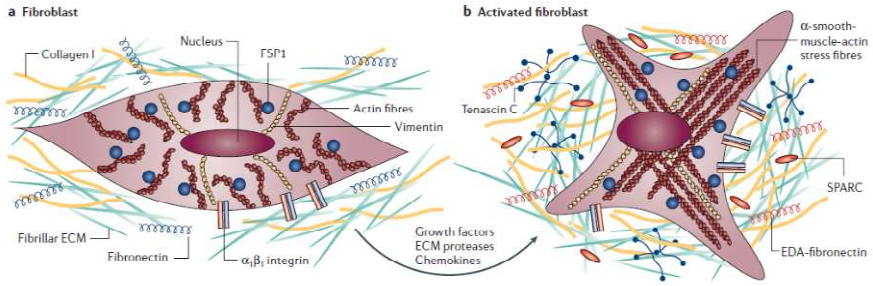

Figure 3: Activated fibroblasts or myofibroblasts. (A) Normal fibroblasts are embedded within the ECM of connective tissue. (B) Fibroblasts can acquire an activated phenotype, which is associated with an increased proliferative activity and enhanced secretion of ECM proteins. Activated fibroblasts are characterized by the expression of αSMA. Numerous growth factors but especially TGF-β mediate the activation of the fibroblasts[10].

The ability of fibroblasts to be activated and become myofibroblasts was first observed during wound healing[11]. A short but intense injury to the parenchyma cells results in a wound healing response that try to restore tissue homeostasis and repair damage. The inflammatory response induces cell proliferation and myofibroblastic differentiation[12]. Myofibroblast that are activated under these stimuli including TGF-β[13] are the responsible for the contraction of the skin to close the wound. Fibroblasts cultured from a healing wound secrete more ECM elements and proliferate more than

fibroblasts isolated from healthy tissue[14] as a result of mechanical and autostimulatory feedback signalling. Once the wound is repaired stimulatory and feedback signalling disappears and the number of activated fibroblasts decreases being the myofibroblast differentation a transient and reversible process.

1.2.2. Myofibroblasts in fibrosis and cancer

In vivo, myofibroblast were later found in tissues with acute and chronic inflammation[15]. In all cases, stimulatory molecules were generated by tissue cells in response to some insult. When injuries turn to be chronic, the repair response is maintained (Figure 4) and epigenetic mechanisms may restrict the regression of activated fibroblasts to quiescence. The consequence of this constant activation is the formation of a pathological fibrous tissue in a process known as fibrosis.

Similar persisting tissue repair responses and chronic inflammation[16] can also occur in cancers, as tumours can act like wounds that never heal[17]. This is because accumulation of cancer cells in a tissue can be sensed as an injury that generates a continuous repair response. In these cases, cancer cells recruit activated fibroblasts (known as CAFs, for cancer associated fibroblasts) similar of those present during wound healing and fibrosis that generate a fibrotic like stroma or desmoplastic reaction around tumours.

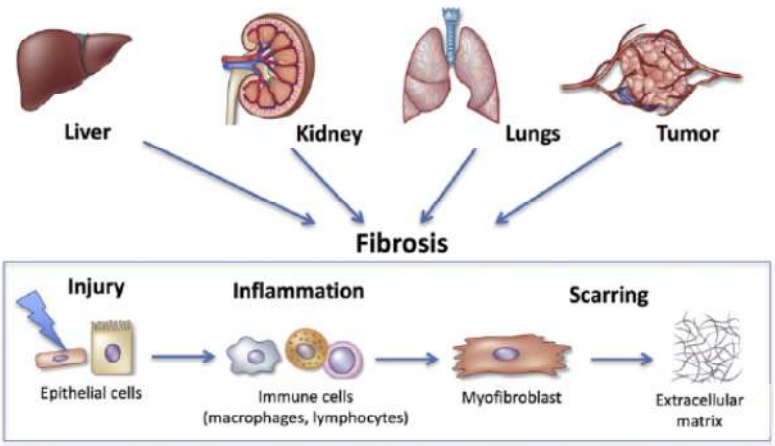

Figure 4: Schematic diagram showing the general fibrogenesis in different organs and tumour. Injury to epithelial cells instigates inflammation. The inflammatory cells secrete growth factors which activate local fibroblasts into myofibroblasts. Eventually myofibroblasts secrete ECM leading to scarring of the tissue[18].

Fibrotic fibroblasts and CAFs express αSMA and show high contractile activity. CAF also express other myofibroblastic markers such as FAP, and Vimentin that vary from one cell to another attesting to the heterogeneity of CAF population.

1.2.3. CAFs and cancer progression

The activity of CAFs affects the evolution of the tumour as its presence correlates with poor prognosis in many tumours[19]. Curiously, chronic fibrosis predisposes the affected tissues to develop cancer[20]. Therefore, fibrosis could be generating tumorigenesis and tumour progression might be instigating

chronic fibrosis. It remains unclear whether CAFs and fibrotic myofibroblasts possess unique traits that differentiate them. Hence, it is logical to assume that effective targeting drugs that interfere with one will also interfere with the other[21].

TGF-β release upon injury is considered the main growth factor for the recruitment of fibroblasts, inducing CAFs activity, tumour progression and metastasis[22]. Metastasis initiation in colorectal cancer is dependent on a TGF-β program in stromal cells[23]. TGF-β is also required for fibroblasts activation in wound healing and fibrosis. Fully activated fibroblasts secrete TGF-β in an autocrine loop sustaining themselves in an active state. TGF-β treatment induces activation of RhoA, a GTPase that promotes stress fibre formation, as well as αSMA synthesis allowing an efficient ECM remodeling[24].

The role of myofibroblasts in wound healing is well understood; however, their paper in tumour progression and metastasis is more complex. As mentioned, the presence of CAFs in the tumour stroma is, in general, interpreted as a force promoting cancer progression. Experimentally, for example, has been shown that normal prostate epithelial cells give rise to intraepithelial neoplasia in mice when co-injected with CAFs but not when co-injected with normal fibroblasts[25]. Subsequently, such studies were reproduced in other cancer systems. CAFs can enhance metastasis by releasing growth factors and cytokines to stimulate directly or indirectly cancer

cell growth and their invasive features. Moreover, CAF activity modifies the ECM properties around primary tumours facilitating and guiding tumour cell invasion towards blood and lymphatic vessels[26]. Thus, the presence of CAFs in a wide range of tumours generate a supportive atmosphere stimulated by cancer cells and targeting tumour CAFs has emerged as a new therapeutic window to treat those tumours[27].

In contrast to this view of CAF actions, some studies have suggested that CAFs can restrain pancreatic ductal adenocarcinoma (PDAC) by reducing fibrosis[28]. In these lines, another study shows that the depletion of αSMA positive cells reduces fibrosis and survival in mice with PDAC[29]. These contradictory studies unveil the complexity of the tumour-stroma interactions and the subtle line between a favourable treatment and a detrimental one.

1.2.4 Paracrine signalling by CAFs

CAFs sustain and promote cancer progression at various levels. Angiogenesis, inflammation, proliferation, growth and survival of the cancer cells are promoted largely throught secretion of growth factors and cytokines by CAFs.

There is a bidirectional cross-talk between tumour cells and CAFs; cancer cell-released TGF-β acts upon CAFs and enhances their potential to secrete tumour promoting

chemokines (such as IL-11[23], CXCL12, Tenascin C[30], HGF or Neuregulin1[31], PGE_2[32]) , which then act back on the malignant cells to promote their proliferative, migratory, and invasive properties[33].

Moreover, activation of CAFs, promotes a NF-κB proinflammatory gene signature that sustains cancer progression by recruitment of macrophages, neoangionesis and subsequently an increase in tumour growth[34]

1.2.6 CAFs signalling through the Extracellular matrix

The ECM is a network composed by fibrous proteins such proteoglycans, fibronectin, collagens and laminins. Fibroblast within the stroma are the producers but also the remodellers of this ECM, synthesizing both fibrillar proteins and ECM-degrading matrix metalloproteinases.

The ECM is a physical and biochemical scaffold that regulates the three-dimensional organization of the tissues, supporting and organizing cells. Its physical properties allow it to act as a physical barrier when ECM forms a disorganized network around the cells. Although tightly controlled during organ homeostasis, the ECM is commonly deregulated in diseases such as cancer or fibrosis. Thus, the extracellular matrix, ECM, resulting from a tumoural desmoplastic reaction bears a striking resemblance to the ECM typical of chronic fibrosis including deposition of fibrillary collagens, Col-I and –III and a severe remodelling of the fibrillary architecture[35].

The remodelled ECM structure provide a physical guidance during tumorigenesis, influencing cell migration, invasion and metastasis[36] and aligned ECM serves as natural trails on which cancer cells migrate[37].

Moreover, the ECM can bind different growth factors limitating their diffusion and their accessibility to receptors, or acting directly as a co-receptor. ECM can initiate signalling indirectly as signal presenter or directly, providing fragments upon metalloproteinase action.

Finally cells directly sense the biomechanical features of the ECM, such as the stiffness and change a wide variety of cell behaviours accordingly (Figure 5).

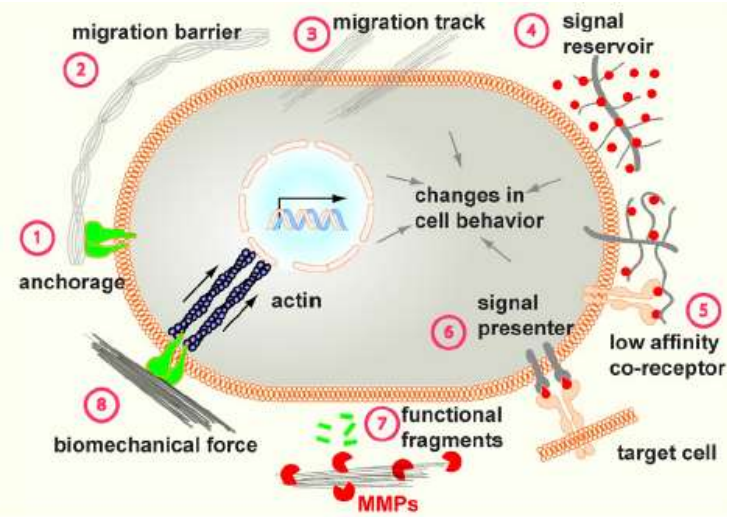

Figure 5: Mechanism of ECM function. Schematic representation of the different functions of the ECM[38].

Fibronectin initiates ECM assembly promoting the assembly of other fibrous proteins such as collagen, fibrillin, thrombospondin-1 and tenascin C[39]. Fibronectin fibrillogenesis requires conformational changes promoted by the binding of a Fibronectin dimer to integrins in the focal contacts. Upon binding, Fibronectin linearize and the binding domains for other members of the ECM and Fibronectin itself are exposed promoting the formation of a dense mesh. The interaction with integrins links the ECM with the actin cytoskeleton[40]. Rho-mediated contractibility of the cytoskeleton exposes the binding sites of Fibronectin and induces Fibronectin matrix assembly[41]. Myofibroblasts nuclei and cell shapes depend on the tensional status of the tissue[42].

Linearization of the ECM fibrils has been observed *in vitro* when fibroblasts from tumour samples were used to produce ECM[43]. ECM derived from tumour fibroblasts activates the tumorigenic capacity of benign cells, and ECM derived from normal fibroblasts represses the tumorigenic phenotype in cancer cells[44].

In breast cancer, the progressive stages within the ECM fibre remodelling correlates with metastasis progression being the presence of aligned collagen fibres a prognostic signature for poor survival[45] (Figure 6).

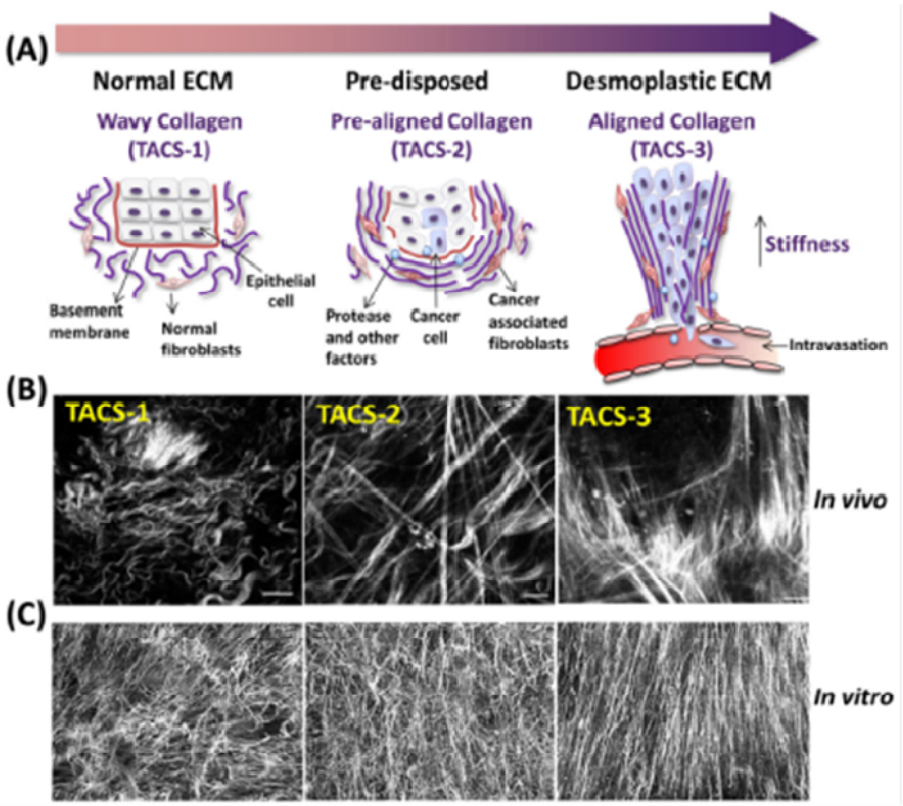

Figure 6: Stromal ECM fibre remodelling stages. (A) Schematic diagram representing progressive remodelling within collagen fibres of ECM during tumorigenesis. TACS (tumour associated collagen signature) TACS-1 (normal stage), TACS-2 (pre-disposed) and TACS-3 (aligned stage) (B) Micrographs acquire using multiphoton laser scanning microscopy illustrating TACS in Wnt-1 mouse breast model. (C) Representative reconstituted confocal images obtained from *in vitro* fibroblast-derived ECM associated with murine squamous cell carcinoma[36].

1.3 Snail1 an essential transcription factor for stromal activation

1.3.1 General characteristics

Snail1 is a zinc-finger transcription factor. It belongs to the Snail superfamily of repressors together with Snail2 (Slug) and Snail3 (Smuc). They are characterized by three different

domains: the zinc-finger C-terminal domain, a highly conserved region that contains four to six zinc fingers that mediate sequence specific interaction with the DNA; the central part which is involved in protein stability and localization; and a more variable N-terminal region.

Snail1 was first described in Droshophila melanogaster for its contribution during development, playing an important role in mesoderm formation[46]. In vertebrates Snail1 also participates in the migration of the neural crest[47]. In fact Snail1 KO mouse embryos exhibit defects in gastrulation and an early embryonic mortality[48]. Snail1 mediates the repression of the epithelial phenotype and promotion of the mesenchymal one essential for the formation of the embryonic tissues of the gastrulation.

Snail1 has four zinc fingers motifs that directly bind to E-box DNA sequences located in target promoters and that are required for transcriptional repression. Additionally, a SNAG domain located in the N-terminal region recruits co-repressors such as the chromatin remodelers HDAC1 and HDAC2[49], the polycomb grup of proteins (PRC2)[50] and the arginine methyltransferase 5 (PRMT5)[51] among others. The binding of the co-repressors is not direct but mediated by Sin3a and AJUBA (Figure 7).

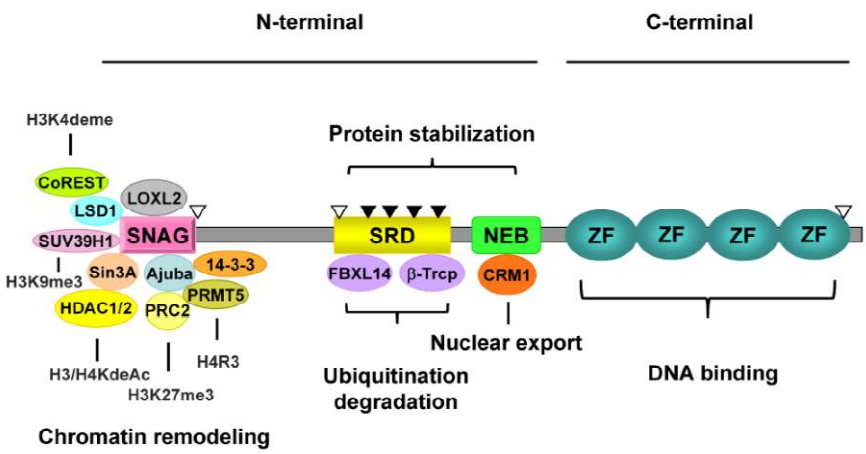

Figure 7: Structure of Snail1. Snail contains an N-terminal SNAG domain and C-terminal zinc finger domains. The N-terminal SNAG domain interacts with several co-repressors and epigenetic remodeller complexes, and the C-terminal zinc finger domains are responsible for the DNA binding. The serine-rich domain (SRD) and the nuclear export sequence (NES) control de Snail1 stability and subcellular localization. Phosphorylation sites are indicated as triangles[52].

As a transcriptional repressor, Snail1 acts on E-cadherin and triggers epithelial-to-mesenchymal transition (EMT) (see chapter 1.3.2); however, Snail1 has also been described to act as a transcriptional activator of typical mesenchymal genes, such as Fibronectin (*FN1*), in epithelial cells undergoing EMT and fibroblasts. The interaction of Snail1 with the FN1 promoter is not direct. p65-NF-κB anchors Snail1 to the *FN1* promoter where these components form a complex together with PARP1[53]. Although the Snail1-activator complex is much less characterized that the classical repressor one.

1.3.2 Snail1 and EMT

As mentioned above, the cell transition from an epithelial to a mesenchymal phenotype is known as epithelial to mesenchymal transition (EMT). EMT provides static epithelial cells with migratory properties allowing them to change tissue and organ location. EMT program includes loss of adherent junctions, loss of apical-basal polarity, rearrangement of the cytoskeleton and conversion to a low proliferative state. During the process, epithelial cells acquire a spindle-like shape, front-back polarity along with an increase of invasion and survival capabilities of the mesenchymal cell. Snail, Zeb and Twist family of proteins are the transcription factors leading EMT and they are usually called EMT-TFs (Figure 8).

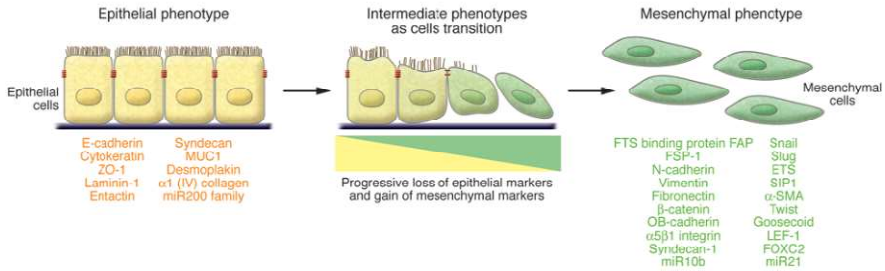

Figure 8: EMT. An EMT involves a functional transition pf polarized cells into mobile ECM-secreting mesenchymal cells. The epithelial and mesenchymal cell markers are listed. Co-localization of these two sets of distinct markers defines an intermediate phenotype of EMT[54].

Snail1 expression is up-regulated by the EMT inducer TGF-β[55], and is also regulated by NF-κB[56] and Wnt[57] pathways as

well as γ-irradiation[58] and hypoxia[59] (Figure 9). In the absence of environmental signals, intracellular Snail1 is rapidly degraded. Thus, post-transcriptional regulation of Snail1 protein levels is essential for its function. EMT is a cell plasticity switch and Snail1 is also involved in controlling cell stem and cell fate programs[60] as well as the acquisition of chemoresistance.

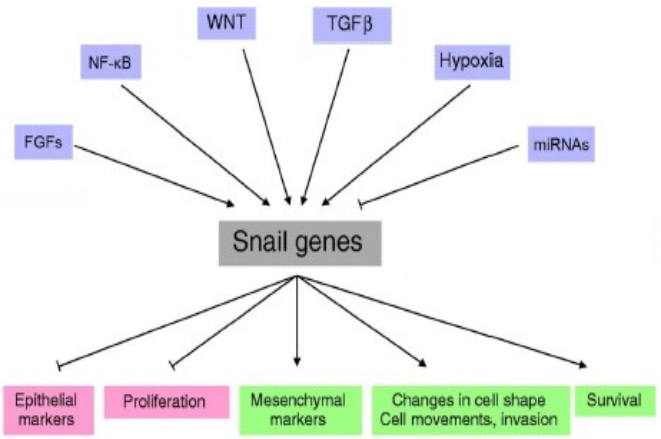

Figure 9: Regulation network of Snail1. Simplified representation of the described regulators of Snail1. Adapted from[61]

Molecularly, EMT is characterized for the loss of E-cadherin expression, a protein present in the adherent junctions, and the acquisition of mesenchymal markers. As mentioned, Snail1 directly repress the transcription of E-cadherin triggering the loss of cell-cell contacts[62,63] and activates the transcription of FN1 a typical mesenchymal gene[53].

In vivo, EMT is indispensable for a normal embryo development. *In vitro*, EMT provides cells with invasive capabilities as well as stem cell properties although its role *in vivo* during tumorigenic processes is still under debate. In mice models, transient Snail1 expression in breast cancer is necessary for metastasis[64] but it has no effect in metastasis on pancreatic cancer although it is inducing chemoresistance[65].

The classical model is that EMT allows tumour cells to escape the primary tumour and intravasate into the circulation. At secondary sites, cell would undergo an inverse transition; mesenchymal to epithelial transition (MET), recovering the epithelial phenotype observed in metastasis (Figure 10). Though, a clear demonstration *in vivo* of this process is still lacking. Lack of clear *in vivo* evidences for this model can be explained by the possibility that cancer cells undergo partial EMT, exhibiting both epithelial and mesenchymal traits. Some studies suggest that this incomplete EMT is associated with improved metastasis and chemoresitance[65]; others suggest that metastasis occur without the requirement of any EMT[66]. Therefore, EMT role during cancer metastasis formation is still an open debate.

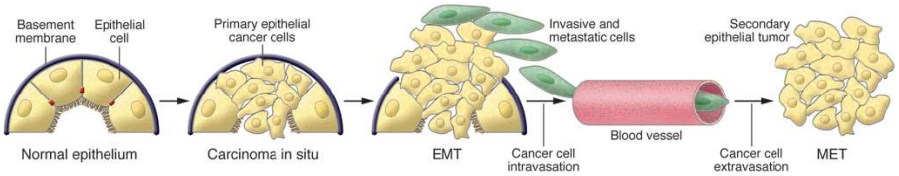

Figure 10: Contribution of EMT to cancer progression. Progression from normal epithelium to metastatic cancer involves EMT, enabling cancer cells to enter the circulation and exit blood stream to a remote site, where they may form metastasis, which may involve MET and thus a reversion to an epithelial phenotype[54].

1.3.3 The role of Snail1 in fibroblasts

Despite Snail1 was initially described as a TGF-β target gene that promotes EMT during developmental programs and tumour progression, accumulating data show that Snail1 is preferentially expressed in mesenchymal cells independent of its EMT function[67–69].

In adult tissues, Snail1 expression is restricted to transitory conditions like wound healing and pathological situations such as fibrosis. Thus, the factor is expressed in wound healing myofibroblasts[70] and its depletion delays wound healing by preventing the activation of the myofibroblasts and the organization of the ECM in the granulation tissue[69] (Figure 11).

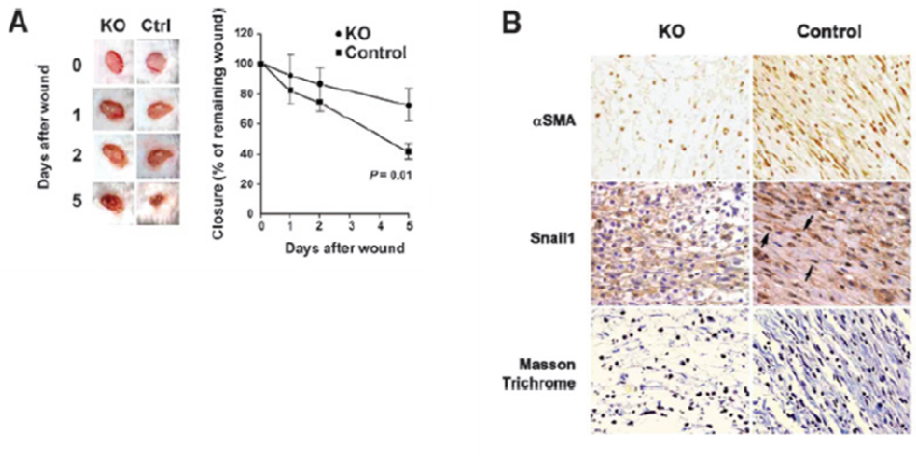

Figure 11: Snail1-deficient mice display ECM defects related to myofibroblast activity in wound healing. (A) Skin wound healing in Snail$^{+/flox}$ (control) and Snail$^{flox/del}$ (KO) mice treated with tamoxifen. Photographs of representative wounds are shown. Plots represent the mean for percentage of remaining wound still open. (B) Immunohistochemistry for αSMA, Snail1 and Masson Trichrome (collagen) in the granulation tissue of the wounds[69].

Snail1 is probably a master regulator of fibroblast activation given that its anomalous expression in fibroblasts is linked to exacerbated fibroblast activity leading to fibrosis in; hepatic stellate cell activation to myofibroblast upon hepatic damage[71], in cardiac fibrosis following hypoxic injury[72] and also in cutaneous fibrous disorders[73].

In tumours, Snail1 is predominantly detected in stromal CAFs, at the tumour-stroma boundary[70]. These Snail1 expressing fibroblasts are more active than regular fibroblasts. Interestingly, in early breast cancers the stromal areas with positive Snail1 CAFs show more desmoplasia with

Fibronectin and Collagen fibre alignment and are associated with lymph node invasion and a poor patient survival[69] (Figure 12). Snail1 stromal expression in colon is also a poor prognosis marker, associated with a higher risk of metastasis[70].

Snail1-depleted fibroblasts fail to acquire myofibroblastic traits in response to TGF-β, including RhoA activation, formation of αSMA-positive fibres and increased Fibronectin fibrillogenesis. Then Snail1 is crucial for the production of a stiff ECM with oriented fibres (Figure 12). Snail1 expression in CAFs perturbs biomechanical but also biochemical homeostasis that affects tumour progression. Snail1 expressing CAFs hold a specific pro-tumour secretome inducing collective invasion of breast and colon tumour cells trough MCP-3 paracrine expression[74] and Prostaglandin E2 (PGE_2) secretion[32]. Consequently, breast cancer cells orthotopically implanted with Snail1 depleted fibroblasts originate less metastasis that those with control fibroblasts[32].

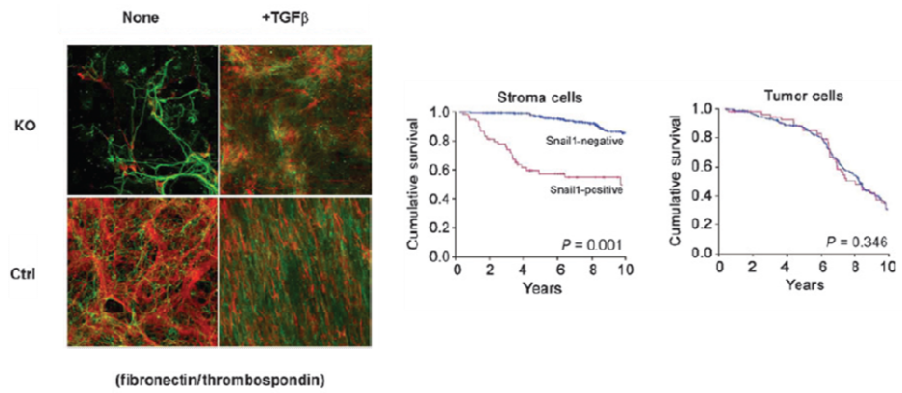

Figure 12: The role of Snail1 in CAFs. (A) TGF-β remodels the ECM generated by MEFs in a Snail1 dependent manner. Immunofluorescence against Fibronectin (green) and Thrombospondin (red). (B) Snail1-expressing fibroblasts in desmoplastic areas of breast cancer correlate with overall survival. Adapted from [69].

In fibroblasts, Snail1 is increased by TGF-β[68] but it is also induced by mechanical signals. ROCK activity indirectly stabilizes Snail1 by increasing ECM stiffness trough integrin signalling to ERK2[75] in this way tumour fibrosis can perpetuate CAFs activation in a feed-forward loop promoting cancer metastasis through regulation of Snail1.

2. PROTEIN METHYLTRANSFERASES

Protein methyltransferases (PMTs) constitute a large class of enzymes that catalyse site-specific methylation of lysine or arginine residues on histones and other proteins posttranslationally. Site-specific histone methylation is a

critical component of chromatin regulation of gene transcription. Methylation of other non-histone proteins affects many cellular processes.

PMTs facilitate the transfer of a methyl (-CH3) group to specific proteins. They share a reaction mechanism in which they use S-adenosyl-L-methionine (Adomet) as the methyl donor for the methyltransferase reaction. Two different kinds of methyltransferases are described: Lysine methyltransferases (PKMTs) and Arginine methyltransferases (PRMTs) depending on the aminoacid that accepts the methyl group.

2.1 The Protein arginine methyltransferase family (PRMTs)

Arginine methylation plays significant roles in diverse cellular processes and various diseases. In mammals this modification is as usual as phosphorylation and ubiquitination[76]. It is found on both nuclear and cytoplasmic proteins and they are involved in different processes such as epigenetic regulation of transcription, pre-mRNA splicing, DNA damage repair, RNA processing, immunologic signaling and glucose metabolism.

Protein arginine methylation is catalysed by nine members of the PRMT family of enzymes[77].They have been classified into type I (PRMT1, PRMT2, PRMT3, PRMT4, PRMT6 and

PRMT8), type II (PRMT5 and 9) and type III (PRMT7) enzymes depending on their specific catalytic activity. Type I catalyses the formation of asymmetric dimethylarginines (aDMA), type II the formation of symmetric dimethylarginines (sDMA) and type III carry out only the formation of monomethylarginine (MMA) a step that in type I and type II enzymes is only an intermediate before the establishment of aDMA or sDMA respectively (Figure 13).

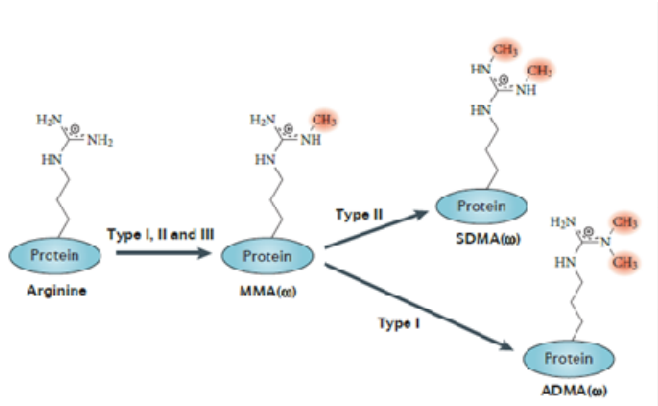

Figure 13: Types of methylation on arginine residues. Type I, II, III protein arginine methyltransferases (PRMTs)[78].

2.2 Biological roles of arginine methylation

PRMTs were first recognized to directly methylate histone substrates; posttranslational modification of histones is known to contribute to the histone code and regulates different

transcriptional states. PRMTs can deposit activating histone marks (H4R3me2a, H3R17me2a)[79,80] by PRMT1 and PRMT4 respectively or repressive (H4R3me2s)[81] by PRMT5 among others. In addition, there are other substrates that are non histones involved in mRNA-splicing, receptor trafficking, protein stability and DNA damage[82]. The arginine methylation marks are regard as very stable, an enzyme or enzymes with clear arginine demethylase activity has not yet been identified.

2.2.1 Transcriptional coactivators

PRMT1 is the main aDMA enzyme (type I). It functions as a transcriptional co-activator by dimethylating H4R3[83], this methylation recruits CBP/p300 complex potentiating the acetylation on lysine residues and favouring the binding of transcription factors[80]. PRMT1 also methylates RNA binding[84] and DNA damage proteins[82]. Interestingly, the loss of PRMT1 activity increases MMA and sDMA proteins owing to substrate scavenging by other PRMTs[85].

PRMT4/CARM1 its known for its transcription coactivator functions by methylating H3R17me2a and H3R26me2a[79] and also by directly recruiting transcription factors. PRMT4 activity is regulated by the association with CBP/p300 acetyltransferase, for example CBP acetylation of H3K13 and H3K23 is sufficient to recruit PRMT4 and methylate H3R17[86].

PRMT4 is also implicated in the regulation of pre-mRNA splicing[87].

PRMT1 and PRMT4 interact functionally with transcriptional activators such as LEF-1/TCF4[88], p53[89] and NF-κB[90]. Thus, protein arginine methylation is likely to be involved in chromatin remodelling and transcriptional regulation through a wide variety of DNA-binding transcription factors. Interestingly, PRMT1 and PRMT4 directly bind to the NF-κB subunit p65 and synergistically co-activate NF-κB-dependent gene expression together with p300/CBP and PARP1[90].

2.2.2 Transcriptional corepressors

PRMT5 is the main type II enzyme in mammals, responsible for the majority of sDMA of proteins. PRMT5 methylates H4R3me2s and acts as transcriptional co-repressor[81]. PRMT5 is also a key component of the Snail1-silencing complex repressing E-cadherin gene expression increasing H4R3me2s in the proximal E-cadherin promoter[51]. Moreover, PRMT5 also methylates non-histones proteins like small ribonucleoproteins (snRNPs) so PRMT5 deficient cells also have defects in splicing[91].

2.2.3 The role of PRMTs in non-histone proteins: mRNA splicing.

The vast majority of PRMTs substrates are associated with RNA[92]. Thus, arginine methylation has been implicated in all aspects of RNA metabolism, including mRNA transcription, splicing, transport, translation and turnover. Direct evidence for a role in splicing came from studies showing that splicing reactions could be block using sDMA- antibodies[93]. Moreover splicing is reduced in hypomethylated extracts.

PRMT4 is a transcription coactivator that impacts alternative splicing. The splicing factors CA150, SAP49, SmB and U1C are substrates of PRMT4 therefore its enzymatic activity contributes to the effects on splicing[94]. Thus, PRMT4 enzymatic activity appears to regulate both transcription and pre-mRNA splicing events. Less characterized is the implication of PRMT1 in the regulation of splicing, a recent report shows that PRMT1 regulates alternative RNA splicing through its interaction with and RNA binding protein named RBM15[84]. PRMT5 is required for the assembly of the snRNP complex to form an activated spliceosome, so the loss of symmetric arginine dimethylation by PRMT5 prevents the spliceosome activation[93].

These findings among others demonstrate that arginine dimethylation regulates the coupling of transcription and

mRNA processing and also has important functions in spliceosome assembly and activation.

2.3 The role of PRMTs in cancer and fibrosis

PRMTs tend to be upregulated in cancer, there are numerous studies showing arginine methylation deregulation in cancer. For example, PRMT1 and PRMT4 are overexpressed in breast and prostate cancers[95,96]. PRMT1 is involved in lung cancer progression and metastasis via methylation of the transcription factor Twist1[97]. PRMT4 promotes breast cancer progression and metastasis by methylating the chromatin remodeler BAF155. This methylation drives the expression of some oncogenes such as c-myc[98]. Also in breast cancer cells PRMT1 modulates EMT and senescence through transcriptional activation of Zeb1[99].

The correlation between cancer and the PRMT missregulation has been focused on their role in the epithelial cancer cells themselves, but it is not clear their function in the surrounding tumour stroma and their role in CAFs.

PRMT1 expression in the fibroblasts has been correlated with chronic pulmonary inflammation and fibrosis. Idiopathic pulmonary fibrosis (IPF) patients show increased PRMT1 levels in myofibroblasts of lung fibrotic lesions[100].

OBJECTIVES

OBJECTIVES

The transcription factor Snail1 is required for a TGF-β response in fibroblasts controlling their differentiation to myofibroblasts. However, the underlaying mechanisms that trigger this transformation still remain to be elucidated.

The main objective of this thesis was thus to find new Snail1-dependent molecular events governing myofibroblast differentiation and to study their role in the context of wound healing, cancer progression and fibrosis. To achieve this aim we focused on two specific objectives:

1. Find Snail1-coactivators necessary for the mesenchymal gene upregulation upon TGF-β.

2. Study their contribution in wound healing, cancer progression and fibrosis by targeting its activity.

RESULTS

RESULTS

1. CHARACTERIZATION OF THE CO-ACTIVATOR COMPLEX INVOLVING PRMT1, PRMT4 AND SNAIL1 IN THE *FN1* PROMOTER

The initial objective of this thesis was to further characterize the molecular mechanism by which Snail1 directs fibroblast activation. It was previously described in our group that upon TGF-β treatment nuclear Snail1 interacts with p65-NF-κB and PARP1 and that this complex enhances the transcription of different ECM genes such as Fibronectin[53]. Previous studies in mouse embryonic fibroblasts (MEFs)[90] have reported that p65-NF-κB interacts also with PRMT1 and PRMT4 (CARM1), two transcriptional coactivators that respectively methylate H4R3 and H3R17.

1.1 PRMT1 and PRMT4 protein levels and activities are increased by TGF-β in a Snail1-dependent manner

The protein levels of PRMT1 and PRMT4 were analysed by Western blot upon activation of MEFs with TGF-β. Accumulation of both enzymes was detected after 1 hour of treatment (Figure 14a) and led to an increase in the levels of the asymmetric arginine dimethylation of a set of proteins (Figure 14b). The levels of methylation were assessed with

an H3R17me2a antibody that recognize asymmetric dimethylation in arginine residues in many other proteins[101].

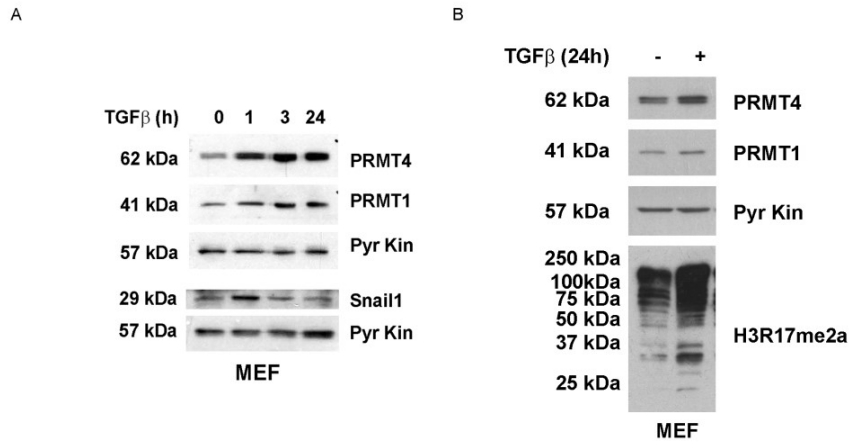

Figure 14: TGF-β increase PRMT1 and PRMT4 protein levels. (A) and (B) MEFs treated with 5ng/ml of TGFβ for the indicated times were lysed with SDS buffer and levels of the indicated proteins were analysed by western blot.

To test if this increase was related to the action of Snail1 we down-regulated Snail1 levels in MEFs treated with TGF-β with a specific siRNA. The siSnail1 decreased the protein levels of both PRMTs (Figure 15a) and, as expected, the degree of asymmetrical dimethylation in arginines (Figure 15b). This reduction in methylation was confident as it was detected by Western blot using two different antibodies, Asym24 and anti-H3R17me2a, obtained from different dimethylated epitopes and that recognize different sets of asymmetrically dimethylated proteins.

The degree of symmetric dimethylation in arginine residues in proteins was assessed with the specific antibody Sym10 (Figure 15b). This mark is manly left by PRMT5 and it was barely altered by the siSnail1, suggesting that Snail1 specifically modulate dimethylation in arginine residues by enzymes such as PRMT1 and PRMT4 that incorporate the methyl groups asymmetrically.

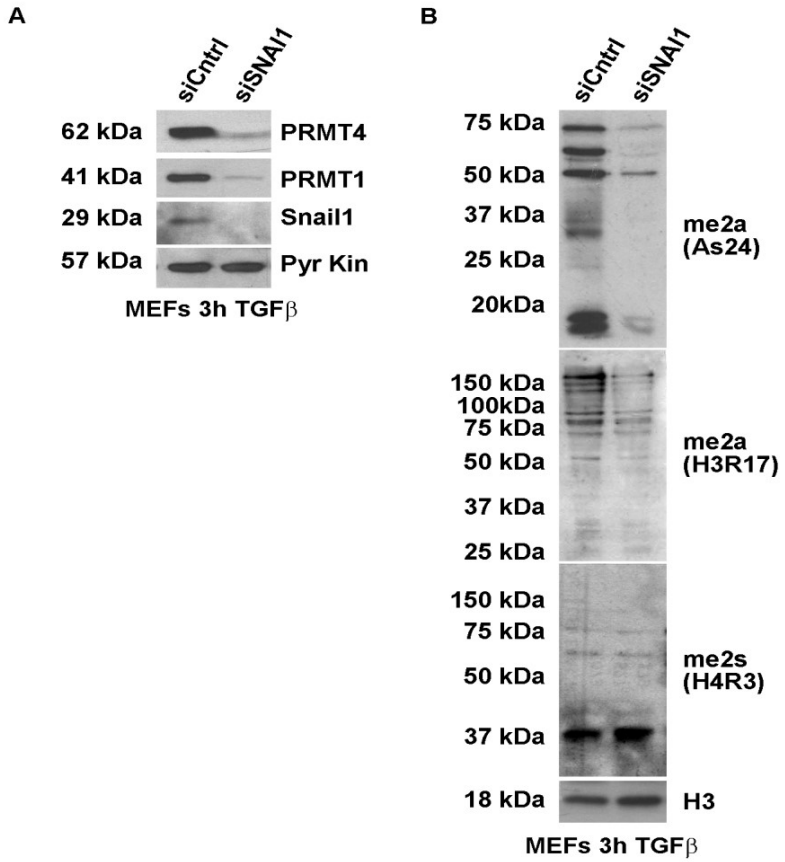

Figure 15: Downregulation of Snail1 in MEFs reduces PRMT1 and 4 protein levels and asymmetric arginine dimethylation of proteins. (A) and (B) MEFs transfected with siRNA Control or Snail1 were treated three hours with TGF-β, lysed with SDS buffer and levels of the indicated proteins were analysed by Western blot.

Similar results were obtained in another fibroblastic cell line. 1BR3G adult human fibroblasts also showed a decrease in the proteins levels of PRMT1 and PRMT4 (Figure 16a) when transfected with siSnail, and the asymmetric marks were also reduced compared with control cells (Figure 16b). Symmetric mark were unaffected corroborating that the effects of TGF-β/Snail1 on arginine methylation are mediated by the increase of PRMT1 and PRMT4 and maybe of other active PRMT catalising asymmetric dimethylation (Figure 16b).

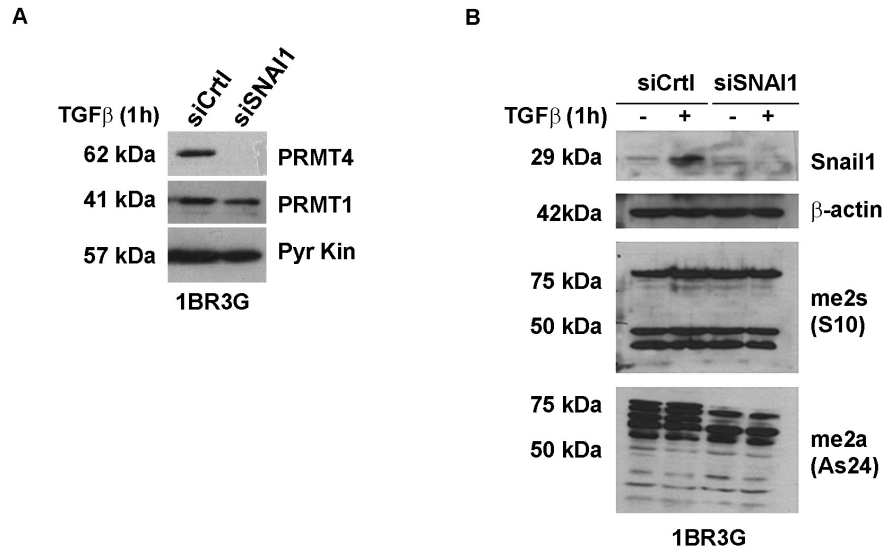

Figure 16: Downregulation of Snail 1 in 1BR3G cell line reduces PRMT1 and 4 protein levels and asymmetric arginine dimethylation of proteins. (A) Adult 1BR3G human fibroblasts were transfected with siRNA Control or Snail1 and were treated for one hour with TGF-β, lysed with SDS lysis buffer and levels of the indicated proteins were analysed by Western blot. (B) 1BR3G fibroblasts transfected with siRNA control or for Snail1 were left untreated or treated one hour with TGF-β, lysed with SDS buffer and the indicated proteins were analysed by Western blot.

1.2 RNA levels of PRMT1 and PRMT4 are mostly insensitive to TGF-β/Snail1 signalling

To check if the decrease in the protein levels of PRMT1 and PRMT4 were due to a transcriptional regulation by Snail1 the levels of RNA of both enzymes were analysed by RT-qPCR in MEFs transfected with siControl or siSnail and treated or not with TGF-β for three hours. Contrasting with the increase in Snail1 RNA levels, PRMT1 and PRMT4 levels were not substantially induced by TGF-β (Figure 17) and were not significantly reduced upon Snail1 downregulation. Therefore, additional posttranscriptional mechanisms are involved in controlling the Snail1-dependent protein downregulation of both enzymes.

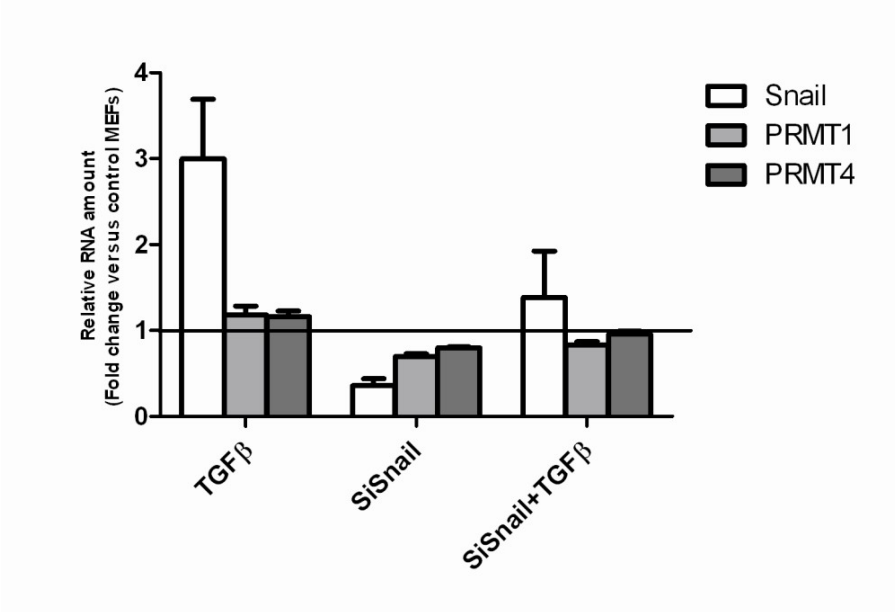

Figure 17: TGF-β does not substantially induce PRMT1 and PRMT4 at RNA levels. RNA from MEFs transfected with Sicontrol or SiSnail1 and treated or not with TGF-β for 3h were analysed by RT-qPCR with specific oligonucleotides for the indicated genes.

1.3 PRMT1 and PRMT4 interact with Snail1 in TGFβ-activated fibroblasts

We reasoned that in TGF-β treated fibroblasts both enzymes could localize into a protein complex with Snail1 and we analysed by co-immunoprecipitation this possibility. Both, PRMT1 and PRMT4 were detected in the immunoprecipitates obtained with anti-Snail1 from RIPA extracts of MEFs treated with TGF-β (Figure 18a). Co-immunoprecipitation of Snail1 and PRMT4 was also achieved using the antibody against PRMT1 (Figure 18b).

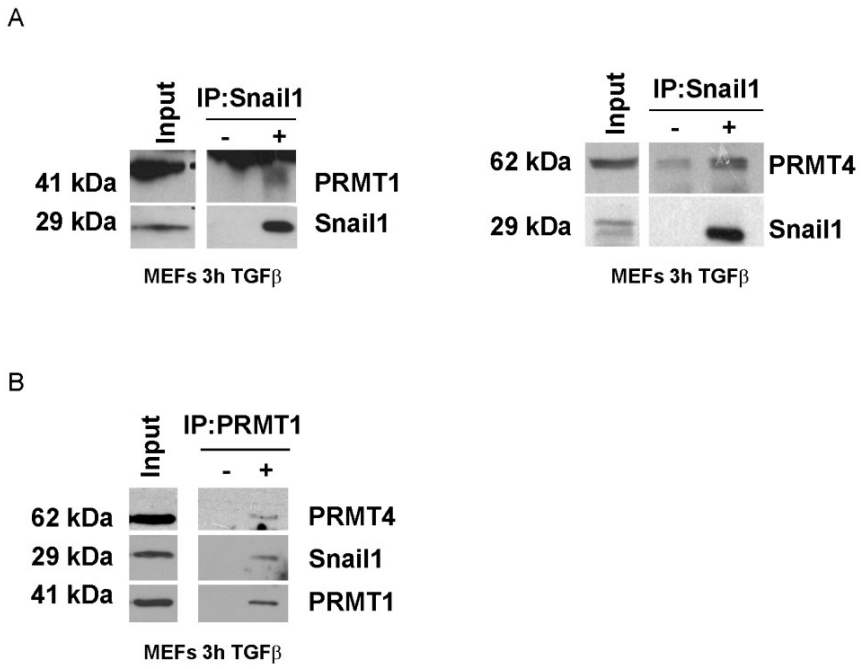

Figure 18: Snail1, PRMT1 and PRMT4 co-immunoprecipitate. Immunoprecipitation was performed from whole cell extracts of MEFs treated 3 hours with TGF-β. (A) Snail1 was immunoprecipitated with a Snail1 antibody. (B) PRMT1 was immunoprecipitated with a PRMT1 antibody.

To confirm that these three proteins coincided in the nuclear compartment we performed immunofluorescence in MEFs treated or not with TGF-β. We could detect both PRMT1 and PRMT4 co-localizing with Snail1 in nuclei especially in TGF-β treated cells (Figure 19).

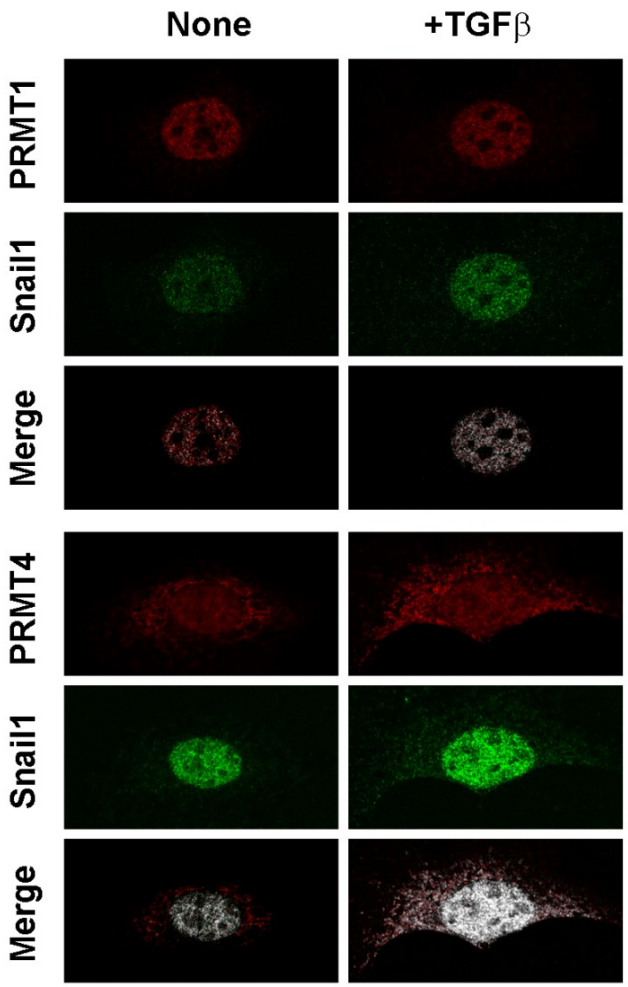

Figure 19: Snail1, PRMT 1 and PRMT4 co-localize in the nucleus of MEFs. MEFs were grown on glass coverslips and fixed with 4% PFA. Snail1, PRMT1 or PRMT4 were analysed by immunofluorescence with specific antibodies and Alexa 488 and 555 conjugated secondary antibodies. White signal in merge corresponds to co-localization calculated with the confocal microscope.

1.4 PRMT1 and PRMT4 interact and methylate the proximal Fibronectin promoter in a Snail1-dependent manner

Given that PRMT1 and PRMT4 interact with Snail1 and catalise the incorporation of activating methylation marks on histones (H3R17me2a and H4R3me2a, respectively), we tested if these PRMTs have a role in the TGFβ/Snail1/p65 dependent transcription of Fibronectin. We performed a ChIP assay to check if PRMT1 and PRMT4 bind to the proximal *FN1* promoter as decribed for Snail1, PARP1 and p65-NF-κB[53] and found that PRMT1 and PRMT4 binding to the proximal Fibronectin promoter was induced by TGF-β treatment. The binding of both PRMTs was associated with an increase of their respective histone marks, H4R3me2a and H3R17me2a in this promoter area detected also by ChIP. Remarkably, both increased events, PRMT binding and me2a levels, were Snail1 dependent, as they were undetected in Snail KO MEFs (Figure 20).

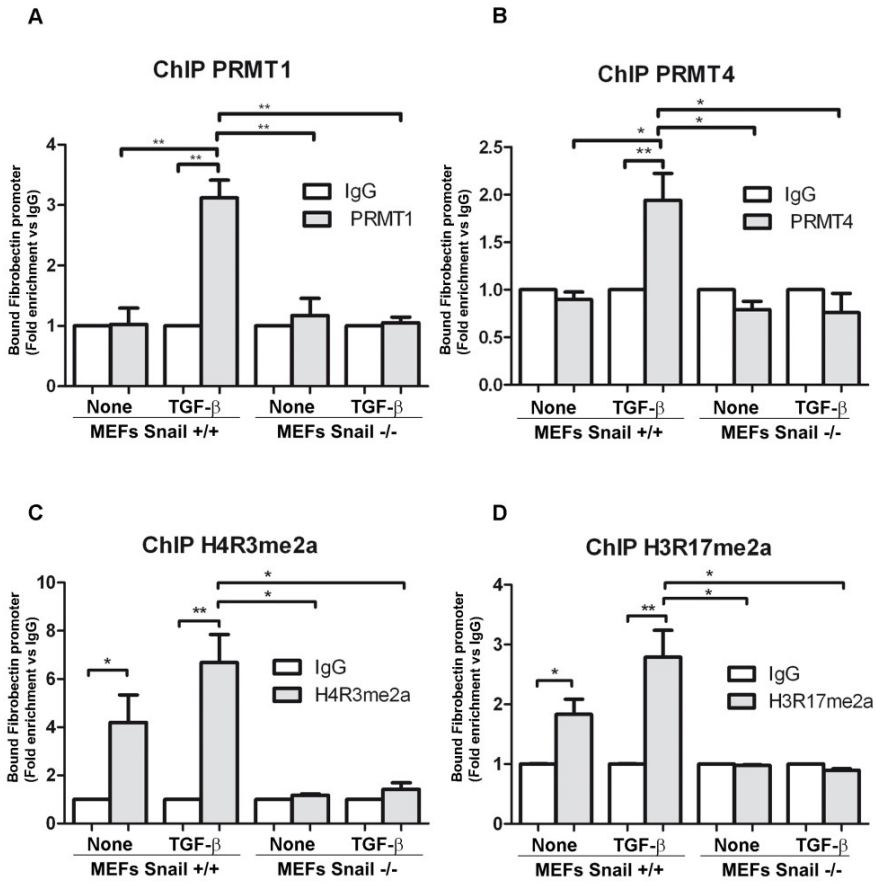

Figure 20: PRMT1 and 4 bind to the proximal FN1 promoter in a TGF-β and Snail1 dependent manner. ChIP in MEFs WT or KO for Snail1 treated or not with 3h of TGF-β. The FN1 promoter (+116/+265) from the immunoprecipitates of the indicated antibodies (A) PRMT1 (B) PRMT4 (C) H4R3me2a (D) H3R17me2a and assay inputs were analysed by qPCR. Bars show FN1 promoter enrichment for each specific antibody relative to an unspecific rabbit IgG. p-value <0.05 (*), p-value<0.01 (**).

Altogether our data indicates that in TGF-β activated fibroblasts Snail1 interacts with PRMT1 and PRMT4 favouring its stabilization and binding to the proximal *FN1* promoter and

the subsequent arginine asymmetrical dimethylation of Arg17 at H3 and Arg3 at H4.

2.SNAIL1 AFFECTS SPLICING OF CYTOSKELETON AND ECM GENES

One of the issues that emerged from the previous findings was the existence of a set of proteins in activated fibroblasts whose arginine methylation depends on Snail1 (Figure 15b). In an attempt to decipher which are these proteins, immunoprecipitates obtained with the Asym24 antibody (recognizes a wide spectrum of asymmetrically dimethylated arginine residues) were analysed by Mass spectrometry. Protein extracts from siControl and siSnail1 transfected MEFs treated 3 hours with TGF-β were used. From the list of around 500 proteins detected, over 60% were previously described as components of the arginine methylome[102,103] and over 30% were increased more than 1.5 fold in the siControl versus the siSnail1; therefore, they were considered as putative Snail1-dependent methylated proteins. A Gene ontology (GO) biological process analysis of these selected proteins showed and enrichment in proteins related to mRNA processing and splicing (Figure 21). Reinforcing this results, functional annotation clustering of the same data showed that RNA-binding, mRNA processing and splicing related proteins as the first significant cluster with an 8.81 enrichment score (data not shown), suggesting that Snail1 may play a role in

the regulation of splicing via methylation of different proteins important for the splicing machinery.

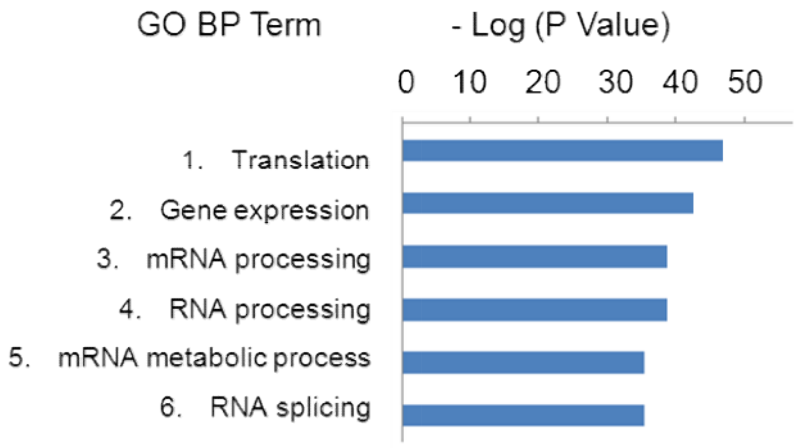

Figure 21: Snail1 down-regulation affected the methylation of proteins related to mRNA processing and splicing. GO biological process (BP) term classification of the first 6 positions from the mass spectrometry list of arginine methylated proteins upregulated in the siControl respect the siSnail condition in TGF-β treated MEFs.

To support the idea that Snail1 plays a role on splicing, we seek for proteins that might interact with Snail1 during the initiation of the fibroblasts activation. Therefore, immunoprecipitates of Snail1 or control Antibody (IgG) from MEFs treated 3 hours with TGF-β were analysed by mass spectrometry and a list of 254 candidates was obtained. Gene ontology biological process analysis of the proteins with a 1.5 fold change in the Snail1 IP versus the IgG also showed an enrichment of proteins related with splicing (Figure 22).

Figure 22: Snail1 immunoprecipitation in TGF-β treated MEFs was highly enriched in proteins related to Splicing and RNA processing. GO biological process (BP) analysis of the first four items of the proteomic data of proteins with more than 1.5 fold change increase versus mouse IgG. Immunoprecipitation was performed from whole cell extracts of MEFs treated 3 hours with TGF-β.

Therefore, we decided to elucidate if Snail1 had a role in splicing by sequencing mRNAs from MEFs wild-type and Snail1 KO treated 3 hours with TGF-β to detect differential splicing events. For these analyses the number of RNA reads per sample was increased until a minimum of $8x10^7$. The RNA-seq data was analysed in collaboration with Dr. Juan Valcarcel laboratory from CRG. The SANJUAN pipeline generated by this laboratory revealed 299 different alternative spicing events in WT respect Snail1 KO MEFs. Among the genes affected a cluster of genes related with actin cytoskeleton or ECM genes were detected, according to GO molecular functional analysis (Figure 23a, experiments performed together with Maria Val and included in her master thesis).

We found Snail1 dependent alternative splicing in ECM genes such as *FN1* and *Col5α1,* and actin cytoskeleton ones like *Myl6, AnIn, Macf1, Tpm2, PP1R12A, FlnC* and *Flnb*.

To validate the alternative splicing of the genes we designed specific oligonucleotide primers covering these splicing events and visualised the RNA isoforms by semi-quantitative RT-PCR in MEFs WT or Snail KO treated or not for 3 hours with TGF-β.

We observed that the inclusion of the exon 33 of the *FN1* gene (Fibronectin) was Snail1 and TGF-β dependent (Figure 23b). TGF-β treatment promoted the inclusion while depletion of Snail1 reduced it. The splicing event in the exon 4 of the *Myl6* gene (Myosin Light Chain 6) was Snail1 dependent but TGF-β independent. Exon 4 is included in a higher proportion in Snail1 depleted cells regardless of TGF-β treatment.

This data indicate that, indeed, Snail1 may play a new molecular regulation during fibroblast activation consisting in a rapid modulation of the alternative splicing of myofibroblastic related genes (such those codifying cytoskeleton or ECM regulatory proteins) probably by regulating the methylation of splicing regulatory proteins. Therefore, we are currently validating some of the candidates that appeared in the mass spectrometry lists and trying to understand the mechanisms and the biological relevance of these Snail1 dependent alternative splicing events.

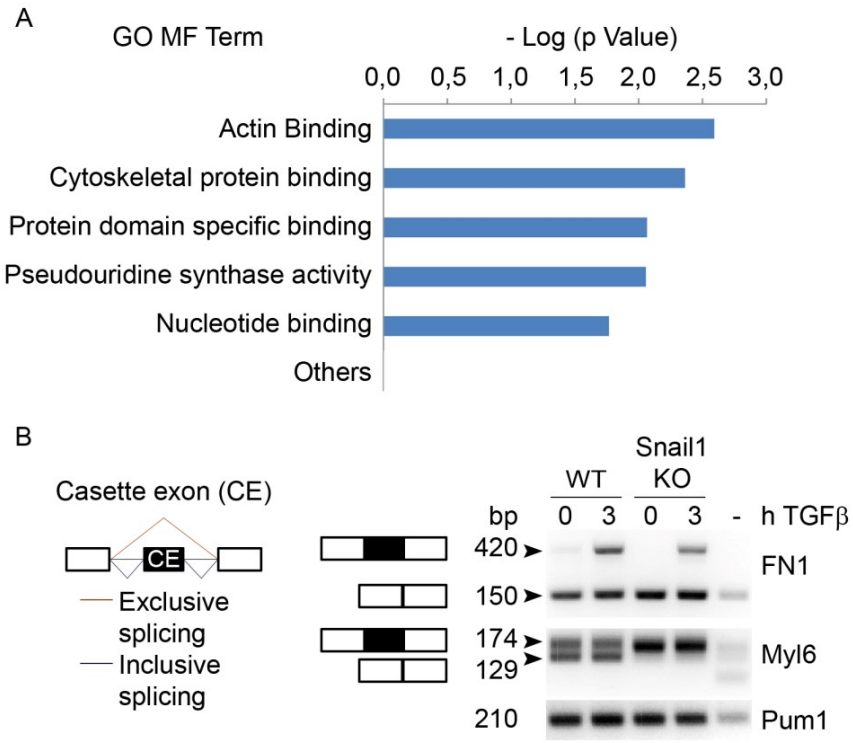

Figure 23: Snail1 dependent splicing of cytoskeleton and ECM genes. (A) GO Molecular Function (MF) term classification of the first 5 terms from RNA sequencing of WT and Snail1 KO MEFs at 3h of TGFβ. (B) Left, schematic representation of cassette exon events. Right, RNAs from WT and Snail1 KO MEFs treated with TGFβ for 3h and without treatment (0h) were retro-transcribed and amplified with specific primers for FN1 and Myl6. Samples were run on a 2% agarose gel and the molecular weight of the amplicon with exon inclusion and with exon exclusion is noted. The fifth lane corresponds to a reaction with no RNA as a test for contamination. Pumilio was used as an amplification and loading control. The image corresponds to one representative experiment of three performed.

3. METHYLTRANSFERASES SUSTAIN FIBROBLAST ACTIVATION SUPPORTING FIBROSIS AND METASTASES

3.1 Inhibition of PRMTs with commercial inhibitors interferes with fibroblast activation in cell culture.

Given the presence of both PRMTs and their histone activating marks in the *FN1* promoter we decided to block the activity of these enzymes with inhibitors and check if they interfere with fibroblast activation by TGF-β. We tested three available commercial inhibitors, AMI-1, Sinefungin and MTA.

PRMTs are a family of methyltransferases that monomethylate or dimethylate the guanidine nitrogen atoms of arginine chains. Strong competitive inhibitors of the methyldonor S-adenosyl-L-methionine (Adomet) such as Sinefungin and Methylthioadenosine (MTA) are usually used to block PRMTs activity. Most methyltransferases and not only PRMTs use AdoMet as a methyldonor. Therefore, Sinefungin and MTA are global inhibitors of methyltransferases.

At the moment to start our research AMI-1 was the most specific commercial PRMT inhibitor. AMI-1 is not a methyldonor competitive inhibitor; it binds the substrate-binding pocket of the enzymes, inhibiting arginine, but not

lysine, methyltransferase activity. Among PRMTs, AMI-1 has more affinity inhibiting PRMT1 and PRMT4[104].

3.1.1 AMI-1 and Sinefungin are non-toxic on MEFs

We first checked if these three molecules were toxic on MEFs by means of cell growth assays (Figure 24). Whereas AMI-1 and Sinefungin did not modify control cell growth, MTA reduced it significantly and was discarded for the following experiments.

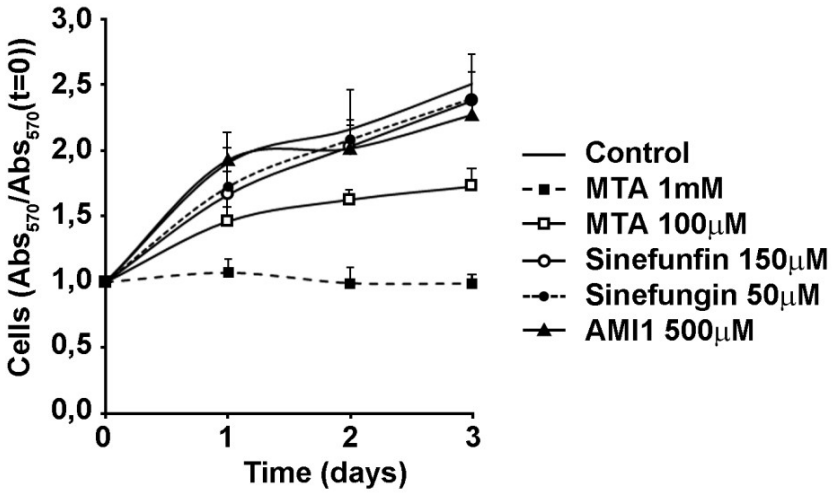

Figure 24: **AMI-1 and Sinefungin are not toxic for MEFs.** MEFs plated in 96 well plates were grown in the presence of the indicated inhibitors and concentrations. Number of cells at 1, 2 or 3 days was estimated with a MTT assay. Each point was measured in quintuplicates.

3.1.2 AMI-1 and Sinefungin prevent the acquisition of myofibroblast markers.

As mentioned in the intoduction, α-SMA is considered a key marker for activated fibroblasts, as the incorporation of this actin isoform into stress fibres empower fibroblasts with the contractibility necessary to remodel the ECM. In vehicle treated MEFs, protein levels of αSMA as well as Fibronectin detected by Western blot were upregulated at 24 hours of TGF-β treatment; however, in AMI-1 or Sinefungin pretreated MEFs this upregulation was prevented (Figure 25).

In contrast, protein levels of Snail1 that pick earlier during the TGF-β treatment were not affected (Figure 25), suggesting that inhibitors target regulatory methylation events downstream of Snail1.

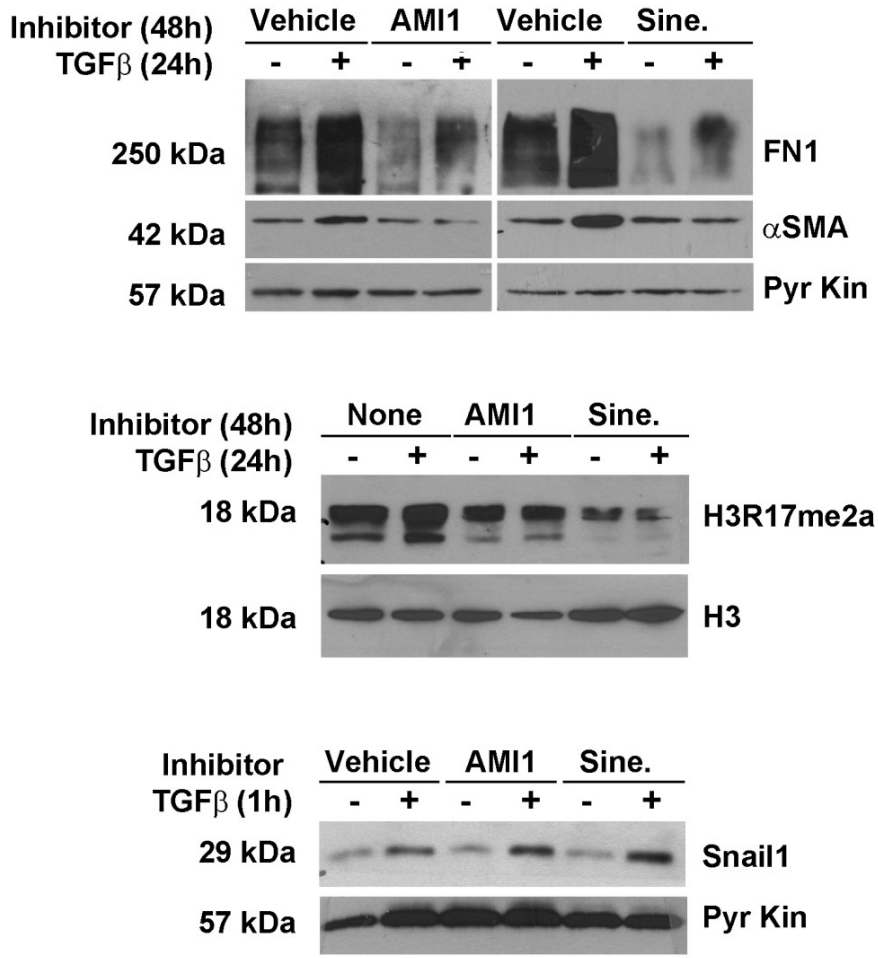

Figure 25: AMI-1 and Sinefungin inhibits TGF-β induced Fibronectin and αSMA expression in MEFs. Parental MEFs were pretreated with none or inhibitors for 24h and then grown 1 or 24h extra hours in the presence of TGF-β. Cells were lysed with SDS buffer and levels of the indicated proteins were analysed by Western blot.

3.1.3 AMI-1 and Sinefungin prevent fibronectin fibrillogenesis by TGF-β.

Activated fibroblasts bear higher ability to polymerize extracellular fibronectin than current fibroblasts. Fibronectin fibrillogenesis was estimated as the amount of extracellular offered Fibronectin cleared by MEFs. Thus, MEFs were plated on Fibronectin coated glass cover slips in the presence or absence of the inhibitors (AMI-1 or Sinefungin) for 24 hours and then cells were fixed with 4% PFA to visualize Fibronectin by immunofluorencese. As reported[69], TGFβ treatment duplicated the capacity of WT MEFs to polymerize extracellular fibronectin monomers (measured as cleared fibronectin areas over the background staining); however, this increase was not detected in the presence of the methyltransferase inhibitors (Figure 26).

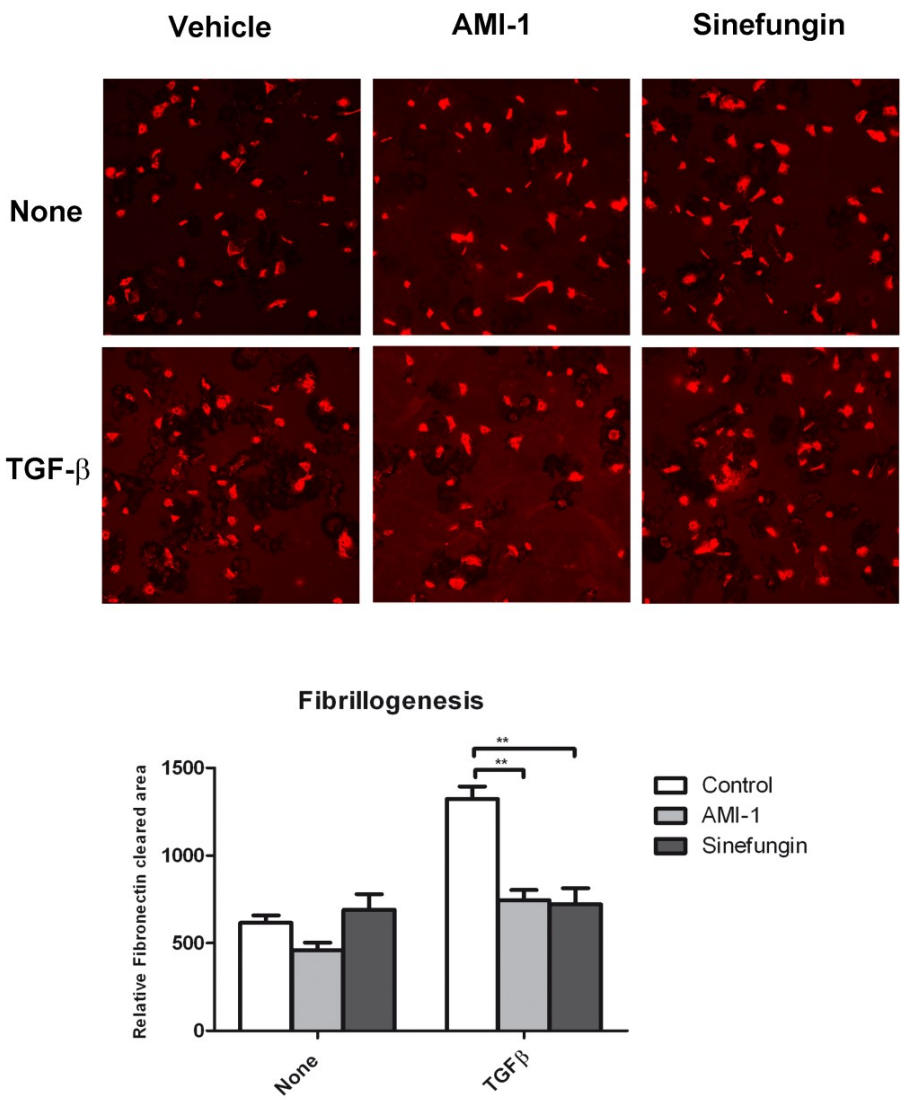

Figure 26: Fibronectin fibrillogenesis by TGF-β was blocked by the PRMTs inhibitors AMI-1 and Sinefungin. MEFs were cultured on fibronectin-coated coverslips for 24h and treated when indicated with TGF-β and inhibitors of PRMTs. Fibronectin was visualized by immunofluorescence (200x). Fibrillogenesis estimation (bars) was quantified as the surface with an intensity value lower that a background threshold. Bars represent the mean from at least six different fields. p-value <0.05 (*), p-value<0.01 (**)

3.1.4 AMI-1 and Sinefungin prevent the formation of organized three-dimensional extracellular matrices by TGF-β.

To further analyse the effect of the inhibitors, we tested if they interfere with the generation of a myofibroblast extracellular architecture. Thus, we allow fibroblasts to generate *in vivo* like three-dimensional extracellular matrices (3D-ECM) following a previously described protocol[105] and challenge their performance with the inhibitors.

Fibroblast alignment into the 3D-ECMs was estimated by measuring the angle of the nuclei and generating distribution histograms (Figure 27a). As previously described[69], fibroblasts in the presence of TGF-β generated matrices with an anisotropic organization: their nuclei became elongated and over 75% shared orientation. Not just nuclei but also the extracellular Fibronectin fibres aligned in the same direction. In untreated MEFs no preferred orientation was observed, over 30% of the fibroblasts oriented in the same direction, corresponding to stochastic orientation.

TGF-β-induced nuclei orientation and Fibronectin fibre alignment into 3D-ECMs were abrogated in the presence of AMI-1 and Sinefungin (Figure 27a). As a control, we also treated cells with a potent antioxidant, Tempol, given that AMI-1 has been described to have antioxidant capacity[106] and no effect was detected (Figure 27b).

We extended our observations in mesenchymal stem cells (MSCs), another population of mesenchymal cells that are activated by TGF-β in a Snail1-dependent fashion[69]. Both inhibitors potently prevent the capacity of TGF-β-activated cells to remodel the extracellular architecture (Figure 28).

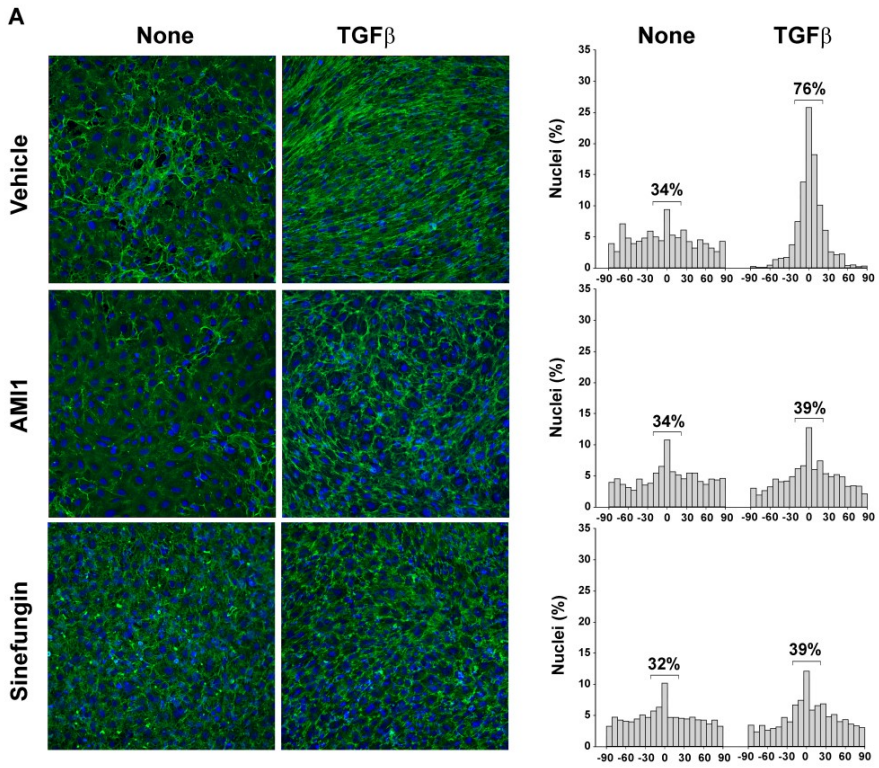

B

MEF Treatment	Alignment (%) None	Alignment (%) TGFβ
Tempol (2mM)	32	76

Figure 27: AMI-1 and Sinefungin prevent the TGF-β dependent alignment of MEFs derived *in vivo* like extracellular matrices. (A) MEFs were seeded on coversplips and allowed to produce extracellular matrix for 10 days. Cells were treated with TGFβ (5ng/mL), AMI-1 (500μM) or Sinefungin (150μM) were indicated. Cells were then fixed with 4% PFA and analysed by IF with anti-fibronectin (green) and DAPI. The nuclei orientation angles were calculated (Image J) from microscope images at 200x and plotted as a frequency distribution centred in the most frequent angle, set as 0˚. (B) Effect of Tempol (2mM). Percentages of the oriented nuclei were represented in the table.

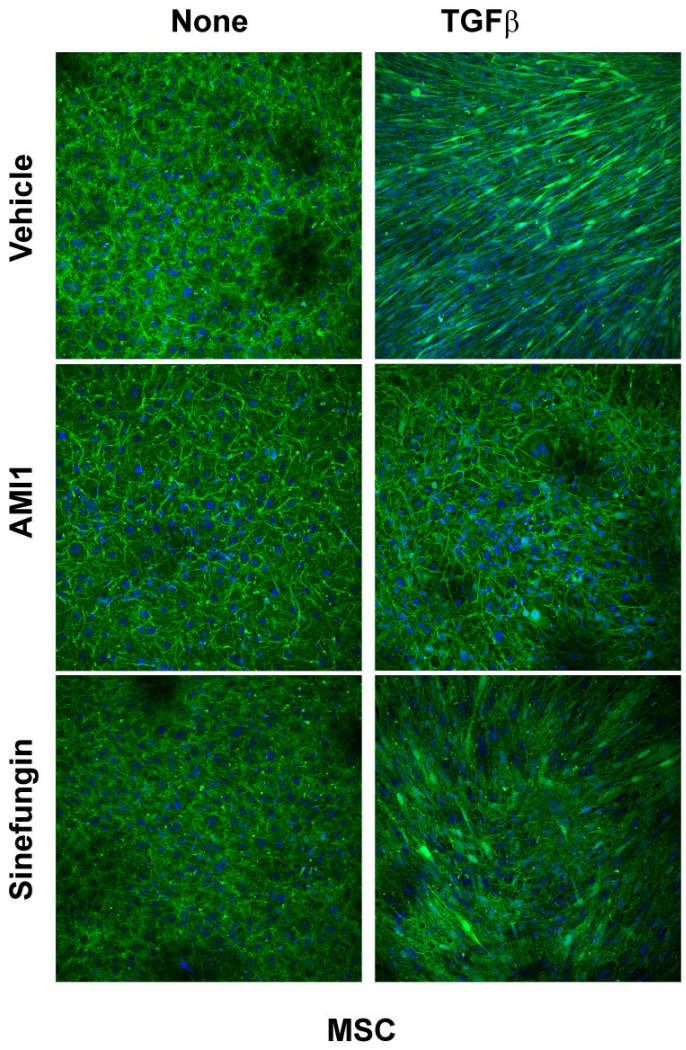

Figure 28: AMI-1 and Sinefungin prevent the TGF-β dependent alignment of MSCs derived *in vivo* like extracellular matrices. Mesenchymal stem cells were seeded on coversplips and allowed to produce extracellular matrix for 10 days. Cells were treated with TGFβ (5ng/mL), AMI-1 (500μM) or Sinefungin (150μM) were indicated. Cells were then fixed with 4% PFA and analysed by IF with anti-fibronectin (green) and DAPI.

3.1.5 The PRMT5 inhibitor EPZ015666 is inefficient in blocking the formation of organized three-dimensional extracellular matrices.

PRMT5 methyltransferase is involved in symmetric arginine dimethylation of proteins, and we found that this kind of methylation was not dependent of Snail1 in MEFs (Figure 15b) or 1BR3G fibroblasts (Figure 16b). To confirm that the activity of this enzyme is irrelevant in fibroblast activation we tested the ability of the inhibitor EPZ015666 that is highly specific for PRMT5 to interfere with the generation of a myofibroblast extracellular architecture. For this propose, *in vivo* like 3D-ECMs were produced in the presence of the inhibitor. No differences with the vehicle-treated condition were observed (Figure 29) reinforcing the idea that PRMT5 activity is not involved in fibroblast activation.

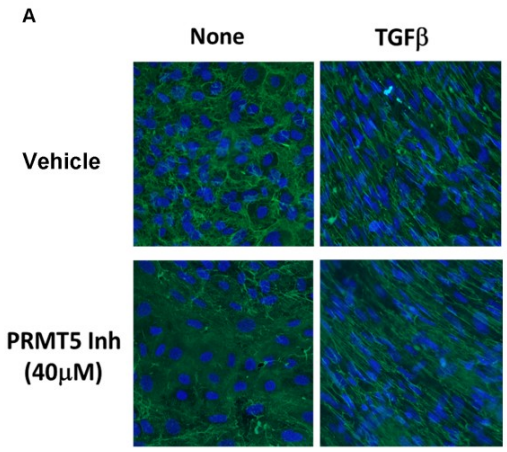

B

		Alignment (Percentage , 5 bars)	
		Control	TGFβ
Vehicle		33,8	75,5
Inh PRMT5 EPZ015666 (GSK3235025)	5uM	32,7	75,8
	10uM	30,0	75,3
	20uM	31,3	70,4
	40uM	33,0	74,1

Figure 29: PRMT5 specific inhibitor does not reduce the alignment of the *in vivo* like extracellular matrices. (A) MEFs were seeded on coversplips and allowed to produce extracellular matrix for 10 days. Cells were treated with TGF-β (5ng/mL) were indicated and the PRMT5 inhibitor at the indicated doses. Cells were then fixed with 4% PFA and analysed by IF with anti-fibronectin (green) and DAPI. The nuclei orientation angles were calculated (Image J) from microscope images at 200x. (B) Percentage of the oriented nuclei was represented.

3.2 PRMT1 and PRMT4 KO MEFs partially recapitulate the effect of the PRMTs inhibitors

Since methyltransferase inhibitors interfere with myofibroblast activity we tested if depletion of PRMT1 and PRMT4 in MEFs using CRISPR/Cas9 technology suffices to recapitulate the effect of the inhibitors.

3.2.1 Simultaneous PRMT1 and PRMT4 depletion barely prevents myofibroblastic markers increase by TGF-β.

We did not succeed producing the PRMT1 single KO accordingly with a previous report indicating that its depletion compromise cell viability[85].

We then took advantage of previously reported inducible cell line[85] that allows maintaining viable PRMT1 KO MEFs for short periods of time. Depletion of PRMT1 blocked αSMA and Fibronectin expression at some extension (Figure 30).

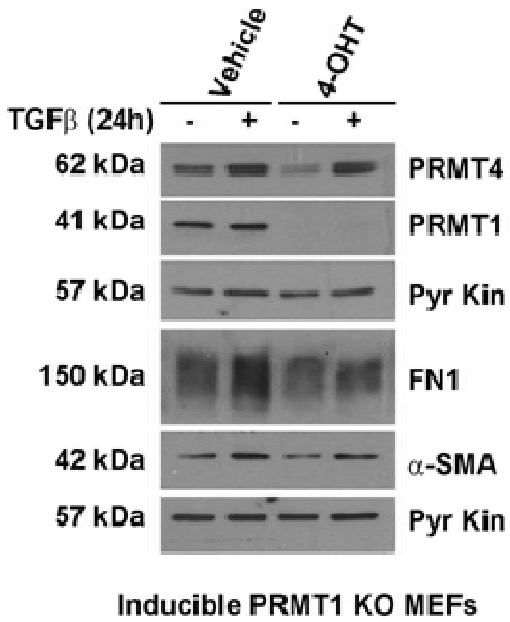

Figure 30: Depletion of PRMT1 affected Fibronectin and αSMA protein levels. Tamoxifen-inducible PRMT1$^{flox/del}$ ER-CRE MEFs treated with 500nM OHT or vehicle during 3 days and with TGF-β when indicated were lysed with SDS lysis buffer and the levels of the indicated proteins were analysed by western blot.

Viable MEFs PRMT4 KO clones were obtained using CRISPR/cas9 technology indicating that PRMT4 activity acts on different cell viability targets than PRMT1.

PRMT4 KO MEFs displayed normal Fibronectin and αSMA induction by TGF-β, indicating that PRMT4 alone does not recapitulate full fibroblast activation (Figure 31a). The levels of its histone mark, H3R17me2a were also assessed by Western blot and the methylation mark was totally abolished in the PRMT4 KO.

Viable PRMT1/4 KO MEFs clones were also obtained (Figure 31b), what was somewhat surprising taking into account that PRMT1 KO was not viable. A possible explanation is that PRMT4 have a negative role in cell survival and its absence in the double KO allows the survival of the cell. Then PRMT1 would have a dominant role against PRMT4 counteracting its effects in wild-type cells.

We confirmed by Western blot that both PRMT1 and PRMT4 histone marks, H4R3me2a and H3R17me2a were respectively downregulated in the double KO clones (Figure 31b) and then we analysed the myofibroblastic markers. A change in the Fibronectin molecular weight was observed in TGF-β treated PRMT1/4 KO MEFs (Figure 31b), suggesting that posttranscriptional or alternative splicing events on fibronectin require of simultaneous PRMT1 and PRMT4 activities. αSMA and Snail1 protein levels were upregulated as usual with TGF-β in the KO MEFs.

Overall these results indicate that PRMT1 and PRMT4 activities modulate myofibroblastic markers in a different and no additive way.

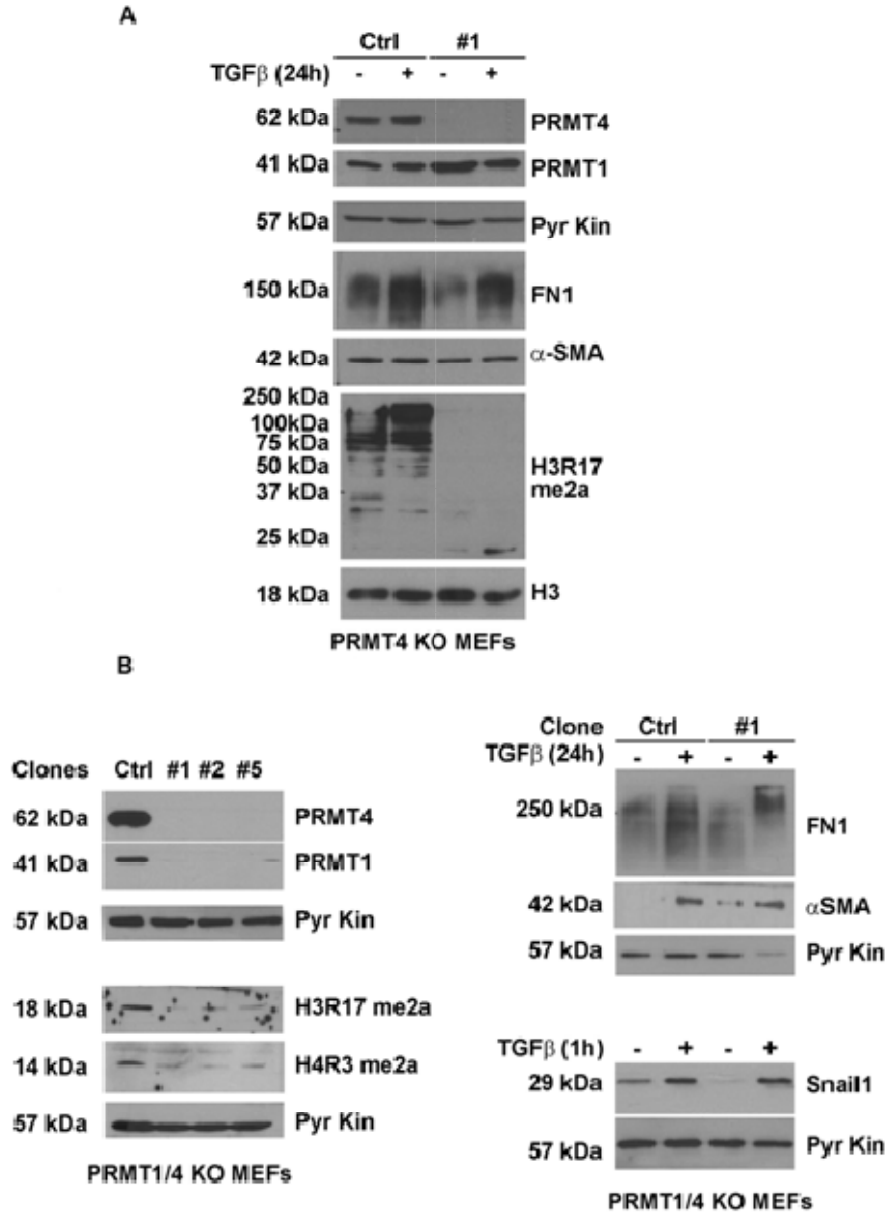

Figure 31: **Protein expression in PRMT4 and PRMT1/4 KO MEFs.** (A) Depletion of PRMT4 did not affect FN1 and αSMA levels. WT or PRMT4 KO MEFS treated or not with TGF-β for 24 hours were lysed with SDS buffer and levels of indicated proteins were analysed by Western blot. (B) PRMT1 and 4 depletion interfere with Fibronectin. WT or PRMT1 and 4 KO MEFs were treated with 1 hour or 24 hours of TGF-β when indicated. MEFs were lysed with SDS buffer and levels of the indicated proteins were analysed by Western blot.

3.2.2 Simultaneous PRMT1 and PRMT4 depletion prevents Fibronectin fibrillogenesis increase by TGF-β.

The capacity to polymerize soluble Fibronectin was also evaluated. As we detected in WT MEFs treated with inhibitors (Figure 26), the fibrillogenesis assay showed that in MEFs PRMT1/4 KO TGF-β also fails to increase the polymerization capacity (Figure 32), indicating that PRMT1 and PRMT4 activities are required for the activation of Fibronectin fibrillogenesis by TGF-β.

Because TGF-β treatment in PRMT1/4 KO MEFs did not increase the fibrillogenesis capacity but still increased αSMA levels, it is likely that PRMT1/4 activities target fibrillogenesis by their action on the Fibronectin molecular weight (Figure 31b).

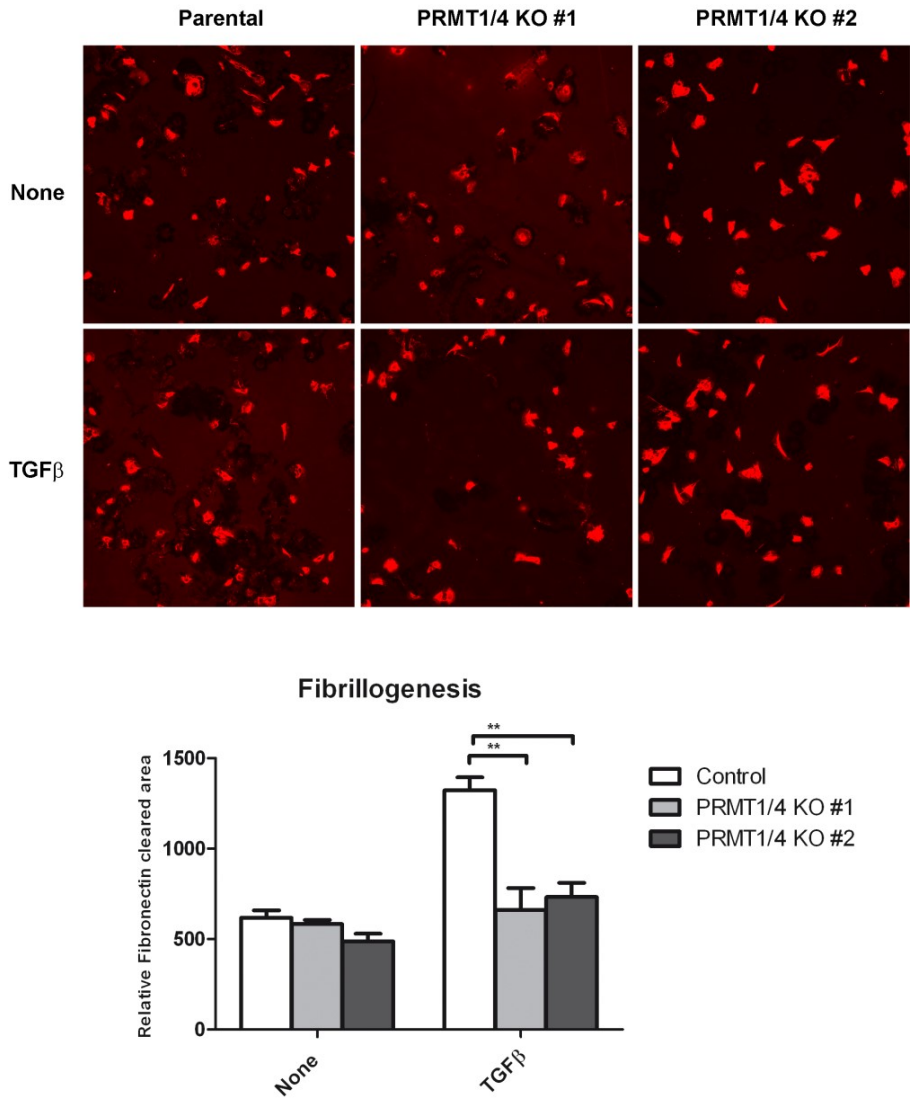

Figure 32: Fibronectin fibrillogenesis by TGF-β was blocked in PRMT1/4 KO clones. MEFs were cultured on fibronectin-coated coverslips for 24h and treated were indicated with TGF-β. Fibronectin was visualized by immunofluorescence (200x). Fibrillogenesis estimation (bars) was quantified as the surface with an intensity value lower that a background threshold. Bars represent the mean from at least six different fields. p-value <0.05 (*), p-value<0.01 (**)

3.2.3 Simultaneous PRMT1 and PRMT4 depletion partially blocks *in vivo* like 3D ECM remodelling by TGF-β.

We also analysed the 3D-ECM produced by these fibroblasts (Figure 33). As shown above (Figure 27), 3D-ECMs produced by TGF-β activated fibroblasts acquire an anisotropic organization with more than 70% of the nuclei oriented in the same direction, while untreated MEFs remained unaligned. Upon TGF-β stimulus 3D-ECMs produced by PRMT4 KO or PRMT1/4 KO MEFs acquired lower orientation (over 50%) compared with parental MEFs.

The different capacity of PRMT KO MEFs and the inhibitors to generate aligned 3D-ECM indicates that other methyltransferases inhibited by AMI-1 and Sinefungin are also required for a complete myofibroblastic activity on the ECM.

A

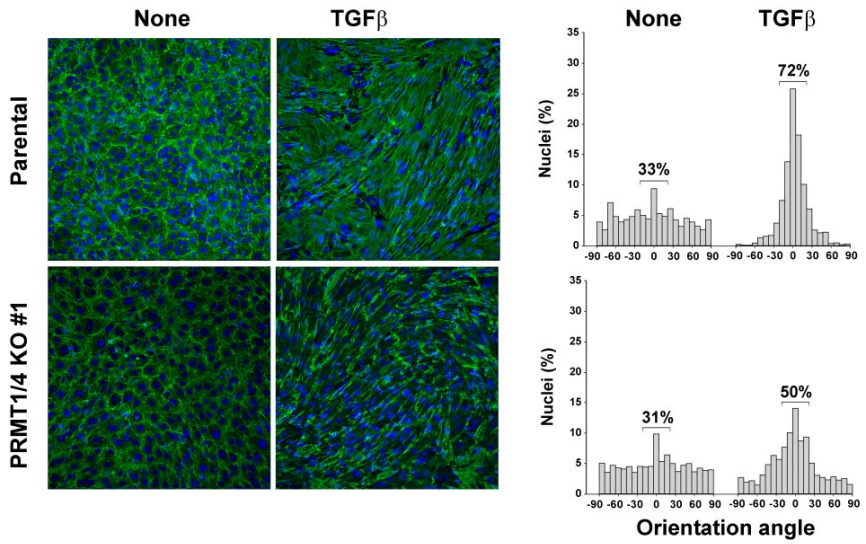

B

MEF Clone	Alignment (%) None	TGFβ
PRMT1/4 KO #2	31	46
PRMT 4 KO #1	33	44

Figure 33: Partial impairment of the TGF-β dependent alignment in PRMT1/4 KO MEFs. (A) MEFs were seeded on coversplips and allowed to produce extracellular matrix for 10 days. Cells were treated with TGF-β (5ng/mL) were indicated. Cells were then fixed with 4% PFA and analysed by IF with anti-fibronectin (green) and DAPI. The nuclei orientation angles were calculated (Image J) from microscope images at 200x and plotted as a frequency distribution centered in the most frequent angle, set as 0˚. (B) Percentage of the oriented nuclei of MEFs PRMT1/4 KO #2 was represented in the table.

3.3 Inhibition of methyltransferases prevents overactivity of Idiopathic pulmonary fibroblasts.

Idiopathic pulmonary fibrosis (IPF) is a chronic lung disease with a median survival time of less than three years following diagnosis[107]. It is characterized by the accumulation of activated fibroblasts (myofibroblasts) in damage lung areas where they secrete and polymerize Fibronectin, fibrillar Collagens and other pro-fibrotic proteins. Growing evidence suggests that inflammatory cells recruited to the site of the injury might contribute to the fibrotic process through the production of pro-fibrotic cytokines such as TGF-β. However the anti-inflammatory therapies based in immunosuppression have been unsuccessful and new options for IPF are needed.

Once established that AMI-1 and Sinefungin reduced the activation of fibroblasts in normal physiologic conditions we wanted to determine if methyltransferase inhibitors were also effective in pathologic conditions such as IPF. Interestingly, prior studies have reported that PRMT1 expression is increased in IPF fibroblasts[100].

We obtained primary IPF fibroblasts from different patients through a collaborative effort with Jordi Alcaraz and tested their response to inhibitors along the few culture passages they maintain a non-senescent phenotype. First we checked the protein levels of some pro-fibrotic markers of these two different IPF patient derived fibroblasts in the presence of the inhibitors. The expression of Fibronectin, FAP and α-SMA

was reduced in the presence of both inhibitors (Figure 34). However, Snail1 levels were maintained, confirming that like in activated MEFs the inhibitors target molecular events downstream the transcription factor. The levels of the H3R17me2a were also assessed in order to control that the inhibitors were effectively inhibiting methylation.

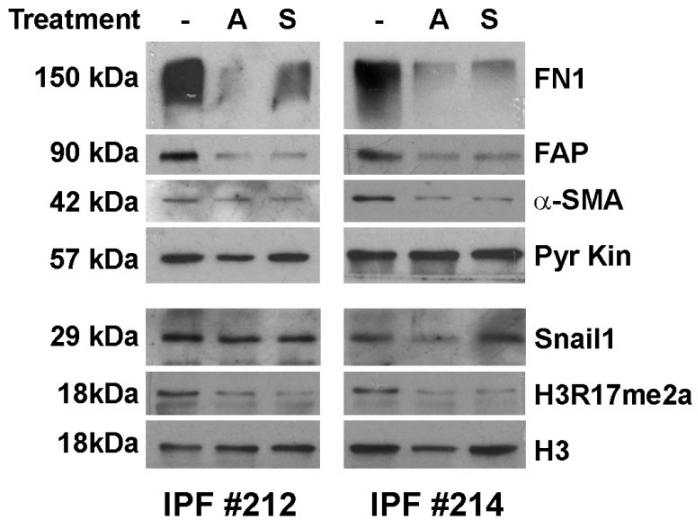

Figure 34: Fibrotic proteins are reduced by AMI-1 and Sinefungin in patient derived fibroblasts. IPF #212 and #214 were treated when indicated with AMI-1 500 µM (A) or Sinefungin 150 µM (S) for 48 hours. Cells were lysed in SDS buffer and the indicated proteins were analysed by Western blot.

We also determined by qPCR the expression of two pro-fibrotic markers such as Col1a1 and Col3a1 that were also downregulated in both conditions (Figure 35)

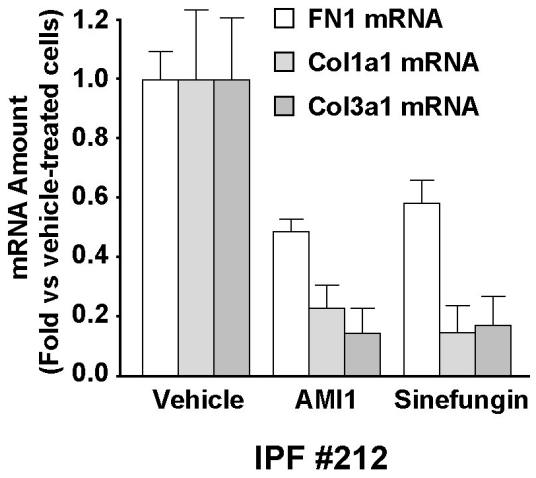

Figure 35: **Fibrotic gene expression is reduced by AMI-1 and Sinefungin in patient derived fibroblasts.** RNA levels of the indicated genes was analysed by RT-qPCR in RNAs extracted from IPF#212 fibroblasts grown in the presence of 500μM AMI-1 or 150μM Sinefungin.

Immunofluorescence analyses were performed in IPF derived fibroblasts to evaluate the co-localization of Snail1, PRMT1 and PRMT4. Both PRMT1 and PRMT4 showed a nuclear staining that matched with Snail1 (Figure 36) resembling what happened in MEFs treated with TGF-β (Figure 19) and suggesting that a similar Snail1 dependent methylation is also active in these cells.

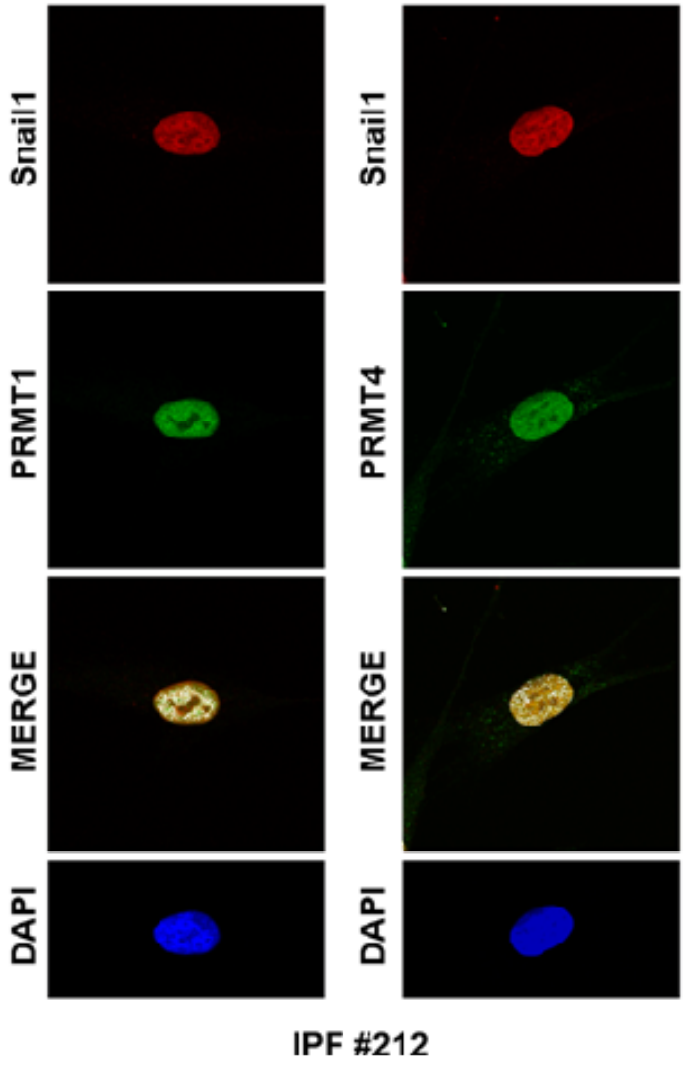

Figure 36: PRMT1 and PRMT4 co-localize with Snail1 in the nuclei of IPF fibroblasts. IPF derived fibroblasts were grown on glass coverslips and fixed with 4% PFA. Snail1, PRMT1 or PRMT4 were analysed by immunofluorescence with specific antibodies and Alexa 488 and 555 conjugated secondary antibodies. White signal in merge corresponds to co-localization calculated with the confocal microscope.

Their capacity to produce organized 3D-ECM was also assessed (Figure 37). An interesting aspect we found is that IPF fibroblasts were able to align themselves and the Fibronectin fibres within 3D-ECMs even in the absence of TGF-β. This property distinguishes IPF derived fibroblasts from MEFs or MSCs and confirms that they are autonomously activated. Both patient derived fibroblasts responded similarly, and the ECM architecture they generate was clearly reduced by the treatment with both inhibitors.

A

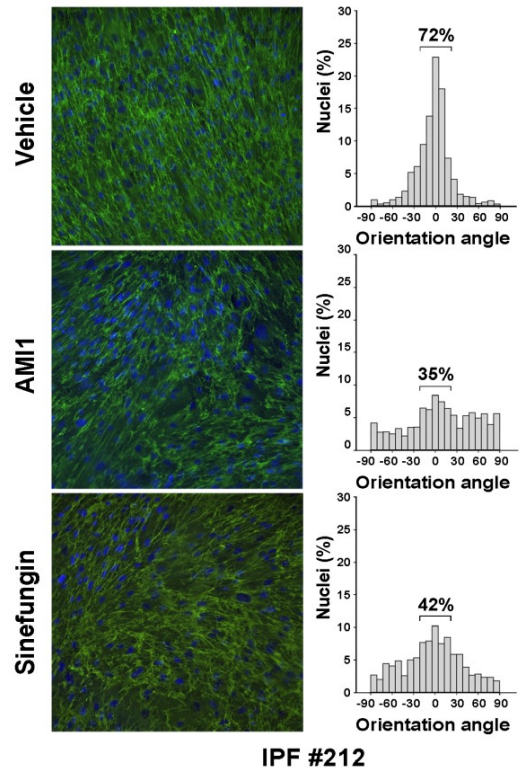

B

Cells	Alignment (%)		
	Vehicle	AMI1	Sinefungin
IPF #212 None	72	35	42
IPF #212 TGFβ	74	36	44
IPF #214 None	72	33	36
IPF #214 TGFβ	73	38	48

Figure 37: AMI-1 and Sinefungin prevent the alignment of Idiopathic pulmonary fibrosis derived fibroblasts in *in vivo* like extracellular matrices. (A) IPF fibroblasts were seeded on coversplips and allowed to produce extracellular matrix for 10 days. Cells were treated with TGF-β (5ng/ml), AMI-1 (500μM) or Sinefungin (150μM) were indicated. Cells were then fixed with 4% PFA and analysed by IF with anti-fibronectin (green) and DAPI. The nuclei orientation angles were calculated (Image J) from microscope images at 200x and plotted as a frequency distribution centred in the most frequent angle, set as 0˚. (B) Summary of the different conditions in percentage of the oriented nuclei was represented in the table.

3.4 AMI-1 or Sinefungin block myofibroblastic activity delaying *in vivo* wound healing

Physiological myofibroblasts are present during *in vivo* wound healing and their activation is maintained through TGF-β[15]. It was previously described in our group that Snail1 conditional KO mice display delayed skin wound healing due to defects in myofibroblast activity in the granulation tissue. The absence of Snail1 prevented the alignment of the fibroblasts within the granulation tissue and the wound closure was delayed.

We took advantage of this experimental model to test the potential of AMI-1 and Sinefungin to block physiologic myofibroblast activity.

3.4.1 Intraperitoneal injection of AMI-1 or Sinefungin delays *in vivo* wound healing

Wounds were inflicted in the dorsal skin of FVB mice and they were intraperitoneally treated every other day with Vehicle, AMI-1 or Sinefungin. Wounds were photographed and measured daily until day five when animals were sacrificed. A clear delay of the closure was observed in the treated wounds compared with the Vehicle (Figure 38). At an equal extension that occurred with the lack of Snail1[69].

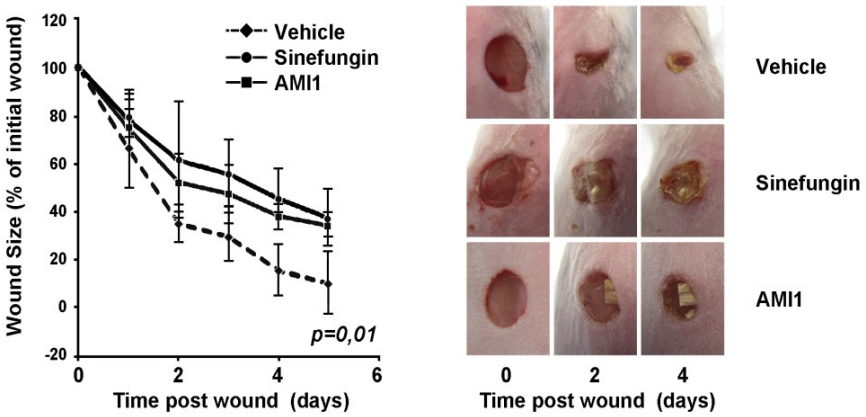

Figure 38: Skin wound healing is delayed in Mice treated with AMI-1 and Sinefungin. Skin wounds (6 mm in diameter) were inflicted on either side of the dorsal midline of FVB mice. Mice were intraperitoneally injected with Vehicle, AMI-1 (20 mg/kg) or Sinefungin (8 mg/kg) every other day until day 5 when the animals were sacrificed. Photographs of representative wounds on the indicated days are shown. Plot represents the mean ± SD for the percentage of closure from a minimum of six wounds performed in different animals. The Student test p value is indicated.

3.4.2 Intraperitoneal injection of AMI-1 or Sinefungin interferes with the granulation tissue architecture

At day five animals were sacrificed and the skin areas containing the wounds were embedded in paraffin for immunofluorescence analysis of the granulation tissue. While in the control animals around 62% of the DAPI stained nuclei of the granulation tissue were aligned in Sinefungin-treated animals fibroblasts aligned randomly (34%) and in AMI-1-treated mice the amount of aligned fibroblasts was clearly decreased (49%). With both treatments a general granulation

tissue disorganization was observed with the Fast green/Safranin staining (Figure 39).

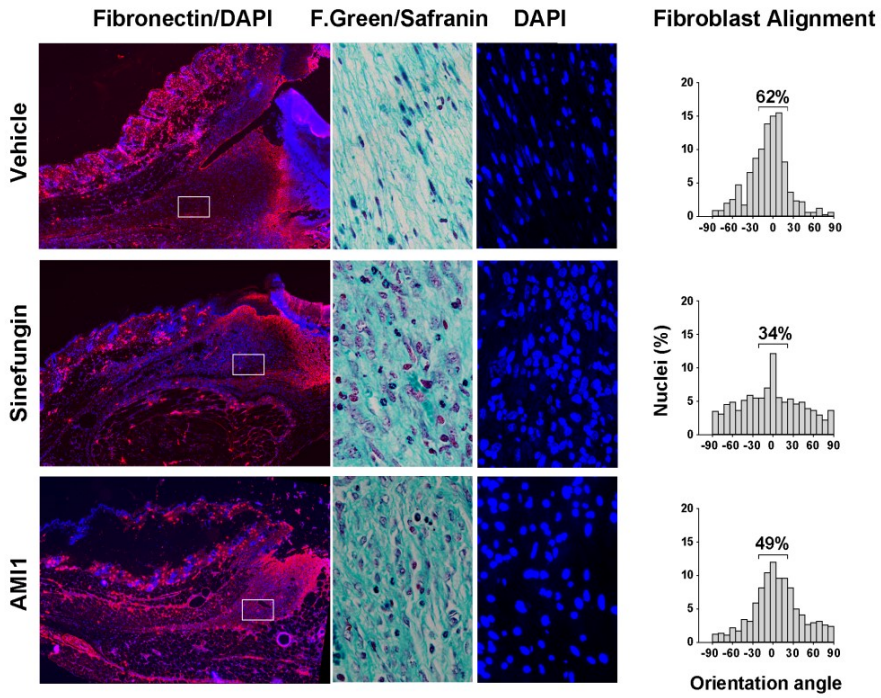

Figure 39: AMI-1 and Sinefungin prevent granulation tissue alignment. Five-day wounds from vehicle or inhibitor-treated mice were analysed from formalin-fixed paraffin embedded wounds by Immunofluorescence or Immunohistochemistry and visualized at x40 (Fibronectin/DAPI) or 400x (Fast Green Safranin and DAPI). The orientation of the angles of DAPI were analysed and plotted as in Figure 27a.

In vehicle treated animals the Fibronectin and Collagen fibres in the granulation tissue aligned towards the wound but this organization was compromised in inhibitor-treated mice (Figure 40).

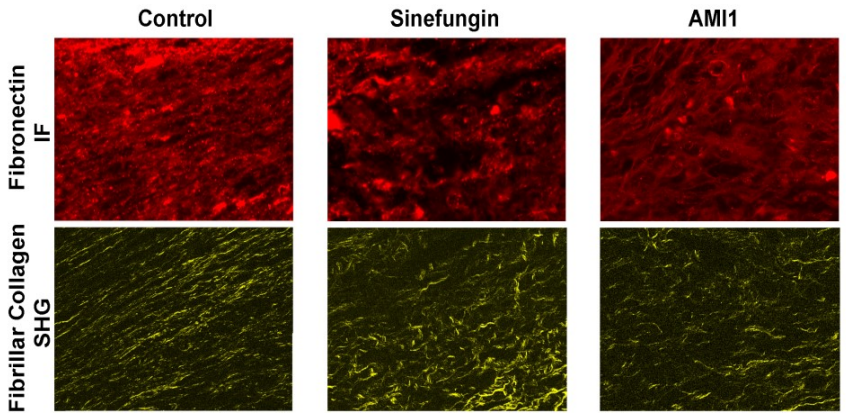

Figure 40: AMI-1 and Sinefungin administration interferes with Fibronectin and Collagen fibre organization within the granulation tissue. Five-day wounds from vehicle or inhibitor-treated mice were analysed from formalin-fixed paraffin embedded wounds by immunofluorescence (Fibronectin) or performing a second harmonic generation (SHG) to visualize fibrillar collagen. Magnification at 400x.

Changes in the expression patterns of αSMA and arginine methylation were also detected in the granulation tissues treated with both inhibitors. In contrast, fibroblastic Snail1 was detected in all conditions indicating that inhibitors affected Snail1-downstream signalling (Figure 41).

This data indicate that both inhibitors but especially Sinefungin are effective blocking the activity of myofibroblasts *in vivo*.

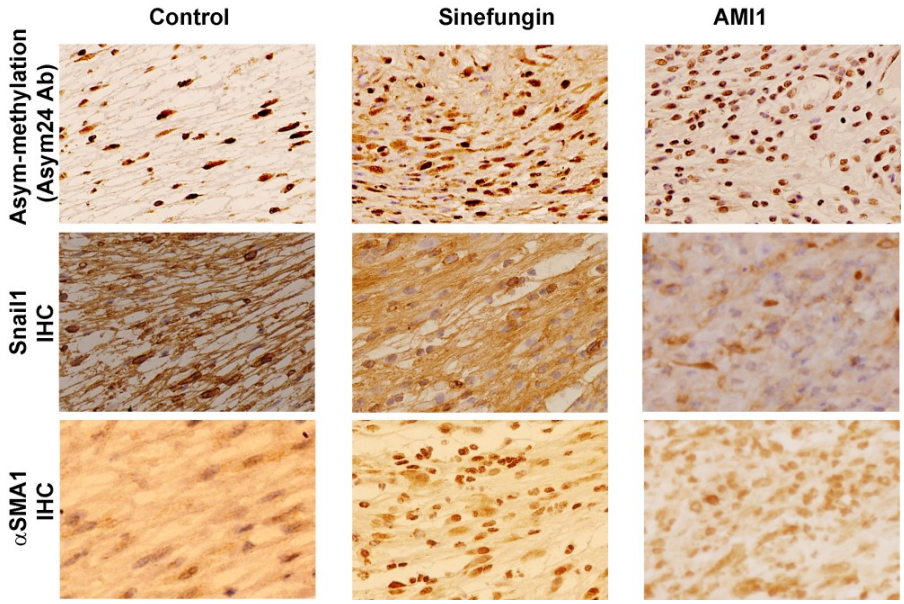

Figure 41: PRMT inhibitors interfere with arginine methylation and αSMA expression within granulation tissue. Five-day wounds from vehicle or inhibitor-treated mice were analysed from formalin-fixed paraffin embedded wounds by immunohistochemistry and visualized at 400x.

3.5 Sinefungin interferes with Fibroblast activation preventing metastasis *in vivo*

It was previously observed that stiff and perpendicular collagen fibres around primary breast tumours associated with tumour invasion and lower patients survival[69]. Similarly, previous analyses in our lab showed that Snail1 expression in breast cancer stroma associates with local anisotropic Fibronectin and Collagen alignment and with a worse outcome. Accordingly with these observations, MDA-MB-231

breast tumour cells showed less invasive capabilities through *in vivo* like 3D-ECMs produced by TGF-β activated Snail KO compared with WT MEFs[69].

3.5.1 AMI-1 and Sinefungin prevent the formation of ECMs that favours tumour cell invasion

We tested if TGF-β activated MEFs treated with inhibitors generate 3D-ECMs that restricts cancer cell invasion. For this propose, MDA-MB-231 cells were seeded above decellularised 3D-ECM produced on invasion inserts.

Similarly to what happened in 3D-ECM generated Snail1 KO MEFs[69], invasion of MDA-MB-231 tumour cells through 3D-ECM generated by activated MEFs in the presence of AMI-1 or Sinefungin was lower compared with in the presence of Vehicle (Figure 42a). In contrast, inhibitors did not affect directly the invasive capacity of MDA-MB-231 cells through Matrigel (Figure 42b), indicating that these methyltransferase inhibitors block specifically the activity of the fibroblasts on the ECM architecture that subsequently limit tumour cell invasion.

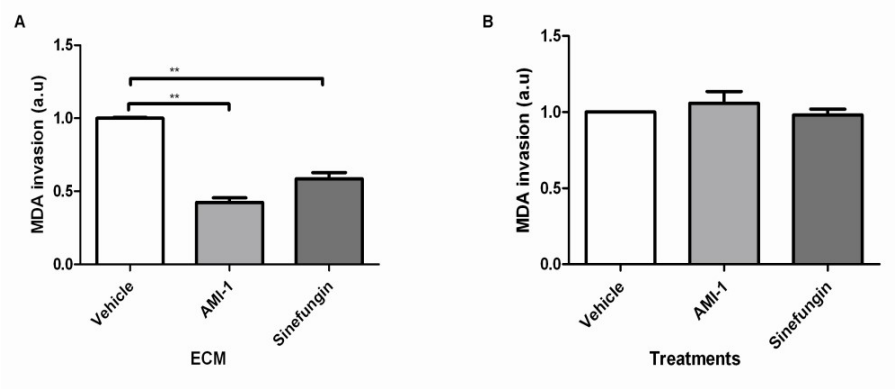

Figure 42: *In vivo* like 3D-ECM generated in the presence of AMI-1 or Sinefungin failed to promote cancer cell invasion. (A) MDA-MB-231 breast cancer cells were allowed to invade for 24 hours in descellularised matrices generated by MEFs treated with Vehicle or PRMTs inhibitors (AMI-1 and Sinefungin) in the presence of TGF-β. Serum was used as a chemoattractant and MDA-MB-231 cells that invaded trough the matrices were fixed, stained with DAPI and quantified on images obtained with the microscope. The relative amount of invasive cells in each condition was plotted. Values represent the mean ± SD of three different experiments. p-value <0.05 (*), p-value<0.01 (**) (B) MDA-MB-231 cells were allowed to invade matrigel-coated Boyden-chambers for 24 hours in the presence or absence of the inhibitors. Serum was used as a chemoattractant and invading cells were quantified and represented as in (A).

3.5.2 Sinefungin treatment limits the stroma component of breast tumours

Given that Sinefungin was effective in the *in vivo* model of wound healing we decided to evaluate the potential of Sinefungin as anti-metastatic acting on CAFs in a mouse model for metastatic disease[108].

We generated synchronized breast tumours by isolating breast cancer cells from MMTV-PyMT mice and orthotopically injecting them 1:1 with mesenchymal stem cells (MSCs) in

immunodeficient NOD-SCID gamma host mice. MSCs favour lung metastasis formation[32], and like MEFs, organize the 3D-ECM in a Snail1 dependent manner[69]. Moreover, Sinefungin and AMI-1 blocked TGF-β induced alignment of 3D-ECMs generated by MSCs (Figure 28). Sinefungin or vehicle was administrated intraperitoneally to mice three times per week until tumours reached 0.2-0.4 cm^3 or 1 cm^3 that were surgically rejected. Animals were maintained alive one extra month to allow the growth of lung metastasis and then were sacrificed.

No significant differences in the weight and volume of the primary tumours at the moment of resection were observed between the two groups (Figure 43) in accordance with the cell culture results that showed that Sinefungin was not toxic (Figure 24).

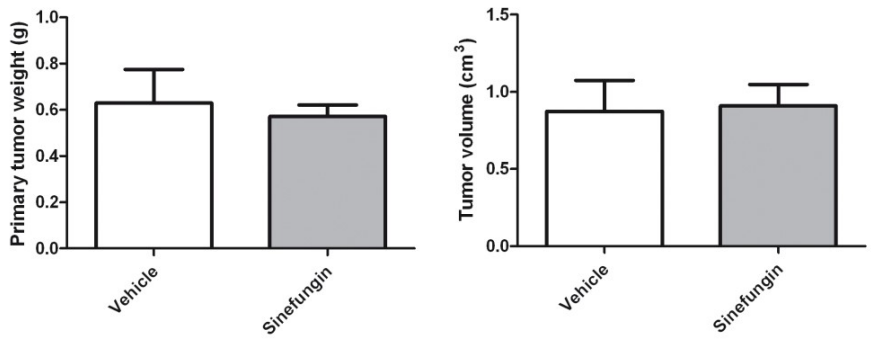

Figure 43: Sinefungin administration does not affect weight and volume of the primary tumours. $5x10^5$ PyMT cells together with $5x10^5$ MSCs were co-injected orthotopically into the mammary fad pad of NOD-SCID gamma mice.

The histological analysis of the 0.2-0.4 cm^3 primary tumours by Haematoxylin and Eosin staining revealed a clear reduction of the stroma compartment in the Sinefungin treated tumours in contrast with the Vehicle (Figure 44).

A deeper histological analysis by immunofluorescence to visualize Fibronectin and Second Harmonic Generation (SHG) for fibrillar Collagen showed a lower deposition of both ECM fibres in the inhibitor condition (Figure 44).

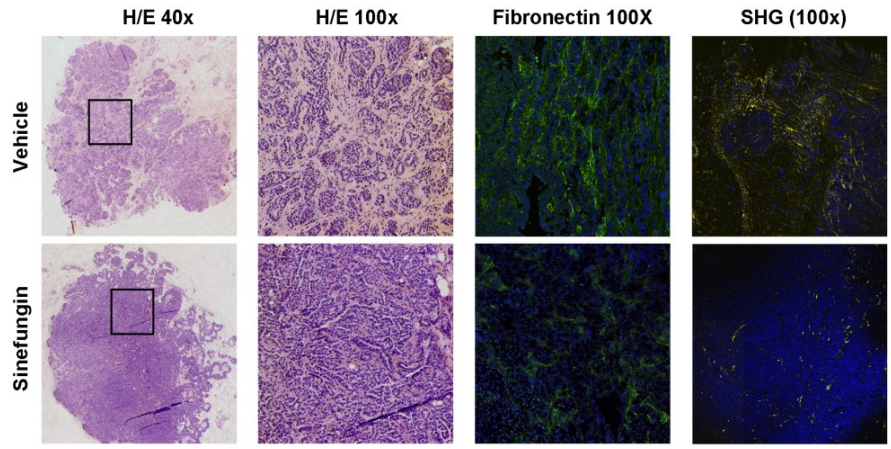

Figure 44: Sinefungin treatment reduces the stromal compartment of the primary tumours. Primary tumours (0.2-0.4 cm^3) were rejected, fixed in formalin, paraffin-embedded and sliced in 5µm paraffin sections. Haematoxylin and Eosin staining, Fibronectin immunofluorescence and Second Harmonic Generation were performed and representative pictures are shown.

Sinefungin treated primary tumours presented also less amount of Fibronectin and FAP, two markers of CAFs, when

protein extracts of tumour samples were analysed by Western blot (Figure 45).

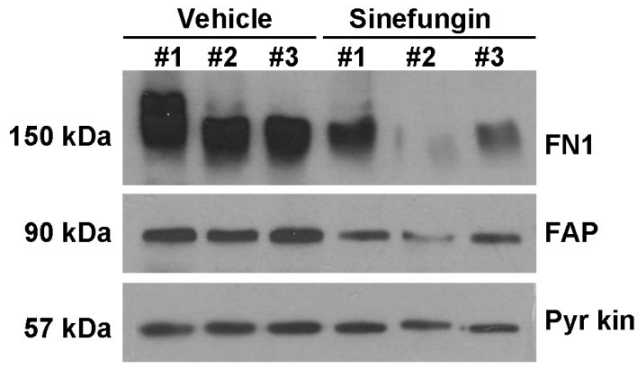

Figure 45: Sinefungin reduces the amount of Fibronectin and FAP in primary tumours. The quantity of the indicated proteins was visualized by Western blot in SDS extracts from fresh primary tumour pieces of Control or Sinefungin treated mice.

3.5.3 Sinefungin treatment reduces the lung metastasis foci

The histological analysis of the $1cm^3$ primary tumours showed a high percentage of necrotic areas in both conditions that impeded to clearly distinguish and assess the dimension of the stroma compartment in the Haematoxylin and Eosin staining.

Finally we assessed the capability of these tumours to metastasize by quantifying the lung metastasis foci. Vehicle treated mice with primary tumours rejected at 1cm^3 developed 6-7 average metastasis foci per animal; however, in Sinefungin treated animals the number of foci was reduced by half (Figure 46a). Mice in which tumours were rejected at 0.2-0.4 cm^3 also developed metastasis (although with less foci) and a tendency was observed with 3/3 vehicle animals with metastases and only 1/3 in the Sinefungin group, reinforcing that Sinefungin reduces metastasis formation and indicating that the metastasis are initiated at the beginning of the tumour process.

As previously observed on MDA-MB-231 cells (Figure 42b), Sinefungin did not alter the invasion of isolated PyMT-tumour cells through matrigel matrices (Figure 46b) suggesting that inhibitors do not directly reduce tumour cell invasion but in an indirect manner.

Taken together, these results support that, *in vivo*, Sinefungin specifically block the activity of CAFs on the organization of the ECM and this interferes with the metastatic potential of the primary tumour.

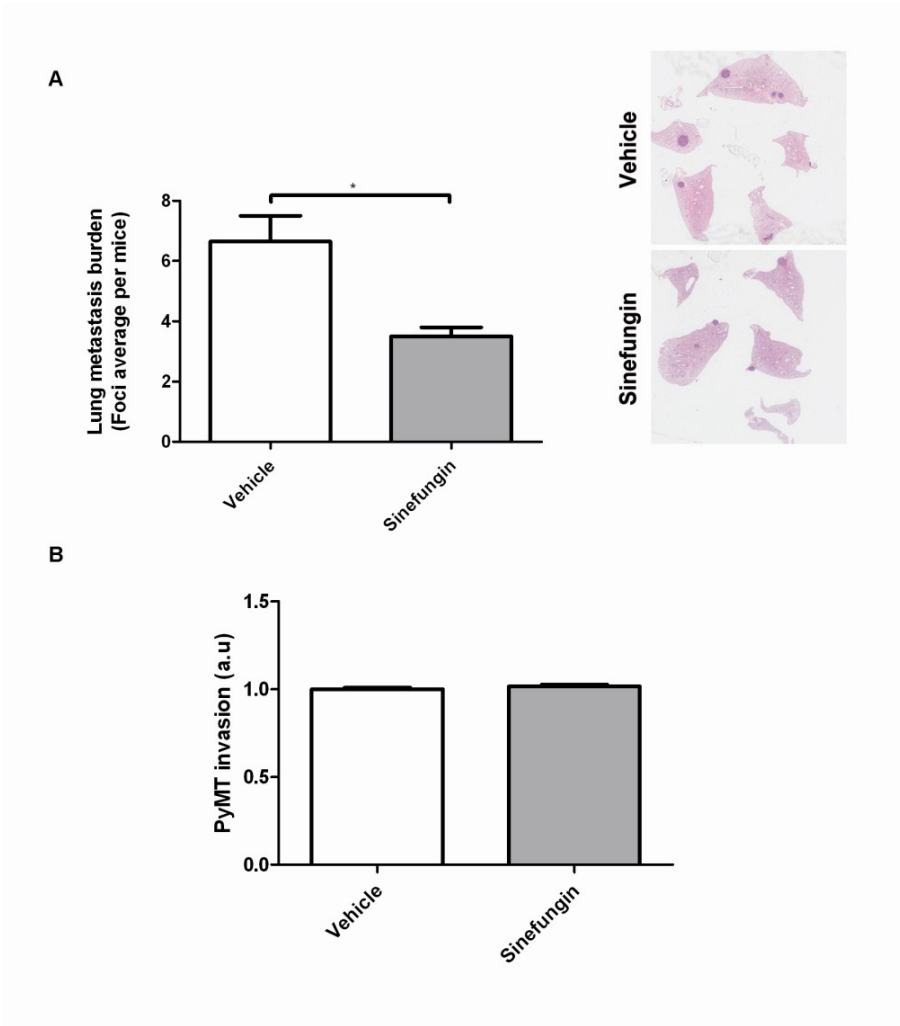

Figure 46: Intraperitoneal Sinefungin administration reduces the number of lung metastasis foci. (A) Mice orthotopically injected with PyMT and MSCs (1:1) developed breast tumours and lung metastasis. Sinefungin was intraperitoneally administrated three times a week (8mg/kg) until tumours were rejected at $1cm^3$. Number of metastatic foci was counted in Haematoxylin and Eosin staining of paraffin sections of the lungs. Average foci of at least ten lungs were plotted ± SD. p-value <0.05 (*). (B) Sinefungin does not affect the intrinsic invasive capability of the PyMT tumour cells. Tumour isolated PyMT cells were seeded in matrigel-coated Boyden chambers in the presence or absence of Sinefungin. Serum was used as a chemoattractant. After 24 hours PyMT cells that invaded through the matrigel coated membrane were fixed, stained with DAPI and quantified on images obtained on the microscope. The relative amount of invasive cells in each condition was plotted. The experiment was done three times with triplicates.

DISCUSSION

DISCUSSION

1. CHARACTERIZATION OF THE SNAIL1-MECHANISMS CONTROLLING FIBROBLAST ACTIVATION.

Wound healing, chronic fibrosis, and cancer progression have a tight relationship. Inflammation, ECM remodelling, cell proliferation, myofibroblastic differentiation and the overexpression of EMT-TFs are common hallmarks of these processes[21].

However, the EMT-TFs downstream effectors that fuel these processes are poorly characterized. Our work focused on characterizing new molecular mechanisms governing myofibroblast differentiation with the idea to offer targetable points interfering with pathological fibroblast activation in chronic fibrosis and cancer progression.

1.1 PRMT1 and PRMT4 the new members of the Snail1-activating complex

Previous research in our laboratory indicates that Snail1 plays a key role in the differentiation from fibroblasts to myofibroblasts. Accordingly with it, we reported that upregulation of αSMA and RhoA by TGF-β is Snail1 dependent and that fibroblasts depleted for Snail1 are not

able to produce a stiff and aligned extracellular matrix when they are activated.

Additionally, we also described that a set of ECM-related genes including *FN1* is under the control of a transcription regulatory complex involving Snail1/PARP1/NF-κB-p65 in fibroblasts[53]. Here, we unveil two extra components of this complex, PRMT1 and PRMT4. Upon TGF-β treatment, the protein levels of these enzymes are up-regulated and they bind to the *FN1* promoter, where their respective histone marks are increased. Indeed, we found both enzymes to interact with Snail1 in the nuclei of activated fibroblast. PRMT1 and PRMT4 binding and histone methylation of the *FN1* promoter does not occur in Snail1 depleted fibroblasts, suggesting that the interaction of PRMTs with Snail1 is essential for *FN1* promoter regulation.

Given that the transcription of a subset of ECM genes was described to be also Snail1 dependent[69], we believe that, through PRMT1 and PRMT4, Snail1 might be coordinating the asymmetrical dimethylation of histone residues in their promoters and enhancing their transcription during myofibroblast differentiation. This hypothesis can be tested by extending our ChIP assays (with anti PRMT1, PRMT4 or PRMT marks) in WT and Snail1 KO MEFs to the promoters of these genes. Our intends to describe all the Snail1 targeted promoters by ChIP-seq have been unsuccessful since only the background signal, measured in Snail1 KO MEFs, was

detected in parental MEFs. We are currently generating Snail1-3xFLAG knock-in MEFs to immunoprecipitate Snail1 more efficiently and solve this problem. We expect that a wider picture of the Snail1-targeted promoters will allow visualizing new targetable Snail1-related molecules or events to block fibroblast activation in tumours and fibrosis.

1.2 PRMT1 and PRMT4 control Fibronectin fibrillogenesis.

For modelling the extracellular matrix, secreted Fibronectin monomers are assembled into fibrillar networks by stromal fibroblasts. Extracellular Fibronectin fibrillogenesis is depending on integrins, which are transmembrane receptors linking extracellular Fibronectin molecules with the cytosolic actomyosin cytoskeleton. This highly contractile cytoskeleton is characteristic of myofibroblasts and it is regulated by Rho family of GTPases. Contracting forces promote the conformational changes on Fibronectin monomers that prime their assembly into fibrils[109]. Therefore, treatments that enhance contractibility stimulate matrix fibrillary assembly whereas inhibition of RhoA GTPase reduces it.

Previous work in the lab showed that Snail1 is required for TGF-β induced Fibronectin transcription, RhoA activation and proper Fibronectin fibrillogenesis[69]. However, the exact molecular mechanism by which Snail1 is regulating active RhoA levels remains elusive. We can speculate that Snail1

may be directly affecting the transcription of GAPs, GEFs or GDIs involved in RhoA regulation. Snail1 may also control Fibronectin fibrillogenesis by modelling Integrin αV levels, since it has been reported that in fibroblasts lacking Snail1 the levels of this Fibronectin receptor are decreased[110]. Moreover, promoter activity of Integrin αV increase when Snail1 is overexpressed, suggesting that Snail1 is activating its transcription, although a ChIP experiment is lacking to confirm that Snail1 directly binds to the promoter.

Here, we found that a similar abrogation of TGF-β dependent fibrillogenesis happened in PRMT1/4 KO MEFs. However, in PRMT1/4 depleted MEFs a shift in the molecular weight of Fibronectin was observed without affecting Fibronectin protein activation by TGF-β.

Fibronectin exhibits different isoforms derived by alternative splicing as well as variation in glycosylation. The organization of Fibronection into fibres is determined by intermolecular interactions involving a subset of domains. Thus, the expression of different splicing variants, which may account for the differences in molecular weight, could explain why fibrillogenesis capacity of these cells is reduced. Another possibility is that Fibronectin suffers changes in its glycosilation status, some reports has shown that glycosilation interferes with fibronectin-integrin interactions[111].

In addition, PRMT1 and PRMT4 may be also involved in the transcriptional regulation of other genes important for Fibronectin fibrillogenesis and that are Snail1 dependent, such as Integrin αV or putative regulators of RhoA activation. Further research is required in order to uncover the precise mechanisms controlled by Snail1 and PRMTs on Fibronectin fibrillogenesis.

1.3 Splicing, a novel Snail1-dependent way to control fibroblast activation

In addition to interact with PRMT, we describe here that transient Snail1 downregulation leads to a decrease in PRMT1 and PRMT4 protein but not RNA levels. Thus, the interaction of both enzymes with Snail1 may favour their stability. As expected, the decrease in PRMT1 and PRMT4 protein levels after Snail1 downregulation was associated with a reduction of asymmetric dimethylation in a set of proteins into a wide range of molecular weight; therefore, Snail1 indirectly modulates the methylation state of proteins other than histones, which may affect diverse cellular processes. Reviewing the literature, the main cellular function of asymmetrical dimethylated proteins is RNA processing and splicing regulation[112], a mechanism interconnected with transcription.

Transcription and downstream RNA processing events are highly coordinated. This notion is supported by the

observation that alternative splicing can be modified by changes in the promoter region of the gene[113] and by data showing that transcription factors regulate subsequent processing events by interacting directly with splicing factors[114,115]. Indeed, transcription and mRNA processing are considered mostly not sequential but simultaneous.

PRMT1 and PRMT4 activities have been associated with the regulation of both mechanisms, transcription and splicing, by catalysing the methylation of histones, splicing factors and RNA binding proteins. PRMT4 methylates proteins of the RNA processing machinery, for instance SmB, SAP49 and U1C, regulating protein-protein interactions that are involved in the ordered assembly of the spliceosome. Additionally, by interacting directly with splicing factors, PRMT4[87] has been described as a transcriptional coactivator involved in transcription-coupled splicing. A molecular crosstalk between transcription and splicing has been characterized in the C-terminal domain (CTD) of RNA polymerase II (Pol II), which serves as a scaffold for many factors involved in the transcript maturation[116]. Although PRMT4 has not been found directly associated with the CTD, it does methylate a CTD-binding protein such as the transcription elongator factor CA150[94]. PRMT1 regulates alternative RNA splicing via reducing RBM15 protein[84]. RBM15 is a RNA binding protein that recruits splicing factors to the sites for alternative splicing.

Thus, the recruitment of PRMT1/4 to sites of transcriptional activation we describe in our work clearly has the capacity to increase the methylation of regulatory substrates impacting alternative splicing, and it is plausible that Snail1 indirectly control the asymmetrical methylation of splicing regulatory proteins in the proximal promoter of its target genes by carrying PRMT1 and PRMT4 on those promoters. Importantly, promoter binding sites occupied by Snail1 (both p65-NF-κB and E boxes) to activate or repress transcription, are always localized near the transcription start site[53] where RNA polymerase II binds. Therefore, Snail1 associated PRMTs can act on the CTD and associated proteins, controlling simultaneously transcription and alternative splicing of specific target genes.

The analysis of proteins with Snail1-dependent arginine methylation we obtained by Mass spec (from IPs obtained with anti-arginine methylation antibodies in Snail1 control and KO MEFs) gave raised conclusions that were in accordance with this hypothesis. Thus, the list of proteins whose arginine methylation depends on Snail1 (Figure 21) was enriched in mRNA processing and splicing related proteins. In the same direction, the list of proteins we obtain in Snail1 immunoprecipitates from TGF-β treated MEFs was also enriched mRNA processing and splicing related proteins (Figure 22). Therefore, our data support that Snail1 may control the methylation of some splicing factors that may interact with Snail1 within the transcriptional complex. Further

experimental approaches are required to characterize some of these factors.

Noteworthy, in a high throughput approach we have detected over 300 alternative splicing events regulated in a Snail1-dependent manner. Among these, we found alternative splicing in *FN1,* thus, Snail1 is regulating *FN1* transcription and alternative splicing. The spliced exon in *FN1* gene encodes for a domain (FN-III) that is involved in the dimerization of FN1 to form fibrils[117]. Moreover, Snail1 also affects the alternative splicing of other ECM genes such as *Col5α1;* therefore, changes in the splicing of these genes may affect the capacity of fibroblast to polymerize ECM fibres.

Genes such as *Anln, Macf1, Tpm2, PPP1R12A, Flnc* and *Flnb* are involved in the regulation of the cytoskeleton: Anln is a GTP-RhoA binding protein coordinating actin, microtubules and septins[118], PPP1CRA regulates myosin contraction and microtubule polymerization[119], and Macf1 (microtubule actin cross-linking factor) connects actin and microtubule filaments[120]. It can be feasible that altogether these splicing events may have a significant impact on CAFs cytoskeleton organization and as a consequence on ECM remodelling.

Of interest, most of the genes spliced in a different way in Snail WT versus KO MEFs also show different expression levels (Data not shown).

The fact that Snail1 affects the alternative splicing was pointed in another work[121] in which ectopic expression of Snail in MDCK cells resulted in changes in alternative splicing of p120 and ZO-1, proteins also involved in actin cytoskeleton. Another study[122] indicates that Snail1 may regulate gene expression post-transcriptionally by modulating the transcription of splicing factors such as SFPQ (Splicing factor, proline- and glutamine-rich).

Therefore, our data and also previous studies[121,122] indicate that Snail1 may modulate alternative splicing, and also mRNA stability and translation of genes important for fibroblast activation. Although we do not precisely know the underlying mechanism, our data support the Snail1 bound to promoters can modulate splicing by interacting PRMT1 and PRMT4 and modulating arginine methylation of splicing factors.

Alterations in the splicing machinery and the process of alternative splicing is involved in many cancers[123,124] and alternative splicing inhibitors have been tested as treatment for some cancers[124,125]. Our data support that targeting alternative splicing in CAFs can be useful to interfere with its activity. Further research may unveil relevant splicing events and allow designing splicing specific antisense oligonucleotides (to specifically favour one splicing isoform with respect to another) that may attenuate CAFs activation and prevent metastasis promotion. Indeed, antisense oligonucleotides to target alternative splicing have already

been proposed for treatment of other diseases[126] and could be a possible new therapeutic approach to target fibroblasts activation in cancer.

2. METHYLATION IS ESSENCIAL FOR FIBROBLAST ACTIVATION

2.1 Methyltransferase inhibitors fully block fibroblast activation

Great efforts are seen in screening and designing potent and selective individual PRMT inhibitors but few of them are currently available. For that reason we started working with general PRMT inhibitors. AMI-1 has been discovered by Bedford as a molecule that specifically inhibits arginine, but not lysine, methyltransferase activity. In particular, AMI-1, has more affinity inhibiting PRMT1 and at less extent PRMT4 among the other PRMTs[127]. It is likely that AMI-1 binds the protein substrate-binding pocket of these enzymes, because it does not compete for the binding of the methyldonor, Adomet.

Nevertheless, some reports have shown that at high concentrations, AMI-1, also affects the methylation capacity of lysine methyltranferases (PKMTs) such as SET7/9[128].

The other methyltransferase inhibitor used in this work is Sinefungin. Sinefungin is an Adomet analogue that competes for Adomet binding and inhibits all Adomet-dependent

methyltransferases. Therefore, Sinefungin function as a general methylation inhibitor, affecting methylation of phospholipids, DNA, RNA and proteins including PRMTs and PKMTs[127].

Herein, we describe that these methyltransferase inhibitors obstructs the myofibroblast phenotype. In cell cultures, they prevent a wide range of TGF-β activated processes in fibroblasts, as the acquisition of the myofibroblast markers Fibronectin and αSMA, the capacity polymerize extracellular Fibronectin and the capability to generate matrices with aligned fibres. Of therapeutic interest, these results were confirmed on cultured primary fibroblasts from Idiopathic lung fibrosis (IPF) patients that retain myofibroblastic treats even in the absence of ectopic TGF-β treatment. Therefore, these results suggest that these methyltransferase inhibitors interfere with the molecular elements that support the exacerbated myofibroblastic activity observed in fibrosis and that they can be used to develop new reagents to treat this pathology.

In vivo, both inhibitors affected myofibroblast activity generated during wound healing. Intraperitoneal administrations effectively prevented the alignment of the fibroblasts and the extracellular fibres within the granulation tissue and delayed the wound closure. Sinefungin was more effective than AMI-1 in this assay. We cannot elucidate the reason but it can be associated either to higher penetrance

into the tissue or higher inhibitory potential on the myofibroblasts generated in wound healing. In the PyMT metastatic cancer model in mice, Sinefungin affected CAFs activity. Intraperitoneal administration visually reduced the stromal compartment of primary tumours and diminished the presence of Fibronectin and Collagen fibres in the stroma. The observed effect was corroborated by the decrease in the myofibroblast markers αSMA, FAP, and Fibronectin by Western blot. These events associated with a reduced number of lung metastatic foci.

AMI-1 was not effective in these experiments, maybe due to a poor penetrance or that *in vivo* this inhibitor has lower inhibitory potential on the myofibroblasts.

We cannot discard that Sinefungin additionally target the secretion of soluble signalling molecules by CAFs, however, the reduced invasion of tumour cells on decellularised 3D-ECMs generated in the presence of the inhibitors indicates that changes in the extracellular matrix are sufficient to reduce malignant behaviour.

Overall, these results indicate that methyltransferase inhibitors can be used to attenuate CAFs activation, reducing its pro-tumorigenic effects and thus preventing metastasis promotion. Therefore, our results support our initial hypothesis that disturbing CAFs activity in breast tumours prevents metastasis formation. The observation that

Sinefungin treated fibroblasts in cell culture generate ECMs similar to control non activated fibroblasts suggest that Sinefungin treated tumours preserve normal fibroblast activity that produce a restrictive stroma that disfavour tumour progression.

Considering that the desmoplastic reaction generated by CAFs resembles the typical fibrotic deposition and the results with the inhibitors in IPF fibroblasts in culture, we expect that Sinefungin would also ameliorate fibrosis in mice models. Altogether, we suggest methyltransferase inhibitors as a new strategy to block myofibroblast activity *in vivo*.

2.2 Methyltransferases other than PRMT1 and PRMT4 may be necessary for full fibroblast activation

AMI-1 action results in the abrogation of fibroblast activation however, at the concentrations we use AMI-1 we cannot assume that we are only affecting PRMT1 and PRMT4. Besides, Sinefungin has a general effect inhibiting a wide spectrum of methyltransferases.

Studying the specific contribution of PRMT1 and PRMT4 on myofibroblast activity is hindered by the fact that PRMT1 causes major defects on DNA integrity[129] and the establishment of a constitutive PRMT1 KO cell line was unsuccessful. Unexpectedly, double PRMT1 and PRMT4 KO MEFs were obtained. It is possible that PRMT1 and PRMT4

have antagonistic activities on survival with PRMT1 dominating the restriction on survival produced by PRMT4.

MEFs depleted for PRMT1 and PRMT4 did not completely recapitulate methyltransferase inhibitors effect on fibroblasts activity. Myofibroblastic markers were barely affected and their capacity to produce aligned matrices in the presence of TGF-β was reduced, although not at the same extent as in the Snail1 KO MEFs or in the presence of the inhibitors. However, the increase in fibrillogenesis capacity upon TGF-β treatment was clearly abolished. We propose that only fibrillogenesis is entirely dependent of PRMT1/4 but other required events for myofibroblast activation are not.

PRMT1 is the primary methyltransferase that catalyses the aDMA mark, accounting for over the 90% of this kind of methylation. A recent publication[85] show that the initial depletion of PRMT1 lead to a striking decrease of aDMA levels but at day-4 post PRMT1 loss there is compensation, as well as novel substrate methylation. This could be due to the cell attempting to compensate for PRMT1-loss with overexpression of other PRMTs. In fact, authors observe an increase in protein levels of PRMT6 and PRMT7 concomitantly with the loss of PRMT1 and suggested that a large number of PRMT1 substrates become targets for other PRMTs. This makes sense with our results because in PRMT1/4 double KO MEFs we did not detect a general reduction of aDMA signal (data not shown) but only of specific

histone residues. Therefore, some of the events regulating myofibroblast activation other than fibrillogenesis may be compensated by the overexpression of PRMT6 and PRMT7.

In addition to compensation, the partial blocking effects in PRMT1/4 KO MEFs could be explained by the effect of the inhibitors on other methyltransferases. We discarded the possibility that PRMT5 activity was required for fibroblast activation using a new specific PRMT5 inhibitor. MEFs treated with specific concentrations for PRMT5 and TGF-β produce normal 3D-ECMs, aligning Fibronectin fibres normally. In addition, we also know that downregulation of Snail1 does not affect sDMA levels (PRMT5 is the main symmetric enzyme) as happens with sDMA, pointing also in the direction that sDMA levels and PRMT5 are not necessary for fibroblast activation.

Reviewing the literature for other candidates, we found that a lysine methyltransferase, named SET7/9, is important for renal fibrosis. *In vitro*, TGF-β activity results in monomethylation of lysine 4 of histone H3 (H3K4me1) through SET7/9 induction, which is important for the transcriptional activation of fibrotic genes such as αSMA. Human samples from patients with renal fibrosis show correlation of SET7/9 expression with fibrotic areas. Moreover, inhibition of SET7/9 ameliorates renal fibrosis in a mouse model of renal fibrosis.

Sinefungin treatment and also AMI-1 (at higher concentrations of 100μM)[128] are able to affect SET7/9 methylation. Moreover, like PRMT1 and PRMT4, SET7/9 is an important member in the p65 gene activation complex regulating NF-κB-dependent inflammatory genes[130].

These studies prompted us to use a new SET7/9 inhibitor called PFI-2[131] in the 3D-ECMs. We abrogated TGF-β induced organization in control 3D-ECMs using PFI-2 inhibitor (concentrations highly specific for SET7/9 inhibition) (Figure 47a). Myofibroblastic markers such as Fibronectin and αSMA were also affected in the presence of the inhibitor (Figure 47b).

3D-ECMs produced by MEFs KO for SET7/9 do present similar disorganization observed with PFI-2 (Figure 47a), suggesting that SET7/9 complements PRMT1 and PRMT4 to sustain fibroblast activation. Hence, methyltransferase inhibitors could affect different processes important for myofibroblast transition.

However, accurate studies of the methylation status in fibroblasts need to be carried out, as H3K27 histone trimethylation, a mark associated with repression of transcription, activates fibroblasts and induce fibrosis[132]. H3K27me3, in contrast to other epigenetic marks, acts as a negative regulator of tissue fibrosis. In that case, inhibiting

this specific methylation would increase fibrosis, an opposite effect that the one we observe in this work.

DNA methyltransferases have been reported to be important also for myofibroblasts differentiation[133,134]. Through hypermethylation of CpG islands, methyltransferases such as DNMT1 and MECP2, repress anti-fibrotic genes perpetuating fibroblast activation. Consequently inhibitors of DNA methylation ameliorate accumulation of activated fibroblasts, reducing their proliferation rate, collagen synthesis and αSMA expression[134]. Interestingly, prostate stromal cells with overexpression of the epigenetic regulator HMGA2 is sufficient to induce prostatic neoplasia[135]. Thus, it is likely that epigenetic changes in the tumour microenvironment could contribute to tumour-promoting activity and that the irreversible activation of fibroblasts might be driven by epigenetic alterations given the rare frequencies of genetic events identified in cancer-associated stroma.

Altogether, our work and the others, demonstrate that methylation determines fibroblast activation. Possibly through various mechanisms including the one described in this thesis. More experimental work has to been done in order to elucidate the specific contribution of each methylation to the myofibroblast phenotype.

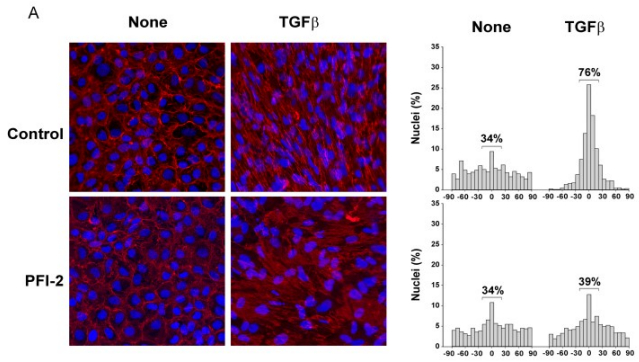

Cells	Alignment (%) Vehicle	TGF-β
MEFs control	33	71
MEFs SET7/9 KO #1	36	36
MEFs SET7/9 KO #2	38	43

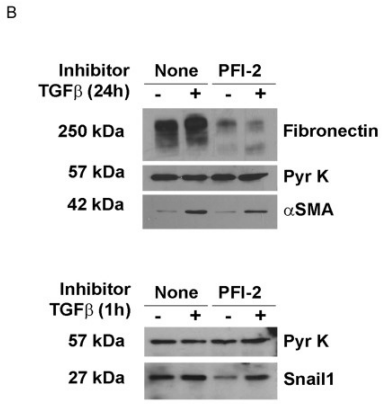

Figure 47: SET7/9 lysine methyltransferase is important for fibroblast activation. (A) TGF-β remodels the ECM generated by MEFs in a SET7/9 dependent manner. MEFs were seeded on coverslips and allowed to produce extracellular matrix for 10 days. Cells were treated with TGF-β (5ng/mL) or PFI-2 when indicated. Cells were then fixed with 4% PFA and analysed by IF with anti-fibronectin (green) and DAPI. The nuclei oriented angles were calculated (Image J) from microscope images at 200x and plotted as a frequency distribution centred in the most frequent angle, set as 0˚. Percentage of the oriented nuclei of MEFs WT or set7/9 KO was represented in the table. (B) Parental MEFs were pre-treated with none or PFI-2 for 24h and then grown 1 or 24h extra hours in the presence of TGF-β. Cells were lysed with SDS buffer and levels of the indicated proteins were analysed by Western blot.

3. THE IMPORTANCE TO TARGET THE STROMAL COMPARTMENT

3.1 Targeting CAFs as a treatment for breast cancer.

A wealth of evidence has now demonstrated that the microenvironment in which a breast cancer cells grow is as critical to its evolution as the genetic mutations it carries[19]. However, there is still relatively little known about how signals from the microenvironment contribute to the early events in the progression to malignancy. Interfering CAFs activity has been envisioned as an anti-metastatic pharmacological strategy[136]. Vaccination with FAP+ stromal cells inhibits breast tumour growth and lung metastasis[137]. In triple negative breast cancer patient-derived xenograft models, the use of an anti-fibrotic agent as well as TGF-β antagonist named Pirfenidone (PFD) in combination with chemotherapy inhibits CAF number, tumour fibrosis and TGF-β signalling strongly, inhibiting tumour growth and lung metastasis. Thus, targeting tumour-stromal interaction has also clinically relevant potential with combination with chemotherapy[138]. TGF-β blockade significantly decreased tumour growth and metastasis in breast cancer by normalizing the tumour stroma and thus, providing intratumoural delivery of doxorubicin[139].

Our results go in the same direction, inhibiting methyltransferases block myofibroblasts *in vivo*, resulting in a

reduced matrix deposition and a normalized fibrotic breast tumour stroma. The mechanical alteration in the ECM architecture may restrict invasion and metastasis. It is likely that inhibitors reduces matrix stiffness generated by CAFs as described for Snail1-depleted fibroblasts[69].

In addition to the putative effect of the inhibitors on drug delivery methyltransferase inhibitors may also prevent mechanical signalling generated by CAFs that reactive epithelial plasticity. EMT provides tumour cell invasiveness, drug-protection[140] and resistance[141]. Our data confirm that tumour cells invade worse in 3D-ECM generated in the presence of the inhibitors. In these lines, rigid substrates has been shown to stabilize nuclear Snail1 in breast tumour cells[75] and drive EMT[142]. There is strong evidence that expression of Snail1 and other EMT-TFs on tumour cells confers invasiveness and stemness[143], a property required to maintain tumour cells in hostile non-epithelial microenvironments and to resist chemotherapy. Data from two different GEMMs of breast cancer show that transient expression of Snail1 in tumour cells is necessary for metastatic competence[64]. Therefore, a modulation of the stromal mechanics by inhibitors is probably preventing epithelial cell motility and stemness associated to EMT.

Apart from mechanical alteration, methyltransferase inhibitors could be also interfering with the secretion of paracrine factors released by the fibroblasts, as MCP-3[74] and PGE_2[32]

that are secreted in Snail1-dependent manner and promote tumour cell invasion. It would be interesting to test this possibility to better determine the potential of the inhibitors.

3.2 Snail1 is essential for epithelial and stromal plasticity in cancer.

Mechanistically, previous studies performed in the lab analysed the dynamics of Snail1 in normal murine mammary gland cells (NMuMG) that are routinely used as a physiological model of EMT. Upon TGF-β treatment there was a rapid accumulation of Snail1 after 1 hour of treatment and, accordingly with its classical described role, Snail1 was bound to E-cadherin promoter (*CDH1*) to mediate transcriptional repression. The repressing complex acting on epithelial genes includes corepressors as PRMT5[51], PRC2[50], SIN3A[49], and LSD1[144]. After eight hours of TGF-β treatment Snail1 was found to bind preferably to mesenchymal promoters such as *FN1* promoter, concomitantly with NF-κB-p65 nuclear accumulation, and being this NF-κB-p65 pool the principal recruiter of Snail1 to the promoters of the mesenchymal genes activating its transcription[53]. The Snail1/NF-κB-p65 complex on the *FN1* promoter was E-cadherin dependent because active adherens junctions retain NF-κB-p65 associated with the plasma membrane and they impede its nuclear activity as a transcription factor[145].

We also observed that PRMT1 and PRMT4 co-immunoprecipitated with Snail1 in epithelial cells overexpressing ectopic Snail1-HA (Figure 48a). Interestingly, both proteins were upregulated by Snail1 overexpression (see protein levels in the inputs). Moreover, significant levels of both proteins were found bound to the *FN1* promoter in SW620 cells, a metastatic cancer cell line that expresses lower E-cadherin and higher Fibronectin levels than other non-metastatic epithelial cancer cells (Figure 48b). The entrance of NF-κB-p65 to the nuclei depends on adherens junctions and at the same extend, their presence determines also the PRMTs cofactors that are bound to Snail1. Snail1 interacts with the corepressor PRMT5 in the presence of E-cadherin and with the coactivators PRMT1/PRMT4 in their absence (Figure 48c).

As described for activated fibroblasts in this thesis, PRMT1 and PRMT4 may be also present in the Snail1 complex formed in the *FN1* promoter after eight hours of TGF-β treatment during EMT, and it is probable that methyltransferase inhibitors would block the capacity of epithelial cells to undergo EMT. Overall, it is noteworthy to realize that epithelial and fibroblastic plasticity processes in breast cancer are interdependent processes and that both are triggered by the activity of Snail1 and methyltransferases; therefore, Sinefungin may directly target both compartments and efficiently disrupt the positive feedback fuelling epithelial and stromal plasticity involved in metastasis formation.

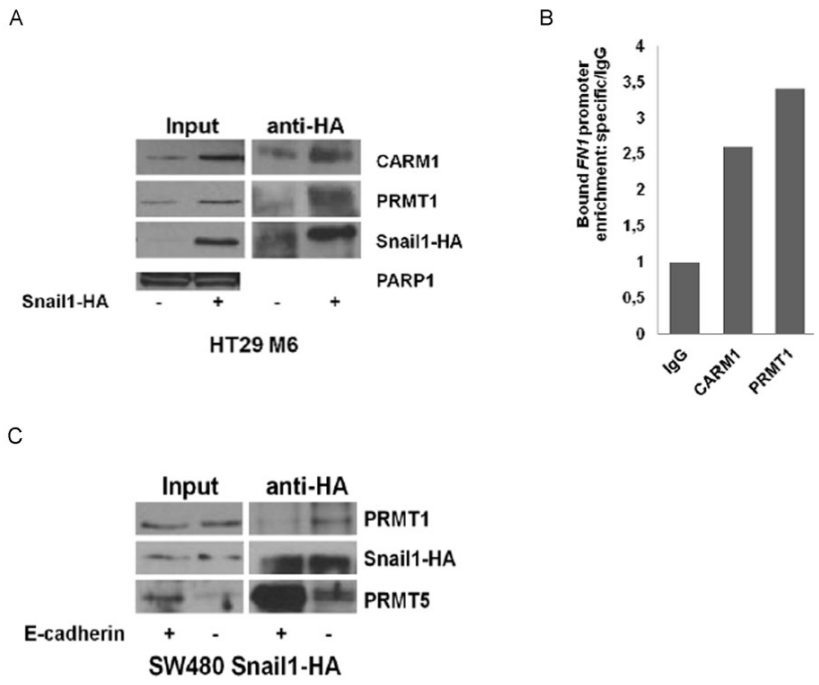

Figure 48: PRMT1 and PRMT4 bind FN1 promoter in epithelial cells forced to undergo EMT and E-cadherin controls its interaction with Snail1. (A) PRMT1 and PRMT4 co-immunoprecipitate with Snail1. Snail1-HA was immunoprecipitated using anti-HA from nuclear extracts of HT29 M6 cells expressing or not ectopic Snail-HA. PARP1 was used as nuclear loading control. (B) PRMT1 and PRMT4 bind to the FN1 promoter in epithelial cells. ChIP in SW620 cells. The FN1 promoter from immunoprecipitates of the indicated antibodies and assay inputs were analysed by qPCR. Bars show FN1 promoter enrichment for each specific antibody relative to an unspecific IgG. (C) E-cadherin controls the interaction of Snail1 with its cofactors. Snail1-HA was immunoprecipitated using nuclear extracts of SW480 Snail-HA cells expressing or not ectopic E-cadherin. Experiments done by Jelena Stanisavljevic.

4. PROPOSED MODEL OF THE EFFECT OF METHYLTRANSFERASE INHIBITORS IN BREAST CANCER

Our work demonstrates that treating breast tumours with the methyltranferase inhibitor Sinefungin reduces stromal compartment in the primary tumour and the formation of lung metastasis. A simplified model of the effect of Sinefungin is summarized in Figure 49. For all these results we suggest methyltransferase inhibitors as good future candidates to treat breast cancer in combination with the existing therapies.

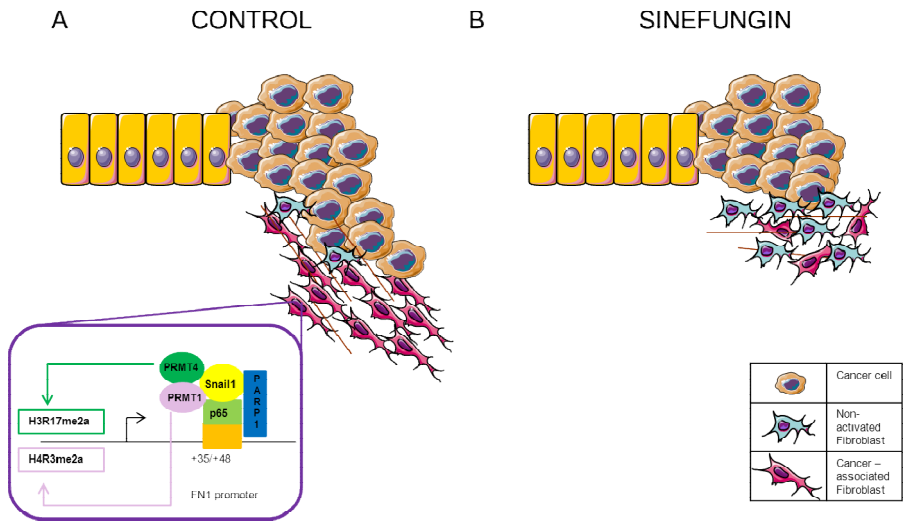

Figure 49: Simplified model of the effect of methyltransferase inhibitors in breast cancer. (A) CAFs are able to synthesize and align ECM components such as *FN1*. Snail1 complex involving PRMT1 and PRMT4 is able to bind *FN1* promoter enhancing its transcription. Moreover this complex is also important for the correct polymerization of Fibronectin. Overall, proper CAF activation lead to an activated stroma with aligned and stiff ECM that guides tumoural cells facilitating invasion and metastasis. (B) Upon methyltranferase inhibitor treatment (Sinefungin) fibroblasts within the stroma are less activated, showing fewer Fibronectin and Collagen deposition. Apart from mechanical alteration in the ECM architecture, biochemical stimuli from CAFs to tumoural cells or to other stromal components such as blood vessels or immune system may be altered as well. The final output is a normalized stroma that is less permissive and allows smaller numbers of metastasis in mice treated with Sinefungin.

CONCLUSIONS

CONCLUSIONS

1. PRMT1 and PRMT4 interact with Snail1 in TGFβ-activated fibroblasts.

2. PRMT1 and PRMT4 interact with the proximal *FN1* promoter and methylate promoter-associated Histone 3 in a TGF-β/Snail1-dependent manner.

3. Alternative splicing is a Snail1-dependent mechanism during fibroblast activation.

4. PRMT1 and PRMT4 depletion prevents Fibronectin fibrillogenesis induced by TGF-β.

5. In culture, methyltransferase inhibitors AMI-1 and Sinefungin block fibroblast activation by TGF-β and prevent the overactivity of IPF fibroblasts.

6. AMI-1 and Sinefungin delay *in vivo* wound healing by impairing myofibroblast activity in the granulation tissue.

7. Sinefungin reduces the stromal compartment in primary PyMT breast tumours and leads to a decreased number of lung metastasis.

MATERIALS AND METHODS

METHODS

1. CELL CULTURE

1.1 Stable cell lines

Cells were grown in DMEM (Invitrogen) supplemented with 2 mmol/L glutamine, 100 U/mL penicillin, 100 mg/L streptomycin, and 10% FBS (GIBCO) and maintained at 37°C in a humid atmosphere containing 5% CO2.

MDA231MB, 1BR3G cells were acquired from the repository stock of our centre. Mouse embryonic fibroblasts (MEFs) and Mesenchymal stem cells (MSCs) were previously established in our laboratory[68].

Inducible PRMT1 KO MEFs were kindly provided by Dr.Stephane Richard, from the Lady Davis Institute for Medical Research, Canada. Tamoxifen-inducible PRMT1 flox/del ER-cre MEF line is treated with 500nM hydroxytamoxifen (OHT) to induce PRMT1 knockout. Two days after induction, genomic DNA locus was completed knocked out but we waited for four-six days for protein completely knocked-out. Usually, we incubate cells with OHT for three-four days and then culture the cells without OHT for one day to avoid OHT effect on the cells. We made 5mM OHT stock in 100% ethanol.

Parental MEFs were transfected with CRISPR vectors from Santa Cruz Biotechnology (sc-420952 for PRMT1 and sc-425576 for PRMT4). Individual GFP positive cells were sorted and cultivated to obtain single or double KO cells. PRMT1 and PRMT4 expression was confirmed by Western blot.

1.2 Primary cell isolation and culture

1.2.1 Epithelial PyMT cells

Single epithelial cell suspensions from breast tumours from MMTV-PyMT mice model[108], kindly provided by Dr. Angel Nebreda (IRB, Barcelona, Spain), were obtained by combining mechanical dissociation and enzymatic degradation using a tumour dissociation kit (MACS, Miltenyi Biotec) and a separation kit (STEMCELL Technologies). Isolated cells were seeded in Epicult-B medium (STEMCELL Technologies) supplemented with EGF 10 ng/mL, FGF 10 ng/mL, heparin 4 µg/mL, and 2% FBS. After 24 hours, serum was removed, and cells were used during the first week after isolation for experiments. Protein expression determined by Western blot indicated that the isolated cells were positive for the epithelial marker E-cadherin and negative for the mesenchymal markers Vimentin and Snail1 (data not shown).

1.2.2 Primary fibroblasts from Idiopathic fibrosis patients

Primary fibroblasts from two patients were isolated by outgrowth of tissue explants from pulmonary tissue as reported previously[146]. All protocols were approved by the Ethics Committees of the Hospital Clínic de Barcelona and the Universitat de Barcelona, and patients gave their written informed consent. Tissue samples from IPF patients were obtained from lung biopsies of patients exhibiting the histopathological pattern of usual interstitial pneumonia. Isolated cells were provided by Dr.Jordi Alcaraz, from the Hospital Clínic. Primary fibroblasts were propagated in standard 2D cultures as previously described[147,148]. In brief, fibroblasts were fast thawed and maintained in fibroblast culture media containing DMEM supplemented with 10% FBS and antibiotics. Fibroblasts were used up to six passages to prevent replicative senescence and guarantee their phenotypic stability.

1.3 Cell treatments

Treatment	Concentration
TGF-β1 (100-21, Prepotech)	5 ng/mL
AMI-1 (ALX-270-440-M025, Enzo)	500μM
Sinefungin (S8559, Sigma)	150μM
MTA (D5011, Sigma)	100μM
EPZ015666 (S7748, Selleckchem)	40μM
PFI-2 (S7294, Selleckchem)	25μM

Table 1. Cell treatments

1.4 Tranfections

For transient transfection with siRNA, 1BR3G or MEFs were grown to 60–80% confluency and transfected with the siGFP or siSnail using the Dharmafect reagent. Cells were kept in complete medium for 48 hours before testing gene expression by RT-qPCR or 72 hours protein analysis by IP, IF or WB.

2. *IN VITRO* EXPERIMENTS

2.1 Three-Dimensional Extracellular Matrices

Three-dimensional ECMs were generated following a previously-described protocol[105]. For 24 wells plates, $5x10^5$

fibroblasts were seeded on gelatine cross-linked glass coverslips and for Boyden Chamber inserts, $1x10^5$ fibroblasts were seeded in gelatine cross-linked inserts, using 100 µl of medium to prevent media leaking through the insert pores. Cell culture media was supplemented with 50 µg/ml ascorbic acid and, where indicated, 5 ng/ml TGF-β or methyltransferase inhibitors listed in Table1. To foster ECM deposition by the plated cells, media was replaced every two days for ten days. Cultures were then washed with pre-warmed (37ºC) PBS and either fixed with 4% PFA for immunofluorescence analysis, or decellularised with 20 mM NH_4OH and 0.5% Triton X-100 in PBS for later use as a cell culture substrate.

2.2 Fibronectin Fibrillogenesis

Glass coverslips were coated overnight with purified soluble fibronectin (2 µg/ml) in PBS. After extensively washing with PBS, cells were plated, grown for 24 and then fixed with 4% PFA in PBS. Background fibronectin left unpolymerized by cells was visualized by immunohistochemistry, and fibronectin fibrillogenesis was estimated using ImageJ software as the fibronectin-cleared background area (with an intensity value lower that a background threshold level) normalized by the number of cells in a field. An area affected by a minimum of 100 cells per condition was analysed.

2.3 Invasion Assays

For some experiments, 8μm porous membranes of Boyden chamber inserts were coated with 50μl of 0.5μg/μL matrigel and incubated 1 hour at 37℃. For others, decellularised ECMs were generated on transwell membranes as explained previously. Approximately $5x10^4$ cells were then seeded in the upper part of the insert in 0.1% serum, 0.1% BSA media, while 10% serum-containing medium was placed in the well below as a chemoattractant. Cells were allowed to invade the ECM for 24 hours, fixed with 4% paraformaldehyde (PFA) in PBS, and stained with DAPI. Non-invading cells were removed from the insert upper side with a cotton swab. Invading cells were imaged with quantified with Image J.

2.4 Cell viability analysis

MEFs grown for 4 days in 96 well-plates were treated with the indicated doses of AMI-1, Sinefungin or MTA for 24 hours, 48 hours or 72 hours. To analyse the amount of viable cells at the end of each treatment 0.5 mg/ml of 3-(4,5-dimethylthiazol-2-yl)-2,5-diphenyltetrazolium bromide (MTT; Sigma) was added to the medium for 3 hours at 37°C. Subsequently, cells were solubilized in DMSO: isopropanol (1:4) and the absorbance at 590 nm in each well was determined. Absorbance quantifies the amount of formazan produced by the cleavage of MTT in mitochondria, and it is proportional to

the number of viable cells. Each treatment was performed in quintruplicates.

3. CELLULAR AND MOLECULAR PROCEDURES

3.1 RNA extraction, reverse transcription and real time qPCR

RNA was extracted with the GenElute TM Mammalian Total RNA Miniprep Kit (Sigma-Aldrich). For quantitative analysis, 1 mg RNA was retrotranscribed with the Transcription First Strand cDNA Synthesis Kit (Roche), and 20ng of the cDNA obtained was used as the template for quantitative SYBR Green-based PCR with specific oligonucleotides (see Table 2). Correct product size was confirmed in agarose gels. The amount of RNA calculated was systematically normalized to the amount of Pumilio RNA.

Primer	Sequence 5′-3′
mPRMT1 sense	5′GAGAATTTTGTAGCCACCTTGG
mPRMT1 antisense	5′-CTTCTCACTACTTTCTGCTTGG
mPRMT4 sense	5′-CCTCATCCAGTTTGCCACAC
mPRMT4 antisense	5′CTGGAAGTACTGCACAGCTGAG
mSnail sense	5′-GCGCCCGTCGTCCTTCTCGTC
mSnail antisense	5′-CTTCCGCGACTGGGGGTCCT
hmPumilio sense	5′-CGGTCGTCCTGAGGATAAAA
hmPumilio antisense	5′-CGTACGTGAGGCGTGAGTAA
hmFibronectin sense	5′-CGAAGCCGGGAAGAGCAAG
hmFibronectin antisense	5′-CGTTCCCACTGCTGATTTATCTG

Table 2. Oligonucleotides used for RNA analyses

3.2 Immunofluorencence analysis

Cells were grown for at least 48 hours on ethanol-sterilized glass coverslips following a standard IF protocol. All steps were carried out at room temperature. Cells were fixed with 4% paraformaldehyde (PFA) for 10 minutes. PFA autofluorescence was quenched by incubating with 50 mM NH_4Cl in PBS for 5 minutes, and cells were then permeabilized with 0.2% Triton X-100 for 5 minutes. Blocking was carried out for 1 hour with PBS containing 3% bovine serum albumin (BSA). Coverslips were incubated for either 1 hour or overnight with a specific primary antibody in blocking solution, and then for 45 minutes with a secondary antibody. For co-localization, cells were initially incubated with a solution containing all of the primary antibodies and then with a solution containing all of the secondary antibodies. Negative controls were performed in parallel, in which the cells that were incubated in a solution lacking the indicated primary antibodies. Nuclei were counterstained with DAPI and coverslips were mounted with fluoromont G.

3.3 Protein extracts and Western blot analyses

For total protein extraction, cells were washed twice with cold PBS and were scraped off the dish in SDS buffer (2% SDS, 50mM TRIS pH 7.5, 10% glycine). Lysates were syringed 5 times and then centrifuged 10 min at top speed. Protein

concentration of the supernatant was quantified by Lowry method.

Depending on the experiments 1-20 ug of protein mixed with sample buffer was loaded into SDS-polyacrylamide gel electrophoresis, samples were run in TGS buffer at 120V. Proteins were transferred into a nitrocellulose membrane at 400mA 90 min. Once the proteins were transferred membranes were blocked with 5% milk at room temperature for 1 hour and then incubated with primary antibody overnight at 4 ˚C with shacking. Primary antibodies used are listed in Table 3. After three washes with TBS-Tween membranes were incubated with Horseradish peroxidase (HRP)-conjugated secondary antibody (DAKO) 1h at room temperature and washed again with TBS-Tween. The detection was carried out using HRP enhance chemiluminiscence (ECL) reactive (Millipore) and exposing to autoradiographic films.

Antibody	Specie	Dilution
Snail (Hybridoma,Francí et al., 2006)	Mouse	1:10
Fibronectin (A0245, Dako)	Rabbit	1:10000
α-SMA (A2547, Sigma)	Mouse	1:5000
Pyruvate kinase (Chemicon)	Goat	1:10000
α-tubulin	Mouse	1:10000
β-actin (Abcam ab8227)	Rabbit	1:10000
Prmt1 (Bethyl A300-722A)	Rabbit	1:2000
Prmt4 (Bethyl A300-421A)	Rabbit	1:5000
FAP (Abcam, Ab28244)	Rabbit	1:1000
H3 (Abcam, Ab1791)	Rabbit	1:10000
Me2a Asym24 (Millipore, 07-414)	Rabbit	1:2000
Me2a H3R17 (Millipore, 07-214)	Rabbit	1:2000
Me2a H4R3 (Abcam, Ab194683)	Rabbit	1:2000
Me2s Sym10 (Millipore, 07-412)	Rabbit	1:2000

Table 3. Antibodies used for Protein Analysis

3.4 Immunohistochemistry and Second harmonic generation analysis

Harvested tissue samples were fixed in formalin and embedded in paraffin. Sections of 4 μm were obtained with a microtome and then subsequently dewaxed and rehydrated. Antigens were retrieved by boiling the samples in Tris/EDTA (50 mM Tris/HCl, 1 mM EDTA, and 10 mM NaCl, pH 9.0) for 15 minutes. Endogenous peroxidase activity was quenched for 15 minutes with 4% hydrogen peroxide in PBS containing 0.1% sodium azide. After several rinses with PBS, sections were incubated with PBS containing 1% BSA to block non-

specific binding and then washed with PBS. Sections were incubated with the indicated antibodies overnight at 4°C. After several rinses with PBS, bound antibody was detected using anti-mouse or anti-rabbit Envision. Sections were counterstained with haematoxylin and mounted for microscopy analysis.

Some paraffin sections were stained with Fast Green safranin. For second harmonic generation analyses was used the multiphoton microscoe in the Advanced Light Microscopy Unit of the CRG (Centre of Genomic Research) at PRBB (Barcelona Biomedical Research Park). Dewaxed and dehydrated tissue slices were directly mounted with fluoromont DAPI).

3.5 Immunoprecipitation assay

For immunoprecipitation, indicated antibody was added to 1 mg of total RIPA extracts pre-cleared with protein-A or -G agarose beads and incubated overnight at 4°C. Antibody-bound proteins were then pulled-down with protein-A or -G agarose beads and washed three times with RIPA buffer. The washed beads were resuspended in sample buffer and used for western blot analysis. For mass spectrometry analysis, beads were washed in 200mM Ammonium bicarbonate (ABC) buffer, resuspended in 6M urea solution, reduced with DTT, alkylated with Iodoacetamide (IAM) and digested with

Trypsin. Finally samples were desalted using C18 stage tips and dried before mass-spectometry analysis.

3.6 Chromatin immunoprecipitation

Cells seeded the day before were washed with warm phosphate buffered saline (PBS) and then cross-linked for 10 minutes at 37°C with 1% formaldehyde in DMEM. To stop the reaction, cells were incubated for 5 minutes more after adding glycine at final concentration of 0.125M. Cells were washed twice with cold PBS and scrapped off with cold soft lysis buffer (50mM Tris pH 8.0, 2mM EDTA, 0.1% Nonidet P-40, 10% glycerol). Lysates were incubated 10 minutes on ice and then centrifuged for 15 minutes at 3000rpm in cold. Pellet was resuspended in SDS lysis buffer (1% SDS, 10mM EDTA, 50mM Tris pH 8.0) and sonicated using 40% of the sonicator's amplitude (Branson DIGITAL Sonifier UNIT Model S-450D) in order to generate DNA fragments ranging from 200 to 1000 kb in length. Lysates were incubated for 20 minutes on ice and centrifuged at maximum speed for 10 minutes. Optionally, the length of the fragments was confirmed running a small volume of the sample on 2% agarose gel.

Protein concentration was determined by Lowry and the desired amount of protein per immunoprecipitation (usually between 250µg and 1mg) was diluted ten times in dilution

buffer (0.001% SDS, 1.1% Triton X-100, 16.7mM Tris pH 8.0, 2mM EDTA, 2mM EGTA, 167mM NaCl).

In order to reduce background, samples were incubated for 3 hours at 4°C with IgGs of the same specie as the used antibody and protein G or protein A beads. 10% of the sample was kept apart for the input and the samples were divided in half and incubated with either the specific antibody or the IgG of the same species overnight at 4°C with agitation. Beads were blocked overnight with BSA 0,5%.

The next day beads were washed with dilution buffer and added to all the samples and incubated 4 hours at 4°C with agitation. Afterwards, five washes were performed on ice with each in each of the given buffers: low salt buffer (0.1% SDS, 1% Triton X-100, 2mM EDTA, 20mM Tris, pH 8.0, and 150mM NaCl), high salt buffer (the same as low salt but with 500 mM NaCl), LiCl Buffer (250mM LiCl, 1% Nonidet P-40, 1% Sodium deoxycholate, 1mM EDTA, and 10mM Tris, pH 8.0), and TE buffer. Beads were recovered and samples were eluted with the elution buffer (100mM Na2CO3, 1% SDS) at 37°C. Elutes were recovered by centrifugation (3 minutes, 2000rpm). To each sample and to the inputs NaCl was added at final concentration of 250mM and both the samples and the inputs were decrosslinked by incubation at 65°C overnight, following by digestion with proteinase K for 1 hour. DNA was purified and quantitative PCR was performed.

Primer	Sequence 5′-3′
mFibronectin promoter sense	5′-GTTGAGACGGTGGGGGAGAGA
mFibronectin promoter antisense	5′-CCGTCCCCTTCCCCA
mTERRA 18q _7 sense (ChIP control)	5′-CATCATTGCAATCTTCGAGTG
mTERRA 18q _7 antisense (ChIP control)	5′TGGAGATTACAGTGTTGTGAATG

Table 4. Oligonucleotides used for chIP.

3.7 Proteomic analyses

Samples were analysed in the proteomics facility of CRG by Liquid Chromatography–Mass Spectrometry using a MEDI_CID method in the nanoLC LTQ Orbitrap XL. Samples were searched against SwissProt (Mice) database and filtered based on the 5% False Discovery rate.

3.8 RNA sequencing and validation

Total RNA was extracted from cultured cells with GenElute Mammalian Total RNA Miniprep kit (Sigma). Samples were paired-end sequenced in CRG Sequencing Unit until reaching 80M reads/sample. For splicing analysis, the SANJUAN software designed by P. Papasaikas was run with a threshold of 0.15 delta Percentage Spliced In (https://github.com/ppapasaikas/SANJUAN).

For splicing variants validation, DNA was obtained by using Transcriptase First Strand cDNA Synthesis Kit (Roche). For

semi-quantitative PCR, 1ng of cDNA was amplified with Biotaq (Bioline) in the provided buffer. Primers used are described in Table 5.

Primer	Sequence 5′-3′
mFibronectin exon 32 sense	5′-CCCTGGTTCAAACTGCAGTG
mFibronectin exon 34 antisense	5′-GGTTGATTTCTTTCATTGGTCCTG
mMyl6 exon 3 sense	5′-TAGAGATGCTAGTGGCGGGG
mMyl6 exon 5 antisense	5′- CAGAAATCACACTGGGCAAGG

Table 5. Oligonucleotides used for RNAseq validation

4. ANIMALS

Animals were maintained in a specific pathogen-free area and fed *ad libitum*. All the procedures were approved by the Animal Research Ethical Committee from the Parc de Recerca Biomèdica de Barcelona (Barcelona, Spain) and by the Generalitat de Catalunya.

4.1 *In Vivo* Wound Healing

FVB mice were anesthetized with isoflurane for skin wounding. After cleaning the exposed skin with 70% ethanol, full-thickness excisional skin wounds were made aseptically on either side of the dorsal midline using a 6 mm biopsy

punch. Two wounds were usually made on the same animal. Wounds were photographed and measured every day. The wound tissue and surrounding skin from the wound margin were harvested from mice at five days post-wounding, fixed in formalin, embedded in paraffin, and sectioned in 4 μM slices for immunohistological analysis. For drug treatment, mice were intraperitoneally injected every other day starting the day before wounding.

4.3 Mammary Orthotopic Transplantation and rejection

MMTV-PyMT mice were kindly provided by Dr. Angel Nebreda (IRB, Barcelona, Spain). This murine line expresses the polyomavirus middle T antigen (PyMT) under the control of the mouse mammary tumour virus promoter (MMTV); female mice develop mammary tumours with lung metastases

Synchronized primary tumours were generated by implanting isolated mammary epithelial from MMTV-PyMT tumours and mesenchymal stem cells (MSCs) at 1:1 ratio in matrigel. Eight week old NOD-SCID (Non Obese Diabetic/Severe Combined ImmunoDeficiency) females were anesthetized with isoflurane and two inguinal mammary fad pats per mice were injected. Growth of the tumour was followed every other day. When tumours reached 0.2-0.4 or 1 cm mice underwent surgical resection of the primary tumour. For surgery, mice were anesthetized as described above and wounds closed with

surgical clips. Mice were maintained alive and extra month to allow the growth of metastasis and then sacrificed to quantify tumour lung metastatic foci. Metastases were counted in haematoxylin and eosin stained slides of formalin fixed paraffin embedded lungs. Approximately fifteen slides per lung were analysed. For both mammary fad pad transplantation and tumour resection mice were treated with buprenorphine 0.1 mg/kg and anesthetized with isoflurane 3.5-2.5% plus 0^2 0,8 L/min following the procedure approved by the ethical committee.

BIBLIOGRAPHY

BIBLIOGRAPHY

1. Mehlen, P. & Puisieux, A. Metastasis: A question of life or death. *Nat. Rev. Cancer* **6,** 449–458 (2006).
2. Joyce, J. A. & Pollard, J. W. Microenvironmental regulation of metastasis. *Nat. Rev. Cancer* **9,** 239–252 (2009).
3. Hanahan, D. & Weinberg, R. A. The hallmarks of cancer. *Cell* **100,** 57–70 (2000).
4. Luo, J., Solimini, N. L. & Elledge, S. J. Principles of Cancer Therapy: Oncogene and Non-oncogene Addiction. *Cell* **136,** 823–837 (2009).
5. Hanahan, D. & Weinberg, R. A. Hallmarks of cancer: The next generation. *Cell* **144,** 646–674 (2011).
6. Bissell, M. J. & Hines, W. C. Why don't we get more cancer? A proposed role of the microenvironment in restraining cancer progression. *Nat. Med.* **17,** 320–329 (2011).
7. Virchow, R. *Die cellularpathologie in ihrer Begruendung auf Physiologische und Gewebelehre*. (1858).
8. Duvall, M. Atlas d'Embyologie. (1879).
9. Parsonage, G. *et al.* A stromal address code defined by fibroblasts. *Trends Immunol* **26,** 150–156 (2005).
10. Kalluri, R. & Zeisberg, M. Fibroblasts in cancer. *Nat. Rev. Cancer* **6,** 392–401 (2006).
11. Gabbiani, G., Ryan, G. B. & Majno, G. Presence of modified fibroblasts in granulation tissue and their possible role in wound contraction. *Experientia* **27,** 549–550 (1971).
12. Wynn, T. a. Mechanism of fibrosis: therapeutic transplation for fibrotic disease. *Nat. Med.* **18,** 1028–1040 (2013).
13. Micallef, L. *et al.* The myofibroblast, multiple origins for major roles in normal and pathological tissue repair. *Fibrogenes. Tissue Repair* **5,** S5 (2012).

14. Strutz, F. & Zeisberg, M. Renal Fibroblasts and Myofibroblasts in Chronic Kidney Disease. *J. Am. Soc. Nephrol.* **17,** 2992–2998 (2006).

15. Hinz, B. *et al.* The myofibroblast: One function, multiple origins. *Am. J. Pathol.* **170,** 1807–1816 (2007).

16. Fuxe, J. & Karlsson, M. C. I. TGF-beta-induced epithelial-mesenchymal transition: A link between cancer and inflammatio. *Cancer Inflamm. Mech. Chem. Biol. Clin. Asp.* **22,** 23–39 (2014).

17. Dvorak, H. F. Tumors: Wounds That Do Not Heal--Redux. *Cancer Immunol. Res.* **3,** 1–11 (2015).

18. Yazdani, S., Bansal, R. & Prakash, J. Drug targeting to myofibroblasts: Implications for fibrosis and cancer. *Adv. Drug Deliv. Rev.* **121,** 101–116 (2017).

19. Dumont, N. *et al.* Breast Fibroblasts Modulate Early Dissemination, Tumorigenesis, and Metastasis through Alteration of Extracellular Matrix Characteristics. *Neoplasia* **15,** 249–IN7 (2013).

20. Junyao, L. *et al.* Idiopathic pulmonary fibrosis will increase the risk of lung cancer. *Chin. Med. J. (Engl).* **127,** 3142–3149 (2014).

21. Rybinski, B., Franco-Barraza, J. & Cukierman, E. The wound healing, chronic fibrosis, and cancer progression triad. *Physiol. Genomics* **46,** 223–244 (2014).

22. Calon, A., Tauriello, D. V. F. & Batlle, E. TGF-beta in CAF-mediated tumor growth and metastasis. *Semin. Cancer Biol.* **25,** 15–22 (2014).

23. Calon, A. *et al.* Dependency of Colorectal Cancer on a TGF-β-Driven Program in Stromal Cells for Metastasis Initiation. *Cancer Cell* **22,** 571–584 (2012).

24. Kardassis, D., Murphy, C., Fotsis, T., Moustakas, A. & Stournaras, C. Control of transforming growth factor signal transduction by small GTPases. *FEBS J.* **276,** 2947–2965 (2009).

25. Olumi, A. F. *et al.* Carcinoma-associated Fibroblasts Direct Tumor Progression of Initiated Human Prostatic Epithelium Carcinoma-associated Fibroblasts Direct

Tumor Progression of Initiated Human. 5002–5011 (1999).

26. Condeelis, J. & Segall, J. E. Intravital imaging of cell movement in tumours. *Nat. Rev. Cancer* **3,** 921–930 (2003).

27. Orozco, C. A. *et al.* Targeting galectin-1 inhibits pancreatic cancer progression by modulating tumor–stroma crosstalk. *Proc. Natl. Acad. Sci.* 201722434 (2018). doi:10.1073/pnas.1722434115

28. Rhim, A. D. *et al.* Stromal elements act to restrain, rather than support, pancreatic ductal adenocarcinoma. *Cancer Cell* **25,** 735–747 (2014).

29. Özdemir, B. C. *et al.* Depletion of carcinoma-associated fibroblasts and fibrosis induces immunosuppression and accelerates pancreas cancer with reduced survival. *Cancer Cell* **25,** 719–734 (2014).

30. De Boeck, A. *et al.* Differential secretome analysis of cancer-associated fibroblasts and bone marrow-derived precursors to identify microenvironmental regulators of colon cancer progression. *Proteomics* **13,** 379–388 (2013).

31. De Boeck, A. *et al.* Bone marrow-derived mesenchymal stem cells promote colorectal cancer progression through paracrine neuregulin 1/HER3 signalling. *Gut* **62,** 550–560 (2013).

32. Alba-Castellón, L. *et al.* Snail1-dependent activation of cancer-associated fibroblast controls epithelial tumor cell invasion and metastasis. *Cancer Res.* **76,** 6205–6217 (2016).

33. Mishra, P., Banerjee, D. & Ben-Baruch, A. Chemokines at the crossroads of tumor-fibroblast interactions that promote malignancy. *J. Leukoc. Biol.* **89,** 31–39 (2011).

34. Erez, N., Truitt, M., Olson, P. & Hanahan, D. Cancer-Associated Fibroblasts Are Activated in Incipient Neoplasia to Orchestrate Tumor-Promoting Inflammation in an NF-κB-Dependent Manner. *Cancer Cell* **17,** 135–147 (2010).

35. Provenzano, P. P. *et al.* Collagen reorganization at the tumor-stromal interface facilitates local invasion. *BMC Med.* **4,** 1–15 (2006).

36. Malik, R., Lelkes, P. I. & Cukierman, E. Biomechanical and biochemical remodeling of stromal extracellular matrix in cancer. *Trends Biotechnol.* **33,** 230–236 (2015).

37. Gaggioli, C. *et al.* Fibroblast-led collective invasion of carcinoma cells with differing roles for RhoGTPases in leading and following cells. *Nat. Cell Biol.* **9,** 1392–1400 (2007).

38. Lu, P., Weaver, V. M. & Werb, Z. The extracellular matrix: A dynamic niche in cancer progression. *J. Cell Biol.* **196,** 395–406 (2012).

39. Purva Singh, Cara Carraher, and J. E. S. Assembly of fibronectin into extracellular matrix. *Annu Rev Cell Dev Biol* **3,** 214–222 (2010).

40. Lee, S. H. & Dominguez, R. Regulation of actin cytoskeleton dynamics in cells. *Mol. Cells* **29,** 311–325 (2010).

41. Zhong, C. *et al.* Rho-mediated contractility exposes a cryptic site in fibronectin and induces fibronectin matrix assembly. *J. Cell Biol.* **141,** 539–551 (1998).

42. Khatau, S. B. *et al.* A perinuclear actin cap regulates nuclear shape. *Proc. Natl. Acad. Sci.* **106,** 19017–19022 (2009).

43. Amatangelo, M. D., Bassi, D. E., Klein-Szanto, A. J. P. & Cukierman, E. Stroma-derived three-dimensional matrices are necessary and sufficient to promote desmoplastic differentiation of normal fibroblasts. *Am. J. Pathol.* **167,** 475–488 (2005).

44. Castelló-Cros, R., Khan, D. R., Simons, J., Valianou, M. & Cukierman, E. Staged stromal extracellular 3D matrices differentially regulate breast cancer cell responses through PI3K and beta1-integrins. *BMC Cancer* **9,** 1–19 (2009).

45. Conklin, M. W. *et al.* Aligned collagen is a prognostic

signature for survival in human breast carcinoma. *Am. J. Pathol.* **178,** 1221–1232 (2011).

46. Grau, Y., Carteret, C. & Simpson, P. Mutations and chromosomal rearrangements affecting the expression of snail, a gene involved in embryonic patterning in Drosophila melanogaster. *Genetics* **108,** 347–360 (1984).

47. Labonne, C. & Bronner-Fraser, M. Snail-related transcriptional repressors are required in Xenopus for both the induction of the neural crest and its subsequent migration. *Dev. Biol.* **221,** 195–205 (2000).

48. Carver, E. a *et al.* The Mouse Snail Gene Encodes a Key Regulator of the Epithelial-Mesenchymal Transition The Mouse Snail Gene Encodes a Key Regulator of the Epithelial-Mesenchymal Transition. *Mol Cell Biol* **21,** 8184–8188 (2001).

49. Peinado, H., Ballestar, E., Esteller, M. & Cano, A. Snail mediates E-cadherin repression by the recruitment of the Sin3A/histone deacetylase 1 (HDAC1)/HDAC2 complex. *Mol. Cell. Biol.* **24,** 306–19 (2004).

50. Herranz, N. *et al.* Polycomb Complex 2 Is Required for E-cadherin Repression by the Snail1 Transcription Factor. *Mol. Cell. Biol.* **28,** 4772–4781 (2008).

51. Hou, Z. *et al.* The LIM Protein AJUBA Recruits Protein Arginine Methyltransferase 5 To Mediate SNAIL-Dependent Transcriptional Repression. *Mol. Cell. Biol.* **28,** 3198–3207 (2008).

52. Wang, Y., Shi, J., Chai, K., Ying, X. & Zhou, B. The Role of Snail in EMT and Tumorigenesis. *Curr. Cancer Drug Targets* **13,** 963–972 (2013).

53. Stanisavljevic, J., Porta-de-la-Riva, M., Batlle, R., de Herreros, A. G. & Baulida, J. The p65 subunit of NF-κB and PARP1 assist Snail1 in activating fibronectin transcription. *J. Cell Sci.* **124,** 4161–4171 (2011).

54. Kalluri, R. & Weinberg, R. a. Review series The basics of epithelial-mesenchymal transition. *J. Clin. Invest.* **119,** 1420–1428 (2009).

55. Peinado, H., Quintanilla, M. & Cano, A. Transforming growth factor β-1 induces Snail transcription factor in epithelial cell lines. Mechanisms for epithelial mesenchymal transitions. *J. Biol. Chem.* **278,** 21113–21123 (2003).

56. Julien, S. *et al.* Activation of NF-κB by Akt upregulates Snail expression and induces epithelium mesenchyme transition. *Oncogene* **26,** 7445–7456 (2007).

57. Yook, J. I., Li, X.-Y., Ota, I., Fearon, E. R. & Weiss, S. J. Wnt-dependent regulation of the E-cadherin repressor snail. *J. Biol. Chem.* **280,** 11740–8 (2005).

58. Escriva, M. *et al.* Repression of PTEN Phosphatase by Snail1 Transcriptional Factor during Gamma Radiation-Induced Apoptosis. *Mol. Cell. Biol.* **28,** 1528–1540 (2008).

59. Liu, S., Kumar, S. M., Martin, J. S., Yang, R. & Xu, X. Snail1 mediates hypoxia-induced melanoma progression. *Am. J. Pathol.* **179,** 3020–3031 (2011).

60. Nieto, M. A. & Cano, A. The epithelial-mesenchymal transition under control: Global programs to regulate epithelial plasticity. *Semin. Cancer Biol.* **22,** 361–368 (2012).

61. Barrallo-Gimeno, A. The Snail genes as inducers of cell movement and survival: implications in development and cancer. *Development* **132,** 3151–3161 (2005).

62. Batlle, E. *et al.* The transcription factor Snail is a repressor of E-cadherin gene expression in epithelial tumour cells. *Nat. CELL Biol. cellbio.nature.com* **2,** (2000).

63. Cano, A. *et al.* The transcription factor Snail controls epithelial-mesenchymal transitions by repressing E-cadherin expression. *Nat. Cell Biol.* **2,** 76–83 (2000).

64. Tran, H. D. *et al.* Transient SNAIL1 expression is necessary for metastatic competence in breast cancer. *Cancer Res.* **74,** 6330–6340 (2014).

65. Zheng, X. *et al.* EMT Program is Dispensable for Metastasis but Induces Chemoresistance in Pancreatic

Cancer. **527,** 525–530 (2016).

66. Fischer, K. R. *et al.* Epithelial-to-mesenchymal transition is not required for lung metastasis but contributes to chemoresistance. *Nature* **527,** 472–476 (2015).

67. Rowe, R. G. *et al.* Mesenchymal cells reactivate Snail1 expression to drive three-dimensional invasion programs. *J. Cell Biol.* **184,** 399–408 (2009).

68. Batlle, R. *et al.* Snail1 controls TGF-β responsivness and differentiation of Mesenchymal Stem Cells. *Oncogene* **32,** 3381–3389 (2013).

69. Stanisavljevic, J. *et al.* Snail1-expressing fibroblasts in the tumor microenvironment display mechanical properties that support metastasis. *Cancer Res.* (2015). doi:10.1158/0008-5472.CAN-14-1903

70. Francí, C. *et al.* Snail1 protein in the stroma as a new putative prognosis marker for colon tumours. *PLoS One* **4,** 1–7 (2009).

71. Scarpa, M. *et al.* Snail1 transcription factor is a critical mediator of hepatic stellate cell activation following hepatic injury. 316–326 (2011). doi:10.1152/ajpgi.00141.2010.

72. Biswas, H. & Longmore, G. D. Action of SNAIL1 in cardiac myofibroblasts is important for cardiac fibrosis following hypoxic injury. *PLoS One* **11,** 1–18 (2016).

73. Goyal, A., Linskey, K. R., Kay, J., Duncan, L. M. & Nazarian, R. M. Differential expression of Hedgehog and Snail in cutaneous fibrosing disorders implications for targeted inhibition. *Am. J. Clin. Pathol.* **146,** 709–717 (2016).

74. Herrera, A. *et al.* Protumorigenic effects of Snail-expression fibroblasts on colon cancer cells. *Int. J. Cancer* **134,** 2984–2990 (2014).

75. Zhang, K. *et al.* Mechanical signals regulate and activate SNAIL1 protein to control the fibrogenic response of cancer-associated fibroblasts. *J. Cell Sci.* **129,** 1989–2002 (2016).

76. Larsen, S. C. *et al.* Proteome-wide analysis of arginine monomethylation reveals widespread occurrence in human cells. *Sci. Signal.* **9,** 1–15 (2016).

77. Bedford, M. T. & Clarke, S. G. Protein Arginine Methylation in Mammals: Who, What, and Why. *Mol. Cell* **33,** 1–13 (2009).

78. Yang, Y. & Bedford, M. T. Protein arginine methyltransferases and cancer. *Nat. Rev. Cancer* **13,** 37–50 (2013).

79. Chen, D. *et al.* Regulation of transcription by a protein methyltransferase. *Science (80-.).* **284,** 2174–2177 (1999).

80. Wang, H. Methylation of Histone H4 at Arginine 3 Facilitating Transcriptional Activation by Nuclear Hormone Receptor. *Science (80-.).* **293,** 853–857 (2001).

81. Pal, S., Vishwanath, S. N., Tempst, P., Sif, S. & Erdjument-bromage, H. Negatively regulates expression of ST7 and NM23 tumor suppressor genes human SWI / SNF-associated PRMT5 methylates histone H3 arginine 8 and negatively regulates expression of ST7 and NM23 tumor suppressor genes. *Mol. Cell. Biol.* **24,** 9630–9645 (2004).

82. Auclair, Y. & Richard, S. The role of arginine methylation in the DNA damage response. *DNA Repair* **12,** 459–465 (2013).

83. Strahl, B. D. *et al.* Methylation of histone H4 at arginine 3 occurs in vivo and is mediated by the nuclear receptor coactivator PRMT1. *Curr. Biol.* **11,** 996–1000 (2001).

84. Zhang, L. *et al.* Cross-talk between PRMT1-mediated methylation and ubiquitylation on RBM15 controls RNA splicing. *Elife* **4,** 1–28 (2015).

85. Dhar, S. *et al.* Loss of the major type i arginine methyltransferase PRMT1 causes substrate scavenging by other PRMTs. *Sci. Rep.* **3,** 1–6 (2013).

86. Daujat, S. *et al.* Crosstalk between CARM1 methylation and CBP acetylation on histone H3. *Curr. Biol.* **12,**

2090–2097 (2002).

87. Ohkura, N., Takahashi, M., Yaguchi, H., Nagamura, Y. & Tsukada, T. Coactivator-associated arginine methyltransferase 1, CARM1, affects pre-mRNA splicing in an isoform-specific manner. *J. Biol. Chem.* (2005). doi:10.1074/jbc.M502173200

88. Stephen S. Koh‡,§, Hongwei Li‡, Young-Ho Lee¶, Randall B. Widelitz‡, Cheng-Ming Chuong‡, and M. R. S. Synergistic Coactivator Function by Coactivator-associated Arginine Methyltransferase (CARM) 1 and β -Catenin with Two Different Classes of DNA-binding Transcriptional Activators. *J Biol Chem* **51,** 87–100 (2002).

89. An, W., Kim, J. & Roeder, R. G. Ordered cooperative functions of PRMT1, p300, and CARM1 in transcriptional activation by p53. *Cell* **117,** 735–748 (2004).

90. Hassa, P. O., Covic, M., Bedford, M. T. & Hottiger, M. O. Protein Arginine Methyltransferase 1 Coactivates NF-κB-Dependent Gene Expression Synergistically with CARM1 and PARP1. *J. Mol. Biol.* **377,** 668–678 (2008).

91. Neuenkirchen, N., Chari, A. & Fischer, U. Deciphering the assembly pathway of Sm-class U snRNPs. *FEBS Lett.* **582,** 1997–2003 (2008).

92. Pahlich, S., Zakaryan, R. P. & Gehring, H. Protein arginine methylation: Cellular functions and methods of analysis. *Biochim. Biophys. Acta - Proteins Proteomics* **1764,** 1890–1903 (2006).

93. Boisvert, F. M. *et al.* Symmetrical dimethylarginine methylation is required for the localization of SMN in Cajal bodies and pre-mRNA splicing. *J. Cell Biol.* **159,** 957–969 (2002).

94. Cheng, D., Côté, J., Shaaban, S. & Bedford, M. T. The Arginine Methyltransferase CARM1 Regulates the Coupling of Transcription and mRNA Processing. *Mol. Cell* **25,** 71–83 (2007).

95. Kim, Y.-R. *et al.* Differential CARM1 expression in

prostate andcolorectal cancers. **10 OP-B,** 197 (2010).

96. Le Romancer, M., Treilleux, I., Bouchekioua-Bouzaghou, K., Sentis, S. & Corbo, L. Methylation, a key step for nongenomic estrogen signaling in breast tumors. *Steroids* **75,** 560–564 (2010).
97. Avasarala, S. *et al.* PRMT1 Is a novel regulator of epithelial-mesenchymal-transition in non-small cell lung cancer. *J. Biol. Chem.* **290,** 13479–13489 (2015).
98. Wang, L. *et al.* CARM1 Methylates Chromatin Remodeling Factor BAF155 to Enhance Tumor Progression and Metastasis (Cancer Cell (2014) 25 (21–36)). *Cancer Cell* **30,** 179–180 (2016).
99. Gao, Y. *et al.* The dual function of PRMT1 in modulating epithelial-mesenchymal transition and cellular senescence in breast cancer cells through regulation of ZEB1. *Sci. Rep.* **6,** 1–13 (2016).
100. Zakrzewicz, D. *et al.* Elevated protein arginine methyltransferase 1 expression regulates fibroblast motility in pulmonary fibrosis. *Biochim. Biophys. Acta - Mol. Basis Dis.* **1852,** 2678–2688 (2015).
101. Gayatri, S. *et al.* Using oriented peptide array libraries to evaluate methylarginine-specific antibodies and arginine methyltransferase substrate motifs. *Sci. Rep.* **6,** 1–8 (2016).
102. Sylvestersen, K. B. & Nielsen, M. L. Large-Scale Identification of the Arginine Methylome by Mass Spectrometry. *Curr. Protoc. Protein Sci.* (2015). doi:10.1002/0471140864.ps2407s82
103. Uhlmann, T. *et al.* A Method for Large-scale Identification of Protein Arginine Methylation* □ S. doi:10.1074/mcp.M112.020743
104. Cheng, D. *et al.* Small molecule regulators of protein arginine methyltransferases. *J. Biol. Chem.* **279,** 23892–23899 (2004).
105. Cukierman, R. C.-C. and E. Stromagenesis during tumorigenesis: characterization of tumor- associated fibroblasts and stroma-derived 3D matrices. *Methods*

Mol Biol **522,** 14–19 (2009).

106. Fulton, F. C. and D. J. R. An Inhibitor of Protein Arginine Methyltransferases, 7,7?-Carbonylbis(azanediyl)bis(4-hydroxynaphthalene-2-sulfonic acid (AMI-1), Is a Potent Scavenger of NADPH-Oxidase–Derived Superoxide. *Mol. Pharmacol.* **244,** 6049–6055 (2009).
107. Travis, W. D. *et al.* An official American Thoracic Society/European Respiratory Society statement: Update of the international multidisciplinary classification of the idiopathic interstitial pneumonias. *Am. J. Respir. Crit. Care Med.* **188,** 733–748 (2013).
108. Guy, C. T., Cardiff, R. D. & Muller, W. J. Induction of mammary tumors by expression of polyomavirus middle T oncogene: a transgenic mouse model for metastatic disease. *Mol. Cell. Biol.* **12,** 954–961 (1992).
109. Mao, Y. & Schwarzbauer, J. E. Fibronectin fibrillogenesis, a cell-mediated matrix assembly process. *Matrix Biol.* **24,** 389–399 (2005).
110. Haraguchi, M. *et al.* Snail regulates cell-matrix adhesion by regulation of the expression of integrins and basement membrane proteins. *J. Biol. Chem.* **283,** 23514–23523 (2008).
111. Srijita Dhar, Zhe Sun, Gerald A. Meininger1, and M. A. H. NON-ENZYMATIC GLYCATION INTERFERES WITH FIBRONECTIN-INTEGRIN INTERACTIONS IN VASCULAR SMOOTH MUSCLE CELLS. *Microcirculation* **24,** 1–30 (2017).
112. Boisvert, F. O.-M., Cô, J., Boulanger, M.-C. & Phane Richardţ, S. A Proteomic Analysis of Arginine-methylated Protein Complexes*. *Mol. Cell. Proteomics* **2,** 1319–1330 (2003).
113. Cramer, P., Pesce, C. G., Baralle, F. E. & Kornblihtt, a R. Functional association between promoter structure and transcript alternative splicing. *Proc. Natl. Acad. Sci. U. S. A.* **94,** 11456–11460 (1997).
114. Maniatis, T. & Reed, R. An extensive network of

coupling among gene expression machines. *Nature* **416,** 499–506 (2002).

115. Monsalve, M. *et al.* Direct coupling of transcription and mRNA processing through the thermogenic coactivator PGC-1. *Mol. Cell* **6,** 307–316 (2000).
116. Corden, J. L. & Patturajan, M. A CTD function linking transcription to splicing. *Trends Biochem. Sci.* **22,** 413–416 (1997).
117. Johnson, K. J. *et al.* PROTEIN CHEMISTRY AND STRUCTURE : The Compact Conformation of Fibronectin Is Determined by Intramolecular Ionic Interactions The Compact Conformation of Fibronectin Is Determined by Intramolecular Ionic Interactions *. **274,** 15473–15479 (1999).
118. Kinoshita, M., Field, C. M., Coughlin, M. L., Straight, A. F. & Mitchison, T. J. Self- and actin-templated assembly of mammalian septins. *Dev. Cell* **3,** 791–802 (2002).
119. Yamashiro, S. *et al.* Myosin Phosphatase-Targeting Subunit 1 Regulates Mitosis by Antagonizing Polo-like Kinase 1. *Dev. Cell* **14,** 787–797 (2008).
120. Leung, C. L., Sun, D., Zheng, M., Knowles, D. R. & Liem, R. K. H. Microtubule actin cross-linking factor (MACF): A hybrid of dystonin and dystrophin that can interact with the actin and microtubule cytoskeletons. *J. Cell Biol.* **147,** 1275–1285 (1999).
121. Ohkubo, T. & Ozawa, M. The transcription factor Snail downregulates the tight junction components independently of E-cadherin downregulation. *J. Cell Sci.* **117,** 1675–1685 (2004).
122. Larriba, M. J. *et al.* Novel snail1 target proteins in human colon cancer identified by proteomic analysis. *PLoS One* **5,** (2010).
123. Amin, E. M. *et al.* WT1 Mutants Reveal SRPK1 to Be a Downstream Angiogenesis Target by Altering VEGF Splicing. *Cancer Cell* **20,** 768–780 (2011).
124. Calcagno, C., Lobatto, M. E., Robson, P. M. & Millon, A. Modulation of splicing catalysis for therapeutic

targeting of leukemias with spliceosomal mutations. *Diagn Microbiol Infect Dis.* **28,** 1304–1314 (2016).

125. Folco, E. G., Coil, K. E. & Reed, R. The anti-tumor drug E7107 reveals an essential role for SF3b in remodeling U2 snRNP to expose the branch point-binding region. *Genes Dev.* **25,** 440–444 (2011).

126. Lee, J. M. *et al.* Modulation of LMNA splicing as a strategy to treat prelamin A diseases. *J. Clin. Invest.* **126,** 1592–1602 (2016).

127. Cheng, D. *et al.* Small molecule regulators of protein arginine methyltransferases. *J. Biol. Chem.* (2004). doi:10.1074/jbc.M401853200

128. Manuscript, A., Cell, H. & Production, C. Effects of a Novel Arginine Methyltransferase Inhibitor on T Helper Cell Cytokine Production. **277,** 2096–2108 (2011).

129. Yu, Z., Chen, T., Hebert, J., Li, E. & Richard, S. A Mouse PRMT1 Null Allele Defines an Essential Role for Arginine Methylation in Genome Maintenance and Cell Proliferation. *Mol. Cell. Biol.* **29,** 2982–2996 (2009).

130. Li, Y. *et al.* Role of the histone H3 lysine 4 methyltransferase, SET7/9, in the regulation of NF-κB-dependent inflammatory genes: Relevance to diabetes and inflammation. *J. Biol. Chem.* **283,** 26771–26781 (2008).

131. Barsyte-Lovejoy, D. *et al.* (R)-PFI-2 is a potent and selective inhibitor of SETD7 methyltransferase activity in cells. *Proc. Natl. Acad. Sci.* **111,** 12853–12858 (2014).

132. Krämer, M. *et al.* Inhibition of H3K27 histone trimethylation activates fibroblasts and induces fibrosis. *Ann. Rheum. Dis.* **72,** 614–620 (2013).

133. Mann, J. *et al.* Regulation of myofibroblast transdifferentiation by DNA methylation and MeCP2: Implications for wound healing and fibrogenesis. *Cell Death Differ.* **14,** 275–285 (2007).

134. Bechtel, W. *et al.* Methylation determines fibroblast activation and fibrogenesis in the kidney. *Nat. Med.* **16,**

544–550 (2010).

135. Zong, Y. *et al.* Stromal epigenetic dysregulation is sufficient to initiate mouse prostate cancer via paracrine Wnt signaling. *Proc. Natl. Acad. Sci.* **109,** E3395–E3404 (2012).

136. Zhang, J. & Liu, J. Tumor stroma as targets for cancer therapy. *Pharmacol. Ther.* **137,** 200–15 (2013).

137. Meng, M. *et al.* Immunization of stromal cell targeting fibroblast activation protein providing immunotherapy to breast cancer mouse model. *Tumor Biol.* **37,** 10317–10327 (2016).

138. Takai, K., Le, A., Weaver, V. M. & Werb, Z. Targeting the cancer-associated fibroblasts as a treatment in triple-negative breast cancer. *Oncotarget* **7,** 82889–82901 (2016).

139. Liu, J. *et al.* TGF-beta blockade improves the distribution and efficacy of therapeutics in breast carcinoma by normalizing the tumor stroma. *Proc. Natl. Acad. Sci.* **109,** 16618–16623 (2012).

140. Kim, J. H., Shin, B. C., Park, W. S., Lee, J. & Kuh, H. J. Antifibrotic effects of pentoxifylline improve the efficacy of gemcitabine in human pancreatic tumor xenografts. *Cancer Sci.* **108,** 2470–2477 (2017).

141. Coppola, S. *et al.* A mechanopharmacology approach to overcome chemoresistance in pancreatic cancer. *Drug Resist. Updat.* **31,** 43–51 (2017).

142. Spencer C. Wei, Laurent Fattet, Jeff H. Tsai, Yurong Guo, Vincent H. Pai, Hannah E. Majeski, Albert C. Chen, Robert L. Sah, S. S. T. A. J. & Engler, and J. Y. Matrix stiffness drives Epithelial-Mesenchymal Transition and tumour metastasis through a TWIST1-G3BP2 mechanotransduction pathway. *Nat. Cell Biol.* **385,** 1183–1189 (2015).

143. Mani, S. A. *et al.* The Epithelial-Mesenchymal Transition Generates Cells with Properties of Stem Cells. *Cell* **133,** 704–715 (2008).

144. Lin, Y. *et al.* The SNAG domain of snail1 functions as a

molecular hook for recruiting lysine-specific demethylase 1. *EMBO J.* **29,** 1803–1816 (2010).

145. Solanas, G. *et al.* E-cadherin controls -catenin and NF- B transcriptional activity in mesenchymal gene expression. *J. Cell Sci.* **121,** 2224–2234 (2008).
146. Gabasa, M. *et al.* Lung Myofibroblasts Are Characterized by Down-Regulated Cyclooxygenase-2 and Its Main Metabolite, Prostaglandin E2. *PLoS One* **8,** 1–13 (2013).
147. Gabasa, M. *et al.* Epithelial contribution to the profibrotic stiff microenvironment and myofibroblast population in lung fibrosis. *Mol. Biol. Cell* **28,** 3741–3755 (2017).
148. Puig, M. *et al.* Matrix Stiffening and β $_1$ Integrin Drive Subtype-Specific Fibroblast Accumulation in Lung Cancer. *Mol. Cancer Res.* **13,** 161–173 (2015).